The effect of *Cyclopia maculata* on AMPK expression in Wistar rats

Carvern Denver Jacobs

Supervisor: Dr Carmen Pheiffer

Co-supervisor: Prof James Syce

November 2012

Declaration

I Carvern Denver Jacobs do hereby declare that the thesis entitled:

"The effect of *Cyclopia maculata* on AMPK expression in Wistar rats"

is my own work and submitted in partial fulfillment of the degree Magister Scientiae in the South African Herbal Science and Medicine Institute, Faculty of Natural Sciences at the University of the Western Cape and that all research resources I have used in this thesis have been duly acknowledged by means of complete references.

Name : Carvern Denver Jacobs

Signature :

Date : November 2012

Abstract

Being overweight or obese are major factors contributing to the increased morbidity and mortality due to non-communicable diseases such as type 2 diabetes, cardiovascular disease and cancer. The treatment of obesity with pharmaceutical drugs is plagued by side effects. Plants and their phytochemicals possess a number of beneficial health effects including anti-oxidant, anti-mutagenic, anti-inflammatory, anti-obesity and anti-cancer effects, mediated by activation of the adenosine monophosphate protein kinase (AMPK). AMPK controls many metabolic processes including glucose uptake and utilisation, and adipogenesis, and is often referred to as the master regulator establishing cellular homeostasis.

Cyclopia maculata, commonly known as honeybush, is an indigenous South Africa plant possessing anti-oxidant, anti-inflammatory and anti-cancer properties. Recently, others in our laboratory have shown that a hot water extract of fermented *C. maculata* inhibits adipocyte differentiation in 3T3-L1 pre-adipocytes, with some evidence of weight regulatory properties in a Wistar rat model of diet-induced obesity. In the rat study, 21 day old weanlings were fed a high fat, high sugar cafeteria diet for 3 months with (n=10) or without (n=10) *C. maculata* supplementation. This group of rats was referred to as the lean group (n=20). Another group of rats were fed a cafeteria diet for 4 months to induce obesity (obese group, n=20) and thereafter treated as described for the lean rats. The aim of this MSc study was to determine whether *C. maculata* induces AMPK activation.

Proteins were extracted from the liver and muscle tissue of lean and obese Wistar rats using an optimized extraction method with a commercial lysis buffer and the TissueLyser. Treatment with the *C. maculata* extract had no effect on the protein yield in lean and obese rats. Interestingly, the protein yield in the liver of obese rats was significantly higher than that observed in lean rats. Although *C. maculata* treatment slightly increased AMPK activation (calculated as the ratio of phosphorylated AMPK to total AMPK) in the liver of lean and obese rats, the difference was not statistical significant. Conversely, *C. maculata* treatment decreased AMPK activity in muscle of lean and obese rats, with statistical significance observed in the lean group only (2.3-fold, $p<0.05$). Differences in

AMPK activation between the groups were also noted, a 1.3-fold decreased activity observed in obese groups compared to their lean counterparts, although this was not statistically significant. Expression of PPARα, a downstream protein target affected by AMPK activation was reduced in the liver of lean and obese rats after *C. maculata* treatment. Moreover, PPARα expression was significantly higher in obese compared to lean rats (2.7-fold, $p<0.001$). PPARα is a transcription factor mediating fat metabolism (β-oxidation) and its expression is induced by circulating free fatty acids, which are increased in obese compared to lean rats. The expression of PPARα in muscle was too low for Western blot analysis and quantification.

Cyclopia maculata treatment did not affect hepatic expression of UCP2, another protein important in establishing energy homeostasis. The expression of UCP2 was 2.9-fold higher in the liver of obese rats compared to their lean counterparts, although the difference was not statistically significant. The opposite results were observed in the muscle where *C. maculata* treatment decreased UCP2 expression in lean rats (2.8-fold, $p<0.0001$), and UCP2 expression was decreased 1.4-fold in obese rats compared to lean rats, although the difference was not statistically significant.

ELISA results for AMPK activation revealed that *C. maculata* treatment increased AMPK activity, although not statistically significant. Histological analysis of retroperitoneal fat showed that *C. maculata* did not affect adipocyte size and number, although a slight decrease in adipocyte size was observed after treatment

This study has demonstrated that treatment of the cafeteria diet fed Wistar rats with 300 mg/kg of a hot water extract of fermented *C. maculata* does activate AMPK. This study revealed important differences between lean and obese rats. In particular, increased hepatic protein content, PPARα and UCP2 expression was observed in obese rats compared to the lean group. This suggests an adaptive response to the increased circulating free fatty acids during obesity and an increase in β-oxidation in these animals.

Acknowledgements

I would like to thank God the Almighty Father for granting me the opportunity and strength to successfully complete this project.

I would like to express my sincere gratitude and appreciation to my supervisor Dr. Carmen Pheiffer for her assistance and guidance.

I would like to thank Dr. Johan Louw, the director of the Diabetes Discovery Platform for giving me the opportunity to study in the platform and for his support during the project.

I acknowledge the National Research Foundation (NRF) for the bursary funding and running expenses (grant 70525 to Prof Elizabeth Joubert, Agricultural Research Council (ARC) Infruitec-Nietvoorbij).

I acknowledge Prof Elizabeth Joubert, ARC, Infruitec-Nietvoorbij for providing the *Cyclopia maculata* extract and for her support during this study.

I would like to thank the South African Herbal Science and Medicine Institute (SAHSMI) for granting me the opportunity to pursue my M.Sc. studies.

To all my colleagues at the Diabetes Discovery Platform, Medical Research Council (MRC), who provided me with technical assistance, thank you. A special thanks to Ms. Oelfah Patel, Dr. Rabia Johnson, Dr. Micheline Sanderson and Mr. Kwazi Gabuza for their support.

I would like to thank my parents, Carol Gray and David Gray for their love and financial support throughout my academic career. Special thanks to my aunt Shiela for all her support and always believing in me. Special acknowledgement to my son Lincoln for being the inspiration in my life and my partner Clarese for all her love and support.

Table of contents

Declaration 2
Abstract 3
Acknowledgements 5
Table of contents 6
List of abbreviations 10
List of figures 12
List of tables 13
1. Literature review 15
1.1 Obesity 15
1.2 Metabolic syndrome 18
1.3 Obesity-associated disorders 19
1.3.1 Insulin resistance 19
1.3.2 Type 2 Diabetes Mellitus 19
1.3.3 Hypertension 20
1.3.4 Cardiovascular disease (CVD) 20
1.4 Obesity therapeutics 20
1.4.1 Surgery 20
1.4.2 Synthetic compounds 21
1.4.3 Natural products 21
1.4.3.1 Natural products and AMPK 22
1.5. Adeno monophosphate-activated protein kinase (AMPK) 22
1.5.1 Peripheral AMPK activation 23
1.5.2 Central AMPK activation 24
1.5.3 The AMPK complex 25
1.5.3.1 The α subunit 25
1.5.3.2 The β subunit 25
1.5.3.3 The γ subunit 25
1.5.4 AMPK regulation 26
1.5.4.1 The AMP/ATP ratio 26
1.5.4.2 Liver kinase B-1 (LKB-1) 26

1.5.4.3 Calmodulin dependent kinase kinase β (CaMKK-β) 27
1.5.4.4 Transforming growth factor-β-activated kinase 1 (TAK1) 27
1.5.5 Endocrine regulation 27
1.5.5.1 Leptin 27
1.5.5.2 Adiponectin 28
1.5.5.3 Ghrelin 28
1.5.6 AMPK and fuel metabolism 28
1.5.6.1 Glucose uptake and utilization 28
1.5.6.2 Lipid metabolism and β-oxidation 29
1.6 *Cyclopia spp*. "Honeybush" 30
1.6.1 Composition 32
1.6.2 Health benefits 32
1.6.3 *Cyclopia maculata* 33
1.7 The present study 34
2. Materials and Methods 35
2.1 Materials 36
2.2 Buffers and solutions 36
2.3 Protein extraction 36
2.3.1 Cutting and weighing 36
2.3.2 Optimization of protein extraction 37
2.4 Acetone precipitation 38
2.5 Protein concentration determination 39
2.6 SDS-PAGE 41
2.7 Coomassie blue staining 43
2.8 Western blot analysis 43
2.8.1 Transfer 44
2.8.2 Blocking 45
2.8.3 Primary antibody 46
2.8.4 Secondary antibody 47
2.8.5 Protein detection 47
2.8.6 Quantification 48

2.8.7 Stripping 48
2.9 Enzyme-linked immunosorbent assay 48
2.9.1 Acclimatization of reagents and solutions 50
2.9.2 Incubation with standards and protein lysate 50
2.9.3 Incubation with detection antibody 51
2.9.4 Incubation with HRP anti-rabbit antibody 51
2.9.5 Incubation with stabilized chromogenic solution 51
2.9.6 Incubation with stop solution and detection at 450 nm 51
2.9.7 Quantification 52
2.10 Histological analysis of retroperitoneal fat pads 52
2.10.1 Slide preparation and dewaxing 53
2.10.2 Haematoxylin staining 53
2.10.3 Eosin staining 53
2.10.4 Mounting of cover slip 53
2.10.5 Image capturing and analysis 54
2.10.6 Quantification of images 54
2.11 Statistical analysis 54
3. Results 56
3.1 Protein extraction 56
3.1.1 Optimization 56
3.1.1.1 Protein concentration 59
3.1.1.2 Protein yield 60
3.1.1.3 Protein profiling 64
3.1.1.4 Selection of protein extraction conditions 71
3.2 Western blot analysis 71
3.2.1 Protein extraction 71
3.2.2 The effect of *C. maculata* treatment on AMPK expression 74
3.2.2.1 The effect of *C. maculata* on the expression of total AMPK 74
3.2.2.2 The effect of *C. maculata* on the expression of phosphorylated AMPK 76
3.2.2.3 Phosphorylated AMPK as a ratio of total AMPK (Activated AMPK) 78
3.2.3 The effect of *C. maculata* treatment on PPARα expression 80

3.2.4 The effect of *C. maculata* treatment on UCP2 expression 82
3.2.5 Other proteins investigated 85
3.3 Phosphorylated AMPK ELISA 85
4. Discussion 91
4.1 Protein optimization 91
4.2 Lean and obese rats 92
4.3 Western blot analysis 93
4.3.1 Protein yield results 93
4.3.2 *Cyclopia maculata* and AMPK activity (pAMPK/tAMPK) 94
4.3.3 *Cyclopia maculata* and PPARα expression 95
4.3.4 The effect of *C. maculata* on uncoupling protein 2 expression 96
4. 4 Phosphorylated AMPK [pT172] ELISA 97
4.5 Adipocyte size and number 98
4.6 Limitations of study and future work 99
4.7 Conclusion 99
5. References 101
Appendix A 118
Materials 118
Appendix B 124
Solutions 124

List of abbreviations

ACC	Acetyl CoA carboxylase
AHA	American Health Association
AMP	Adenosine monophosphate
AMPK	5’ Adenosine monophosphate-activated protein kinase
pAMPK	Phosphorylated adenosine monophosphate protein kinase
APS	Ammonium persulfate
ATP	Adenosine triphosphate
BMI	Body mass index
CBS	Cystothione binding sequence
CDC	Center for Disease Control
CD	Cafeteria diet
CNS	Central nervous system
CPT1	Carnitine palmityol transferase 1
CVD	Cardiovascular disease
ELISA	Enzyme-linked immunosorbent assay
FAS	Fatty acid synthase
FDA	Food and Drug Administration
FFA	Free fatty acids
GHO	Global Health Observatory
GLUT	Glucose transporter
G6P	Glucose 6 phosphotase
HMC-CoA	3-Hydroxyl-3-methylglutoryl CoA reductase
HRP	Horse reddish peroxidase
NCD	Non-communicable diseases
PEPCK	Phosphoenol-pyruvate-carboxykinase
PMSF	Phenylmethanesulfonyl fluoride
PGC1	Peroxisome proliferator activated receptor-gamma coactivator-1

PPARα	Peroxisome proliferator activated receptor alpha
PPARγ	Peroxisome proliferator activated receptor gamma
PVDF	Polyvinylidene fluoride
RF	Retroperitoneal fat
SDS	Sodium dodecyl sulphate
SNS	Sympathetic nervous system
TG	Triglyceride
T2DM	Type 2 diabetes mellitus
WHO	World Health Organization

List of figures

Figure 1. Worldwide prevalence of overweight. 16
Figure 2. Worldwide prevalence of obesity. 21
Figure 3. A summary of AMPK function on whole body metabolism. 23
Figure 4. Model for the stimulatory effect of AMPK. 30
Figure 5. *Cyclopia maculata*. 31
Figure 6. HPLC chromatogram of the major phytochemicals in *C. maculata*. 34
Figure 7. Experimental layout for optimization of protein extraction. 38
Figure 8. Representative 96 well microtiter plate layout for protein determination. 41
Figure 9. Diagrammatic illustration of Western blot transfer sandwich. 44
Figure 10. Illustration of the AMPK [pAMPK-T172] double sandwich ELISA. 49
Figure 11. Representative 96 well microtiter plate layout for ELISA. 50
Figure 12. Representative picture of H&E straining of retroperitoneal fat. 52
Figure 13. SDS PAGE of proteins before optimization. 57
Figure 14 SDS PAGE of proteins after acetone precipitation. 58
Figure 15. BSA standard curves. 59
Figure 16. Graphical representation of protein yield after optimization. 63
Figure 17. SDS-PAGE using 10 µg of liver protein. 67
Figure 18. SDS-PAGE using 10 µg of muscle protein. 68
Figure 19. SDS-PAGE using 60 µg of liver protein. 69
Figure 20. SDS-PAGE using 60 µg of muscle protein. 70
Figure 21. Graphical representation of the protein yield of liver and muscle tissue. 73
Figure 22. Total AMPK expression. 75
Figure 23. Phosphorylated AMPK expression. 76
Figure 24. Activated AMPK. 79
Figure 25. PPARα expression. 81
Figure 26. UCP2 expression. 83
Figure 27. Phosphorylated AMPK [pT172] ELISA results. 87
Figure 28. Histological results of retroperitoneal fat. 89

List of tables

Table 1. Preparation of the BSA standard curve..... 40
Table 2. Primary antibodies used in study..... 46
Table 3. Secondary antibodies used in study..... 47
Table 4. Protein concentration and yield after optimization..... 61
Table 5. Volumes of proteins (10 µg) for SDS-PAGE profiling..... 65
Table 6. Volumes of proteins (60 µg) for SDS-PAGE profiling..... 66
Table 7. Protein yield of liver and muscle tissue..... 72
Table 8. Activated AMPK expression in liver and muscle of lean and obese rats..... 78
Table 9. Summary of Western blot results for liver tissue..... 84
Table 10. Summary of Western blot results for muscle tissue..... 84
Table 11. ELISA results..... 86
Table 12. Histological results of retroperitoneal fat..... 88

Chapter 1

Literature Review

1. Literature review

1.1 Obesity

Obesity is said to be the silent plague of the future (Prentice, 2006). Traditionally, overweight and obese individuals were thought to exist only in high income countries, such as the United States and Great Britain. However, over the last few decades, obesity has spiraled into a worldwide epidemic affecting all races, cultures and most countries (Flegal *et al*., 2010). More than 2,500 years ago Hippocrates, the "father of medicine", recognized that people who were overweight were at a higher risk of sudden death. Later, in the 18th century, Malcolm Flemyng stated that, "corpulancy" (obesity) may be a disease leading to a shorter life span (Haslam and James, 2005).

Being overweight or obese are considered major factors contributing to a reduced lifespan, increased morbidity and mortality, as well as an escalating financial burden (WHO, 2012). Obesity is characterized by the excessive accumulation of body fat due to an imbalance between energy intake and expenditure, i.e., increased consumption of high fat, nutrient poor foods and decreased physical activity (Misra and Khurana, 2009).

The body mass index (BMI) is a tool used to define obesity, and is calculated by the equation:

$$\text{BMI} = \text{Body weight (kg)}/\text{height (m)}^2$$

Obesity is classified by a BMI of $\geq$ 30 kg/m^2 (WHO, 2012). More recently, abdominal circumference and waist-to-hip ratio are considered to be better predictors of obesity and metabolic syndrome. Studies in normal weight and obese adults have shown that higher abdominal and waist to hip ratios are superior to BMI for predicting increased mortality (Reis *et al*., 2009 and Welborn *et al*., 2003).

The prevalence of obesity has increased dramatically over the last few decades. Finucane *et al*., (2011) estimated that 1.46 billion adults worldwide in 2008 were overweight and 502 million of these people were obese. It is quite evident that overweight and obesity incidences are increasing at a rapid pace, even outdating previous projections of future morbidity. The prevalence of overweight and obesity in South Africa is also estimated to be very high, with more than 29% of men and 56% of woman classified as overweight or obese (Puoane *et al*., 2002). Joubert *et al*., (2007) showed that in 2000, 87% of type 2 diabetes mellitus (T2DM), 68% of hypertensive disease, 61% of endometrial cancers, 45% of ischaemic stroke, 38% ischaemic heart disease, 31% of kidney cancer, 24% of osteoarthritis, 17% of colon cancer and 13% of postmenopausal breast cancers in South Africa were attributable to overweight and obesity.

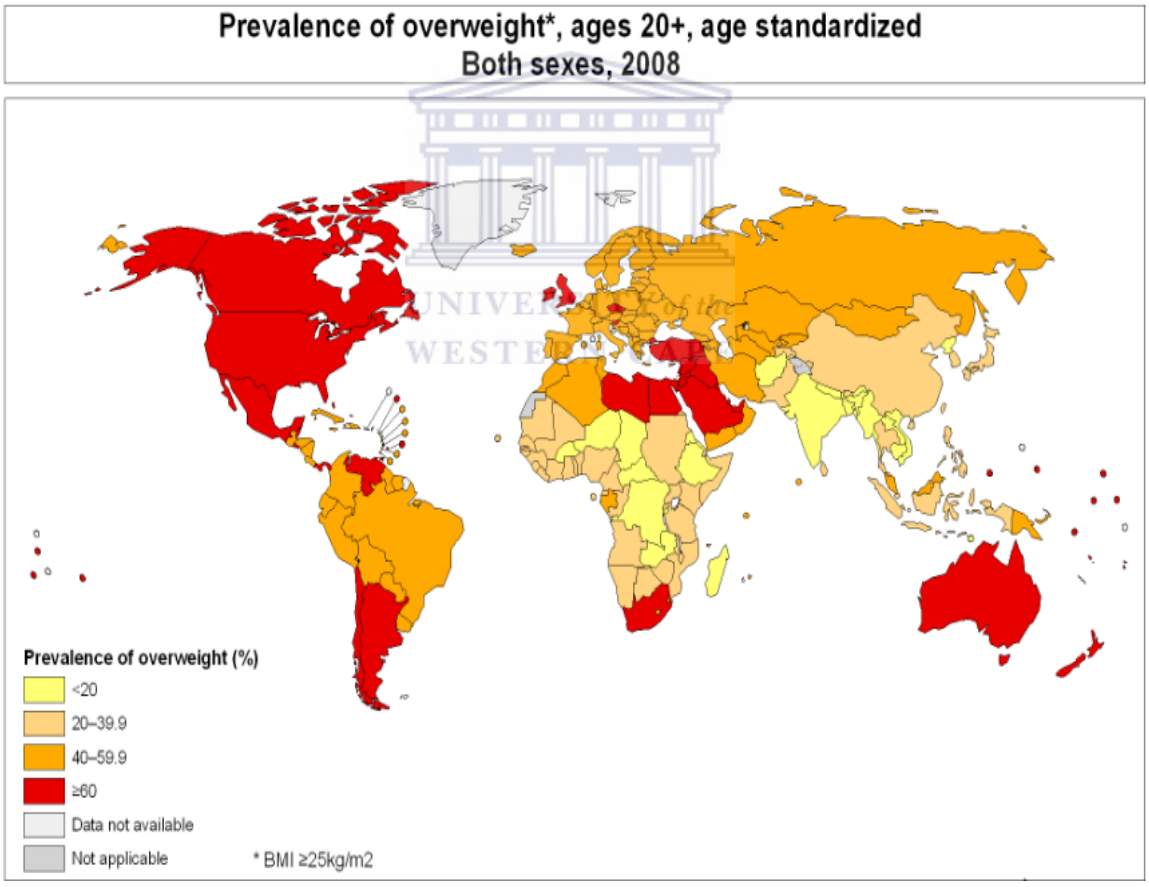

Figure 1. Worldwide prevalence of overweight.

Graphical representation of adult overweight prevalence globally in 2008 (Figure taken from the Global Health Observatory (GHO), Overweight and obesity, WHO, 2012).

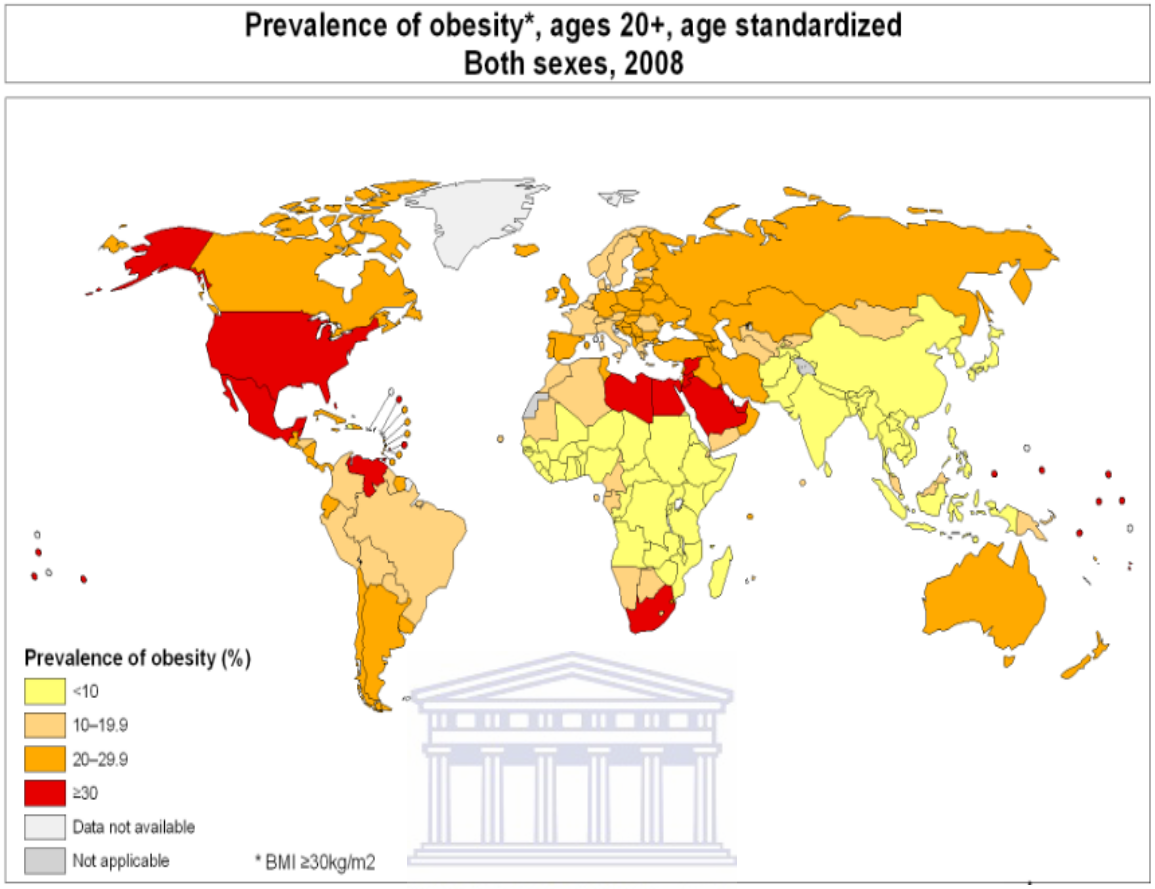

Figure 2. Worldwide prevalence of obesity.

Graphical representation of adult obesity prevalence globally in 2008 (Figure taken from the Global Health Observatory (GHO), Overweight and obesity, WHO, 2012).

The prevalence of obesity has increased in low and middle income countries at the same pace and rate as that in high income countries (Flegal *et al*., 2010). Urbanization has been extensively linked to the increased prevalence of overweight and obesity (Popkin *et al*., 2011). Food has also become highly saturated with processed fats, caloric sweetener additives and preservatives for a longer shelf life and palatable consumption, increasing body weight gain and obesity (Wasir and Misra, 2004). Technological advances in the home and at work has led to decreases in manual energy expenditure, which is considered one of the major drivers of population weight gain and obesity as well as increased morbidity and mortality (Paeratakul *et al*., 1998). Obesity has a genetic component and a

number of genetic variants that increase the risk for obesity has been identified (Loos, 2011). However, genes alone cannot account for the increasing obesity rates worldwide and it is now well known that a complex interaction between environmental factors, such as those described above, together with genetic factors play a role in the development of this multifactorial disorder.

Obesity places huge financial burdens on countries. Overweight and obese individuals are estimated to be responsible for 1% to 3% of the total health care expenditure in most countries, with an average of 5% to 10% in the USA as reviewed by Sassi (2010). In 2008, the estimated medical cost of obesity for the USA was calculated to be $147 billion per year (Finkelstein *et al*., 2009). The percentage is projected to rise to between 16% and 18 % of the USA health expenditure by 2030 (AHA, 2012). The high costs of obesity are especially alarming to health departments of low and middle income countries, such as those in Sub-Saharan Africa which are already burdened with infectious diseases such as the Human immunodeficiency virus/Acquired immune deficiency syndrome (HIV/AIDS) and tuberculosis (TB) (Lalloo and Pillay, 2008).

Being overweight or obese is ranked as the fifth leading risk of global deaths, with a mortality incidence of 2.8 million deaths each year (WHO, 2012). The mortality rate from obesity associated cardiovascular disease (CVD) deaths in developing countries is estimated to increase by 120% for woman and 137% for men, between 1990 and 2020 (Leeder *et al*., 2004).

1.2 Metabolic syndrome

The clustering of metabolic derangements in overweight and obese individuals has been collectively classified as the metabolic syndrome (Galassi *et al*., 2006). Obesity results in the deregulation of metabolic processes such as glucose and fat metabolism, leading to the development of insulin resistance, hyperglycemia, dyslipidemia and hypertension (Redon *et al*., 2008).

Recent epidemiological data has shown that obesity and metabolic syndrome are immediate precursors of type 2 diabetes mellitus (T2DM) and CVD (Ford, 2005; Misra and Khurana 2009). The metabolic syndrome has been shown to double the risk of CVD in patients with hypertension (Andreadis *et al*., 2007 and Scholze *et al*., 2010), and triples the relative risk of T2DM (Segura *et al*., 2007).

1.3 Obesity-associated disorders

The increased prevalence of obesity and metabolic syndrome in developing countries has led towards the increased development of non-communicable disease (NCD) such as hypertension, asthma, cancer, depression, T2DM and CVD (Scholze *et al*., 2010; Misra and Khurana 2009). Deaths due to NCDs were shown to account for 36 million out of 57 million deaths globally in 2008, with nearly 80% of these deaths (29 million) occurring in low and middle income countries (WHO, 2012).

1.3.1 Insulin resistance

Insulin resistance occurs when cells become resistant to the action of insulin, reducing the uptake of glucose from the circulatory system, resulting in hyperinsulinemia, hyperglycemia and dyslipidemia (Samuel *et al*., 2010). Studies have shown that obesity induced insulin resistance occurs independent of genetic heritability (Pi-Sunyer, 2002), and are attributable to increased free fatty acids (Schinner *et al*., 2005 and Samuel *et al*., 2010). Hyperinsulinemia and insulin resistance is associated with T2DM, dyslipidemia, hypertension, hypercoagulability and CVD (Schinner *et al*., 2005 and Hemmingsen *et al*., 2009).

1.3.2 Type 2 Diabetes Mellitus

Type 2 diabetes mellitus is defined by high fasting plasma glucose concentrations of ≥ 7.0 mmol/l (126 mg/dl), and is thought to develop as a consequence of increased peripheral insulin resistance and a reduction in the secretion of insulin by the pancreatic β-cells (Schinner *et al*, 2005). The risk of T2DM increases with the extent and duration of overweight and with the degree of central obesity (Must *et al*., 1999 and Kahn *et al*.,

2006). Type 2 diabetes was estimated to effect 171 million individuals with an estimated increase of 366 million individuals by 2030 (Wild *et al*., 2004).

1.3.3 Hypertension

Epidemiological, clinical and animal studies have shown a strong correlation between obesity and hypertension (Hall *et al*., 2003 and Persell, 2011). Abdominal obesity has been singled as the most important risk factor for hypertension and CVD (Sironi *et al*., 2004). According to the American Heart Association (AHA), about 76.4 million people over the age of 20 were estimated to have high blood pressure in the US (AHA, 2012).

1.3.4 Cardiovascular disease (CVD)

Obesity increases susceptibility to CVD and its related complications (Lavie *et al* 2009 and Marinou *et al*., 2010). CVD associated mortalities were estimated at 17.3 million people in 2008, representing 30% of all global deaths (WHO, 2012). Of these deaths, an estimated 7.3 million were due to coronary heart disease and 6.2 million were due to stroke.

1.4 Obesity therapeutics

1.4.1 Surgery

Bariatric surgery or weight loss surgery includes a variety of procedures performed on the morbidly obese. Weight loss is achieved by reducing the size of the stomach with implanted medical devices (gastric banding), through the removal of a portion of the stomach (sleeve gastrectomy or biliopancreatic diversion) or by resecting and rerouting the small intestines to a small stomach pouch (gastric bypass surgery) (Porrier *et al*., 2011).

These surgical interventions have shown significant long term weight loss, recovery from diabetes, improvement of cardiovascular risk factors and a reduction of mortality from 40% to 23% (Robinson, 2009). Although bariatric surgery can be beneficial it is only conducted on the morbidly obese with a huge financial cost and possible surgical complications (Encinosa and Hellinger, 2008).

1.4.2 Synthetic compounds

Treatment of obesity with synthetic compounds has been plagued with detrimental side effects giving rise to other health complications and morbidities. Phentermine, an appetite suppressant was approved for the short term treatment of obesity by the Food and Drug Administration (FDA) in the USA in 1959 (Khaodhiar and Apovian, 2007). Thereafter, a combination of phentermine and another drug, fenfluramine was sold as "phen-fen", until fenfluramine was withdrawn by the FDA in 1997 due to concerns of developing valvoapthy. Another anti-obesity agent, sibutramine, approved in 1997 for the long term treatment was withdrawn from the market in 2010 due to an increased risk of nonfatal myocardial infarction and stroke in patients with pre-existing CVD and T2DM (James *et al*., 2010).

Currently, Orlistat (Xenical) and Lorcaserin are the only two FDA approved drugs for the long term treatment of obesity. Orlistat acts by inhibiting pancreatic and gastric lipase enzymes blocking 25% to 30% of fat absorption in the gastrointestinal tract (Torgerson *et al*., 2004). It is considered mild in comparison to appetite suppressants. Lorcaserin acts centrally on serotonin receptors promoting the feeling of satiety and reducing food intake (Smith *et al*., 2008(a)). Lorcaserin was proven to function as an anti-obesity drug for chronic weight management in the morbidly obese with a BMI $\geq$ 30 kg/m^2 (Smith *et al*., 2008(b)).

1.4.3 Natural products

The use of natural products to treat obesity has gained considerable interest over the last decade (Hwang *et al*., 2009). Phytochemicals and plants are viewed as safe, effective and affordable alternatives to synthetic treatments with fewer side effects (Wu *et al*., 2010). Numerous anti-obesity herbal compositions and single compounds purified from plants have been shown to regulate body weight gain and obesity (Kang *et al*., 2012; Lee at al., 2010; Wu *et al*., 2010 and Hwang *et al*., 2009).

Lee *et al*., (2010) showed that a herbal mixture consisting of seven herbs inhibited fat accumulation *in vitro* and *in vivo*, through the modulation of the adipogenic pathway.

Citrus peel which has been used in Asia for centuries to treat indigestion (Galati *et al*., 1994 and Ko *et al*., 2010), has recently been shown to regulate weight gain and obesity by enhancing β-oxidation *in vitro* and *in vivo* (Kang *et al*., 2012).

1.4.3.1 Natural products and AMPK

Epigallocatechin gallate (EGCG), a constituent from green tea, mediates its anti-obesity and glucose regulating effects by activating the 5' adenosine monophosphate-activated protein kinase (AMPK) signaling pathway (Hwang *et al*., 2007 and Collins *et al*., 2007). Resveratrol, a polyphenolic compound present in red grapes has been shown to be effective in preventing CVD, obesity, diabetes and cancer (Jiang, 2008). The benefits of resveratrol was found to be associated with increased glucose uptake and decrease accumulation of fatty acids through the modulation of AMPK and associated downstream proteins involve in glucose signaling and lipid metabolism (Ajmo *et al*., 2008).

Nelumbo nucifera or "scared lotus" is a Taiwanese flavonoid rich plant which reduces fatty acid synthesis and accumulation through the stimulation of AMPK signaling (Wu *et al*. 2010). Ginsenoside, curcumin, coffee acid phenethyl ester (CAPE), berberine and theaflavin are a few other natural occurring flavonoid and phenolic compounds which were shown to possess anti-obesity, anti-inflammatory, anti-oxidant and anti-tumour properties through the modulation of the AMPK signaling pathway (Hwang *et al*., 2009).

1.5. Adeno monophosphate-activated protein kinase (AMPK)

The adenosine 5' monophosphate-activated protein kinase (AMPK) is a serine/threonine kinase that plays a central role in energy regulation (Kahn *et al*., 2005 and Lage *et al*., 2008). It is often referred to as the master regulator of energy metabolism controlling carbohydrate, lipid and protein metabolism as well as cellular growth and division (Carling *et al*., 2005; Hardie and Sakamoto, 2006). Activation of AMPK in many tissues switches off ATP consuming processes while switching on catabolic processes that generate ATP. AMPK is activated in response to stresses that deplete cellular ATP supplies such as low glucose, hypoxia, ischemia, and heat shock. It exists as a heterotrimetric complex composed of a catalytic α subunit and regulatory β and γ subunits

(Kahn *et al*., 2005). Binding of AMP to the γ subunit allosterically activates the complex, making it a more attractive substrate for its major upstream AMPK kinase, tumour suppressor liver kinase B-1 (LKB-1). Several studies indicate that signaling through adiponectin, leptin and calmodulin dependant kinase kinase 2 (CaMKKβ) may also be important in activating AMPK (Steinberg and Kemp, 2009). AMPK regulates carbohydrate, lipid and protein metabolism, as well as cell growth and apoptosis through the regulatory control of key transcriptional factors and enzymes involved in energy homeostasis (Figure 3).

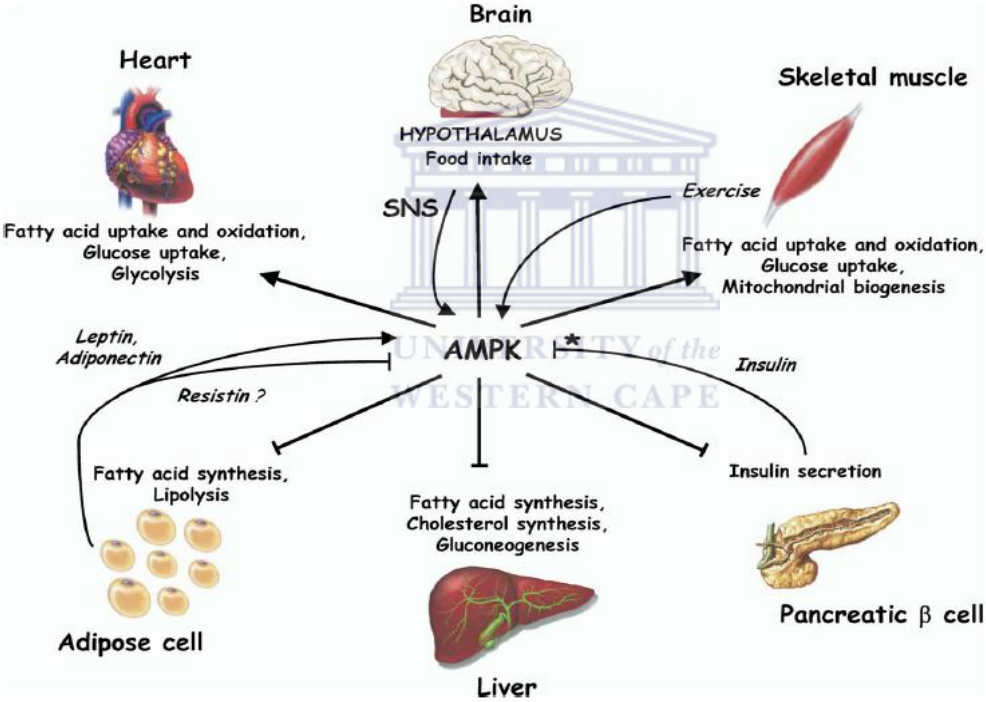

Figure 3. A summary of AMPK function on whole body metabolism.
Sympathetic nervous system (SNS). (Figure was taken from Khan *et al*., 2005).

1.5.1 Peripheral AMPK activation

AMPK is activated by cellular stresses that either interfere with ATP production e.g. (hypoxia, glucose deprivation or ischemia) or physiological stresses which increase ATP consumption e.g. endurance exercise (muscle contraction) (Kahn *et al*., 2005). These

processes lead to depleting circulating ATP levels and a parallel increase in the AMP: ATP ratio, which is believed to be the foremost activator of AMPK and its energy regulatory affects (Fogarty and Hardie, 2010). AMPK activation induces energy generating catabolic processes such as glycolysis and fatty acid oxidation, improving ATP output from glucose and fatty acid utilization (Carling, 2005). At the same time it induces the inhibition of energy consuming anabolic pathways such as gluconeogenesis, lipogenesis, adipogenesis and protein synthesis, preventing further energy loss (Yang *et al*., 2011). Through processes such as these AMPK reestablishes the ATP:AMP ratio, and maintains metabolic energy homeostasis (Steinberg and Kemp, 2009; Fogarty and Hardie, 2010).

1.5.2 Central AMPK activation

In addition to AMPK's role in maintaining cellular energy regulation, it also plays an important role in the regulation of whole body energy metabolism (Carling, 2005 and Lim *et al*., 2010). AMPK is ubiquitously expressed in the brain, especially in areas controlling food intake and neuroendocrine function such as the hypothalamus and the hindbrain (Kola, 2008). AMPK has emerged as a nutrient and glucose sensor in the hypothalamus with appetite and energy regulatory effects (Momcilovic *et al*., 2006). Fasting has been shown to result in the activation of AMPK whereas refeeding inhibits AMPK activity in multiple hypothalamic regions in mice (López *et al*., 2008). Hypothalamic activation of AMPK has been linked to an increase in food intake and weight gain, whereas its inhibition decreases food intake and blunts weight gain. (Andersson *et al*., 2004 and Kola *et al*., 2008).

The appetite and energy regulatory affects associated with hypothalamic AMPK activation has been shown to be controlled by hormones from the gastrointestinal tract (peptide YY, ghrelin, cholecystokinin, glucagon-like peptide 1 (GLP-1) and oxyntomodulin) and adipokines from adipose tissue (leptin, resistin and adiponectin) (Minokoshi *et al*., 2004; Yang *et al*., 2011: Steinberg and Kemp, 2009).

1.5.3 The AMPK complex

AMPK is made up of a heterotrimetric complex comprising of a catalytic α subunit and two regulatory subunits β and γ (Carling, 2005; Hardie and Sakamoto, 2006). Orthologs of the AMPK subunits are found in all eukaryotic species, such as the Snf1 kinase in yeast (Amodeo *et al*., 2007). In mammals each subunit is encoded by multiple genes (α1, α2, β1, β2, γ1, γ2, γ3) resulting in numerous isoforms, which generate 12 possible combinations of the AMPK protein complex (Amodeo *et al*., 2007; Hardie and Sakamoto, 2006).

1.5.3.1 The α subunit

The α subunit contains a classical serine/threonine protein kinase domain close to the N-terminal (Lage *et al*., 2008). When the α subunit forms the heterotrimetric complex with the β and γ subunits, the auto-inhibitory function is abolished and its catalytic function is attained (Pang *et al*., 2008). Phosphorylation of the α subunit at Threonine 172 (Thr172) by LKB-1 or any other upstream kinases is responsible for the activation of AMPK and its energy regulatory effects (Collins *et al*., 2000; Hawley *et al*., 2005).

1.5.3.2 The β subunit

The β subunit serves as a scaffold to the heterotrimetric AMPK complex. This subunit contains a specific sequence that binds to glycogen particles, which have been proposed to be associated with the tight regulation of glycogen metabolism (Hudson *et al*., 2003). Thus, in addition to its scaffolding function it has an important auto-regulatory function in the AMPK complex (Polekhina *et al*., 2003).

1.5.3.3 The γ subunit

The γ subunit contains four tandem repeats of the cystothione-β-synthase sequence (CBS), located at the N-terminus forming two Bateman domains (Bateman, 1997). The Bateman domains selectively bind adenosine containing molecules such as AMP or ATP. Binding of AMP to the CBS moieties in the Bateman domains activates AMPK, whereas ATP antagonizes this process (Scott *et al*., 2004). This allosteric interaction increases the sensitivity of AMPK to short term changes to intracellular levels of AMP (Suter *et al*.,

2006). The unique allosteric regulation between AMP and ATP forms the molecular basis for the on and off switch function of AMPK and is a plausible target for synthetic activators (Suter *et al*., 2006; Sanders *et al*., 2007).

1.5.4 AMPK regulation

1.5.4.1 The AMP/ATP ratio

As previously mentioned, AMPK is activated under stressful conditions which deplete ATP stores and increase AMP content in cells (Fogarty and Hardie, 2010). The binding of AMP to the CBS domains in the γ subunit induces a conformational change in the heterotrimetric complex that promotes the phosphorylation of Thr172 in the α subunit by a upstream kinases (Collins *et al*., 2000; Hawley *et al*., 2005). In addition to AMP's allosteric regulatory effects on the AMPK structure, it also prevents AMPK's dephosphorylation and inactivation by phosphatase action (Suter *et al*., 2006; Sanders *et al*., 2007).

1.5.4.2 Liver kinase B-1 (LKB-1)

The tumour suppressor liver kinase B-1 (LKB-1) which is a serine/threonine kinase has been identified as one of the major upstream kinases that phosphorylate Thr172 in the α-subunit to activate the AMPK (Lizcano *et al*., 2004). LKB-1 was first identified as a tumour suppressor molecule whose inhibition led to an autosomal dominantly inherited cancer in humans called the Peutz-Jerghers syndrome (Hemminki *et al*., 1998; Jenne *et al*., 1998). LKB-1 exists as a heterotrimetric complex with two supporting subunits, the mouse protein 25 (MO25) and STE20-related adaptor protein (STRAD) (Hawley *et al*., 2003). LKB-1 is said to be constitutively active; its activity is not regulated by stimuli that activate AMPK nor is it directly activated by AMP (Hawley *et al*., 2003). However, as previously mentioned the allosteric regulatory effect of AMP on AMPK increases the phosphorylating potential of LKB-1 and enhances its phosphorylating function at Thr172 (Scott *et al*., 2004).

1.5.4.3 Calmodulin dependent kinase kinase β (CaMKK-β)

Another upstream activator of AMPK has been identified as the calmodulin-dependent kinase-kinase-β (CaMKK-β) (Hurley *et al*., 2005). CaMKK-β phosphorylates AMPK at Thr172 independent of cellular ATP levels under the influence of high circulating Ca^{2+} levels (Hawley *et al*., 2005). Activation of CaMKK-β by Ca^{2+} leads to increased fatty acid oxidation and glucose utilisation in muscle and liver tissue in an AMPK dependant manner (Fogarty and Hardie 2010). CaMKK-β has been found to be highly expressed in the brain, with a depolarisation in K^{+} increasing AMPK activation and its appetite regulating effects (Hawley *et al*., 2005).

1.5.4.4 Transforming growth factor-β-activated kinase 1 (TAK1)

Transforming growth factor-β-activated kinase 1 (TAK1) is another upstream kinase that has been identified to phosphorylate AMPK at Thr172 directly (Momcilovic *et al*., 2006). TAK1 was suggested to be activated by tumour necrosis factor α (TNF α) and transforming growth factor β (Srivastava *et al*., 2007).

1.5.5 Endocrine regulation

1.5.5.1 Leptin

Leptin is an adipocyte secreted hormone that plays a crucial role in the regulation of feeding, energy expenditure and neuroendocrine homeostasis (Friedman and Halaas, 1998; Kahn *et al*., 2005). Leptin acts directly in peripheral tissue to increase fatty acid oxidation (Minokoshi *et al*., 2004) and glucose uptake (Brabant *et al*., 2005), as well as inhibiting fatty acid synthesis in an AMPK dependant manner (Andersson *et al*., 2004). Central nervous system (CNS) leptin stimulated modulation of AMPK has been linked to the hypothalamic melanocorticon-sympathetic axis and α-adrenergic signalling in muscle (Minokoshi *et al*., 2002). Hypothalamic activation of leptin seems to inhibit AMPK activity, reducing appetite and food intake while increasing peripheral fatty acid oxidation through the melanocorticon-sympathetic axis (Minokoshi *et al*., 2004 and Andersson *et al*., 2004).

The development of leptin resistance in obesity has been characterised by suppressed rates of leptin stimulated AMPK signalling (Tanaka, 2007). High fat feeding has also shown to inhibit leptin's ability to suppress hypothalamic AMPK signalling (Martin *et al*., 2006).

1.5.5.2 Adiponectin

Adiponectin is an insulin sensitizing adipokine that improves glucose utilisation and fatty acid oxidation in muscle and liver, as well as reducing hepatic glucose synthesis (Goldstein and Scalia, 2004). Adiponectin stimulates the phosphorylation of AMPK in liver and muscle as well as in the CNS (Yamauchi *et al*., 2002). In contrast to leptin, its secretion and plasma concentration is inversely related to adiposity (Lage *et al*., 2008). Plasma adiponectin concentrations are reduced in obese and T2DM individuals (Berg *et al*., 2002). Adiponectin's over expression has been shown to reverse insulin resistance in models of genetic and diet induced obesity (Yamauchi *et al*., 2002).

1.5.5.3 Ghrelin

Ghrelin is a gut derived, appetite inducing hormone that has been shown to increase AMPK activity in the hypothalamus (Barazzoni *et al*., 2005; López 2008). Like leptin, ghrelin elicits tissue specific effects on AMPK activity (Barazzoni *et al*., 2005). Ghrelin inhibits AMPK activity in the liver (Kola, 2008), while activating AMPK activity in the hypothalamus and heart with no effect observed in muscle (Kola, 2008).

1.5.6 AMPK and fuel metabolism

1.5.6.1 Glucose uptake and utilization

AMPK plays an important role in glucose metabolism. AMPK activation in response to contraction of fast twitching (glycolytic) muscles increases glucose uptake independent of insulin (Bergeron *et al*., 2001 and Fujii *et al*., 2006). AMPK increases the uptake of glucose into the cell by stimulating the expression of hexokinase II and glucose transporter 4 (GLUT4), and its enhanced translocation to the cell membrane (Hardie and Sakamoto, 2006). Activated AMPK in skeletal muscle phosphorylates and inhibits glycogen synthase thus inhibiting glycogen synthesis (Jorgensen at al., 2004). AMPK

activity in the liver has been shown to regulate gluconeogenesis by inhibiting the transcription of phosphoenolpyruvate-carboxykinase (PEPCK) as well as glucose-6-phosphatase (Cool *et al*., 2006).

1.5.6.2 Lipid metabolism and β-oxidation

AMPK has been shown to play a major role in the regulation of glucose and fatty acids through the regulation of key substrates (Kahn *et al*., 2005). Activated AMPK phosphorylates and inhibits acetyl-CoA-carboxylase 1 (ACC1) and 3-hydroxy-3-methylglutaryl-CoA reductase (HMG-CoA), decreases fatty acid synthase (FAS) expression and activates malonyl-coA CoA carboxylase, leading to decreased fatty acid and cholesterol synthesis (López *et al*., 2008; Lage et a., 2008 and Steinberg and Kemp, 2009). AMPK stimulates fatty acid oxidation by decreasing malonyl-CoA levels through the phosphorylation of ACC2 (Hardie and Sakamoto, 2006). This leads to an increase in carnitine palmityol transferase (CPT1, CPT2) activity, facilitating the transport of fatty acids such as acetyl-CoA across the mitochondrial membrane and the subsequent activation of fatty acid oxidation (Abu-Elheiga *et al*., 2001; Hardie *et al*., 2006). AMPK has also been shown to stimulate and up regulate the expression of the peroxisomal proliferator activated receptors α, γ and β which consequently increases mitochondrial biogenesis and the rate of fatty acid oxidation (Jager *et al* 2007).

Peroxisomal proliferator activated receptor α (PPARα) is predominantly expressed in tissues with high rates of mitochondrial and peroxisomal fatty acid metabolism such as the liver, heart, brown adipose tissue, skeletal muscle and kidneys (Yoon *et al*., 2009). PPARα functions by regulating the gene expression of key enzymes involved in the transport, uptake and oxidation of lipids such as fatty acid transport protein, carnitine palmityol transferase-1 (CPT1) and the uncoupling proteins (UCP1, UCP2 and UCP3) (Evans *et al*., 2004 and Yoon *et al*., 2009). Uncoupling proteins uncouples ATP energy and heat from the β-oxidation of circulating free fatty acids decreasing adiposity and weight gain (Yonezawa *et al*., 2009; Schrauwen and Hesselink, 2002).

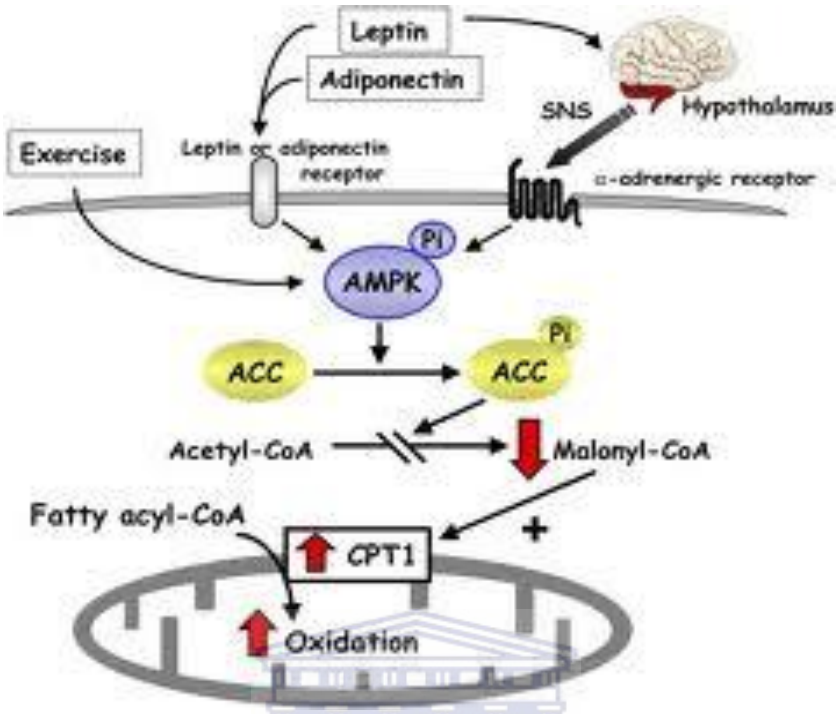

Figure 4. Model for the stimulatory effect of AMPK.

Stressful conditions such as exercise or hormonal stimuli increase the phosphorylation of AMPK, which in turn phosphorylates ACC, inhibiting the conversion of acetyl-CoA to malonyl-CoA. This facilitates the transport of long chain acetyl-CoA into the mitochondria by CPT1 for fatty acid oxidation in peripheral tissue, including the liver and the muscle. (Taken from Khan *et al*., 2005).

1.6 *Cyclopia spp*. "Honeybush"

The *Cyclopia* spp. is commonly known as "honeybush". The *Cyclopia* genus (*Fabaceae* family, *Podalyrieae* tribe) consists of 24 species of endemic shrubs which are found in the Eastern and Western Cape Floristic regions of South Africa ((Du Toit *et al*. 1998; Joubert *et al*. 2011). The honeybush plant is easily recognised by its trifoliate leaves, single flowered inflorescences and sweetly scented bright yellow flowers (Joubert *et al*., 2011).

Figure 5. *Cyclopia maculata*.
Picture of *Fabaceae*: *Cyclopia maculata* 'honeybush' during the flowering period with distinctive, deep yellow flowers which have the characteristic sweet, honey scent. (Picture was taken by Marina Joubert, 2010. Genadendal's hopes for honeybush tea, Science in Africa)

Honeybush is consumed as a herbal tea infusion similar to rooibos tea, having a pleasant sweet taste and aroma (Joubert *et al*., 2011). *Cyclopia subternata* (vleitee), *Cyclopia intermedia* (bergtee) and *Cyclopia genistoides* (kustee) are a few of the commonly known commercial species used for the production of honeybush tea (Joubert *et al*. 2011). The tea is prepared from the leaves and flowers but contain components from the stem as well. It is estimated that approximately 50 to 200 tonnes of honeybush is produced in South Africa each year (Joubert *et al*., 2011). The demand for these teas is growing, partly due to their pleasant taste and aroma and partly due to their health promoting properties (Joubert *et al*., 2011).

1.6.1 Composition

Honeybush tea is low in tannins and is caffeine free with a sweet aromatic flavor (Joubert *et al*., 2008). Honeybush contains minerals including Ca^{2+}, Cu, Fe, K, Mg, Mn, Na and Zn (McKay and Blumberg, 2007). The major phytochemical compounds identified in the *Cyclopia* species have been characterized as the xanthones mangiferin and isomangiferin, as well as the flavanone hesperidin (De Nyssenchen *et al*., 1995 and Joubert *et al*., 2008; 2011). In addition to hesperidin, the presence of other flavanones has been demonstrated. Honeybush extracts, depending on species, also contain flavones, isoflavones, flavonols, coumestans, a benzophenone and a dihydrochalone (Ferreira *et al*., 1998; Kamara *et al*., 2003; Kamara *et al*., 2004: De Beer *et al*., 2009 and Kokotkiewicz *et al*., 2012).

The polyphenolic composition of *Cyclopia* varies according to species, geographical location, harvesting and processing method (Du Toit *et al*., 1998; De Beer and Joubert, 2010; Joubert *et al*., 2011). Fermentation, the oxidation process whereby *Cyclopia* is converted into traditional honeybush tea, reduces the composition and concentration of polyphenols (Joubert *et al*., 2008).

1.6.2 Health benefits

Honeybush was traditionally prepared as a tea from the leafy shoots and flowers, which were dried and fermented to give the sweet honey flavor (Joubert *et al*., 2008). A decoction of *C. genistoides* was used as restorative and as expectorant in chronic catarrh and pulmonary tuberculosis (Bowie, 1980). *Cyclopia* spp. has been shown to possess anti-oxidant, anti-cancer and phytoestrogen properties as reviewed by Joubert *et al*., 2008 and 2011. In a study by Marnewick *et al*., 2000, a fermented and unfermented hot water extract of honeybush in a dose dependant manner significantly reduced mutagenesis induced by 2-acetylaminoflourene (AAF) *in vivo* in the *Salmonella typhimurium* strain TA198 compared to the control.

In a recent publication by Muller *et al*., 2011, it was shown that an aqueous extract of *Cyclopia intermedia* was effective in controlling blood sugar levels. *Cyclopia* has also been shown to contain a substance called pinitol, which has been reported to have blood

glucose lowering effects in the body (Kim *et al*., 2007). Mangiferin, a polyphenol constituent of honeybush exhibits lipolytic activity (Yoshikawa *et al*., 2002), and reduces the accumulation of triglycerides and intracellular free fatty acids by stimulating AMPK activity (Niu *et al*., 2012). Recent work in our laboratory has provided further evidence of the anti-obesity properties of *Cyclopia* spp. (Dudhia *et al*., 2013; Patel *et al*., 2012). Dudhia *et al*. (2013) showed that a fermented, hot water extract of *C. maculata* inhibits adipocyte differentiation in 3T3-L1 adipocytes. Patel *et al*., 2012, illustrated that *C. maculata*, together with a dietary intervention, ameliorated diet-induced obesity in Wistar rats.

1.6.3 *Cyclopia maculata*

Cyclopia maculata grows naturally in the Western Cape Province of South Africa (Joubert *et al*., 2011). *Cyclopia maculata* is not as well studied as other *Cyclopia* spp. but the growing demand for honeybush tea warrants investigation of this species.

High performance liquid chromatography (HPLC) analysis showed that the xanthones mangiferin and isomangiferin, as well as the flavanone hesperidin are present in *C. maculata* (Dudhia *et al*., 2013) as previously reported for other *Cyclopia* spp. (Joubert *et al*., 2008; 2011). Hesperetin, the aglycone of hesperidin is also present in small amounts (Figure 6).

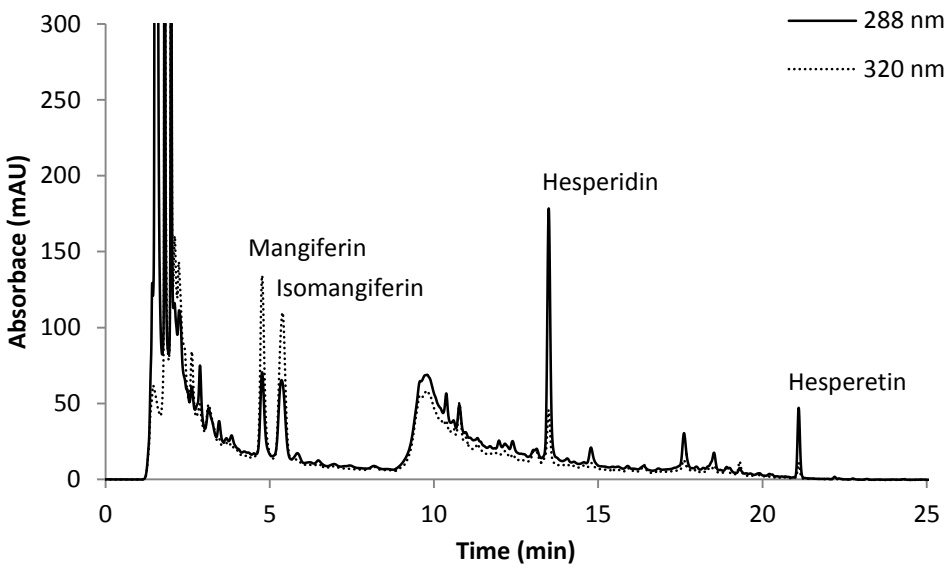

Figure 6. HPLC chromatogram of the major phytochemicals in *C. maculata*.
(Taken from Dudhia *et al*., 2013).

1.7 The present study

A hot water extract of fermented *C. maculata* has demonstrated anti-obesity properties *in vitro* (Dudhia *et al*. 2013), and there is evidence of weight regulatory properties *in vivo* (Patel, 2012). The aim of the present study is to determine whether *C. maculata* treatment effected AMPK activation in high fat, high sugar cafeteria diet (CD)-induced obesity in Wistar rats. The effect of *C. maculata* on AMPK activation will be investigated in the liver and muscle of lean and obese rats fed a CD.

Chapter 2

Materials & Methods

2. Materials and Methods

2.1 Materials

Tissue biopsy samples used in this study were obtained from Ms. O. Patel (Patel, 2012). In Ms. Patel's study 21-day old rats (weanlings) were fed a high fat cafeteria diet (CD) for 12 weeks to induce obesity, with (n=10) or without (n=10) supplementation with a hot water extract of fermented 300 mg/kg *C. maculata*. This was called the lean group. Another group of weanlings, the obese group, were fed the CD for 4 months until they became obese and thereafter fed the CD for 12 weeks with (n=10) or without (n=10) 300 mg/kg *C. maculata*. Rats were terminated after treatment, tissue rapidly excised, and snap frozen in liquid nitrogen, whereafter they were stored at -80°C until analysis.

Cyclopia maculata was harvested from a plantation in Riversdale, South Africa and fermented by a commercial tea processor (Cape Honeybush Tea Company, Mossel Bay, South Africa). A hot water extract of the plant material was prepared by Elizabeth Joubert (Infrutec-Nietvoorbij, Agricultural Research Council). The extract and its phenolic composition are described in Dudhia *et al*., 2013. The dose of 300 mg/kg of *C. maculata* extract used was calculated to be equivalent to 5 cups of tea per day (Patel *et al.*, 2012).

The materials used in the study, together with their suppliers, are listed in Appendix A.

2.2 Buffers and solutions

The recipes of buffers and solutions prepared and used in this study are listed in Appendix B.

2.3 Protein extraction

2.3.1 Cutting and weighing

Liver and skeletal muscle tissue samples were removed from -80°C and placed in liquid nitrogen to prevent thawing. All surfaces and equipment used for weighing were cleaned with 70% (v/v) ethanol to prevent contamination. Thereafter, 100 mg of tissue was weighed using an analytic balance (Ohaus, UK) and immediately placed on ice to preserve sample integrity. Excess hemoglobin was minimized by briefly rinsing tissue

samples with 2 ml of cold phosphate buffered saline, pH 7.5 (PBS) (Sigma-Aldrich, USA) for 5 minutes. Thereafter, samples were centrifuged at 15,000 g for 10 minutes at 4°C. Supernatants were discarded and 1 ml of in-house lysis buffer was added to the tissue and the tissue homogenized with the TissueLyser.

2.3.2 Optimization of protein extraction

The quality and quantity of proteins are crucial for accurate representation by Western blot analysis. Protein extraction from liver and muscle tissue was optimized by comparing two different lysis buffers and two different homogenization methods. Three liver and 3 muscle tissue samples were subjected to protein extraction comparing two lysis buffers, an in-house lysis buffer and a commercial lysis buffer (Tissue Extraction Reagent I, Invitrogen, USA), and two homogenization methods, the TissueLyser (Qiagen, Germany) and the Polytron homogenizer (Brinkmann/Kinematica, Switzerland) (Figure 7).

The in-house lysis buffer (50 mM Tris, 1 mM DTT, 50 mM NaF, 100 µM Na_3VO_4, 1% (v/v) NP40, 1% (v/v) Triton x 114, 25 µg/ml RNase and 1 mM PMSF) and the commercial lysis buffer (50 mM Tris, 250 mM NaCl, 5 mM EDTA, 2 mM Na_3VO_4, 1 mM NaF, 20 mM $Na_4P_2O_7$, 0.02% (w/v) NaN_3 and proprietary detergent) was supplemented with 1x protease and 1x phosphatase inhibitor cocktail tablets (Roche, USA). Protease and phosphatase inhibitor cocktail tablets were added to lysis buffer according to manufacturer's instructions; 1 tablet per 10 ml of buffer or as instructed by our standard operation procedure for the making of the in-house lysis buffer. Protease and phosphatase inhibitor cocktail tablets inhibit a broad spectrum of proteases (serine, cysteine and acidic proteases) and phosphatases (acid, alkaline, serine/threonine and tyrosine phosphatases).

TissueLyser homogenization works by disrupting biological samples through high-speed shaking with beads, which beat and grind samples, releasing the constituents into solution. Homogenization was performed by adding a stainless steel bead (Qiagen, Germany) to tubes containing tissue samples in lysis buffer. Thereafter tubes were placed in pre-cooled adaptors (-80°C overnight) and transferred to the TissueLyser. Tissue samples were

homogenized at 25 Hz for 30 seconds followed by one minute incubation on ice. This process was repeated four times.

Polytron homogenization was performed at the Department of Medical Physiology, Faculty of Health Sciences, Stellenbosch University. Tissue samples and lysis buffer were transferred to a round base centrifuge tube on ice. The serrated probe of the Polytron was placed into the tube and the tissue ground for 4 seconds at a speed of 4, followed by a 40 second incubation on ice. The process was repeated four times. Lysates were clarified by centrifugation at 15,000 g for 15 minutes at 4°C. Supernatants were transferred to 1.5 ml tubes and stored at -20°C until protein concentration determination.

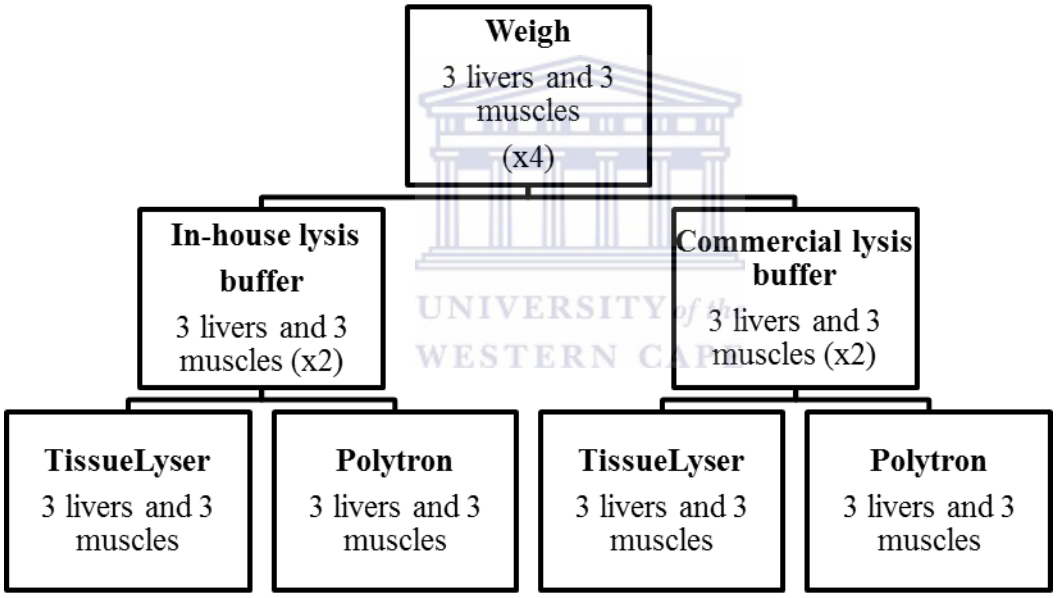

Figure 7. Experimental layout for optimization of protein extraction.
Three liver and 3 muscle tissue samples were weighed in quadruplicate and compared using two different lysis buffers and two different homogenization methods.

2.4 Acetone precipitation

Acetone precipitation is a technique used to remove salts and debris from lysate samples using solvent based precipitation and high speed centrifugation (Pierce Biotechnology Incorporated, 2004). Proteins are insoluble in acetone at low temperatures, whilst many small molecules and debris are soluble.

Acetone precipitation of samples was performed by adding 3x the volume (3 ml) of cold acetone to the lysate, mixed by vortexing and then incubated for 1 hour at -20ºC to allow precipitation. The lysate was vortexed briefly for 5 seconds, then centrifuged for 10 minutes at 13 000 rpm. The supernatant was removed and the protein pellet was air dried for 20 minutes. The pellet was dissolved in 300 µl of lysis buffer and mixed by vortexing for 10 seconds. Thereafter, the pellet was homogenized in the TissueLyser for 1 minute at 25 Hz and left on ice for 10 minutes. The lysate was centrifuged for 5 minutes at 13 000 rpm whereafter the supernatant was transferred to a fresh tube and freezed at -20ºC.

2.5 Protein concentration determination

Protein concentrations were quantified using the RC DC kit (BioRad, USA). The RC DC assay is based on the Lowry method of protein estimation, where proteins react with alkaline copper and subsequently reduces folin reagent, resulting in color development. The RC DC assay is a protein concentration determination kit which is compatible with samples containing reducing agents and detergents, the major interfering agents in protein estimation.

A standard curve was prepared using bovine serum albumin (BSA) (BioRad, USA) (Table 1). To ensure that the absorbance of unknowns fell within the range of the standard curve, it was decided to dilute protein samples 1:20. Proteins were diluted by adding 1 µl of sample to 19 µl of lysis buffer. To minimize interference from lysis buffer constituents, lysis buffer for absorbance readings was diluted 1:2 with double distilled water (ddH_2O) (500 µl of lysis buffer and 500 µl of ddH_2O) and used at a half strength concentration. Five microliters of BSA standards and protein samples were added to separate wells of a 96 well microtiter plate (Sigma-Aldrich, USA) in duplicate (Figure 8). Twenty five microliters of solution A' was added to each well followed by 200 µl of reagent B. Solution A' was made by mixing 20 µl of reagent S and 1 ml of reagent A. Thereafter, the plate was mixed on a plate mixer (Scilogex, USA) for 10 seconds. Plates were left at room temperature for 15 minutes whereafter absorbance was measured at 630 nm using a

spectrophotometer (BioTek, USA). Data was exported to Excel (Microsoft Office, Version 2003, USA) for analysis.

Table 1. Preparation of the BSA standard curve

[BSA] µg/µl	Volume (µl)		
	BSA	Lysis buffer	Total
1.44†	20	0	20
1	13.8	6.2	20
0.5	7	13	20
0.2	2.8	17.2	20
0	0	20	20

†A stock solution of 1.44 µg/µl BSA was used

	1	2	3	4	5	6	7	8	9	10	11	12
A	0	0										
B	0.2	0.2										
C	0.5	0.5										
D	1	1										
E	1.44	1.44										
F												
G												
H												

Figure 8. Representative 96 well microtiter plate layout for protein determination. BSA standards were pipetted in duplicate into wells shaded in blue. Unknown samples were pipetted, in duplicate, in the remainder of the plate. To avoid inaccuracies, the concentrations of no more than 20 unknowns were analyzed per plate.

2.6 SDS-PAGE

Sodium dodecyl sulfate polyacrylamide gel electrophoresis (SDS-PAGE) was used to separate proteins according to their size. SDS is an anionic detergent that binds quantitatively to proteins, denaturing their tertiary structure, and linearizing them (Westermeier, 2000). The polyacrylamide gel is a cross-linked matrix which allows proteins, which are negatively charged due to their binding with SDS, to migrate towards the anode when an electric current is passed through the gel.

Proteins were separated by SDS-PAGE to assess the quality of the extracted proteins, or for Western blot analysis. For the assessment of protein quality, 10 µg of protein was separated by SDS-PAGE and thereafter subjected to Coomassie blue staining for protein visualization. For Western blot analysis, 60 µg of protein was subjected to electrophoretic separation and thereafter transferred to polyvinylidene fluoride (PVDF) membranes. Proteins were separated using a 4% stacking gel over a 10% resolving gel.

One millimetre spacer plates (BioRad, USA) and cover plates (BioRad, USA) were cleaned with dish washing liquid, rinsed with water then wiped with 70% (v/v) ethanol and paper towel. Plates were assembled on assembling racks (BioRad, USA). The resolving gel was poured into plates until it reached 2 cm from the top of the plate, overlaid with water saturated butanol and left to set at room temperature for 30 to 40 minutes. Water saturated butanol was discarded, gels were rinsed with distilled water and blotted with Whatmann paper to get rid of excess water. Thereafter, the stacking gel was overlaid onto the resolving gel; the well combs were inserted and the gel was allowed to set at room temperature for 30 to 40 minutes.

Protein samples were prepared by diluting all samples to the concentration of the most dilute sample. This ensured that the same volume of sample was loaded onto the SDS-PAGE gel. Thereafter, an equal volume of 2x Leammli sample loading buffer (BioRad, USA) was added. Proteins were divided into 100 µl aliquots and stored at -20°C or used immediately. Double the volume of sample corresponding to 10 or 60 µg of protein was transferred to a new tube, and proteins were denatured by heating at 95°C on a heat block (Labnet, USA) for 5 minutes. A double volume was heated at 95˚C in case of protein loss during denaturation, and to ensure that a total of 10 or 60 µg of protein was added to gels. Thereafter, tubes were briefly spun down for a few seconds and placed on ice.

Glass plates containing the set gels were placed into an electrophoresis chamber (BioRad, USA) and half filled with 1x SDS-PAGE running buffer (25 M Tris, 1.9 mM Glycine, 1% SDS). Protein samples were loaded onto gels, tanks were filled with running buffer, and gels were run at 150 V for 70 minutes using the Mini-Protean Tetra Electrophoresis system (BioRad, USA). For protein visualisation with Coomassie blue, 10 µl of the unstained protein ladder (Pierce, USA) was used as molecular weight marker. For Western blot analysis, 10 µl of the prestained protein ladder and 5 µl of the Cruz Marker (Santa Cruz, USA) were used as molecular weight markers. The prestained Fermentes protein ladder (Thermo Scientific, USA) was used as a molecular weight marker to visualise the transfer of proteins to the PVDF membrane (Millipore, USA) and the Cruz

marker, was used as a chemiluminescent molecular weight marker, to asses sizes after Western blot analysis.

After electrophoresis, gels were removed and stained with Coomassie blue or transferred to PVDF membranes for Western blotting.

2.7 Coomassie blue staining

Forty millilitre of Coomassie blue stain (BioRad, USA) was added to gels and incubated at room temperature for 16 to 18 hours shaking. Gels were destained with 10% (v/v) acetic acid and 30% (v/v) methanol 3 washes, 2x 3 hours and 1x for 16 hours until protein bands became visible. Gel images were captured using the BioRad, USA ChemiDoc^{TM} XRS^{+} image illuminator and Quantity One software.

The camera, ChemiDoc system and the computer were switched on a few minutes in advance before use. The Quantity One software programme was opened and the ChemiDoc XRS file selected to open the acquisition window. The UV plate converter was placed on the glass plate in the imager. An A4 sheet containing a hole the size of the gel was placed on the UV plate converter to orient the gel. A piece of paper, with a black cross, was cut to the same size as the gel and was placed in the hole to facilitate focusing. The Trans UV option on the imager and the UV Trans option in the acquisition window were selected and the image oriented and focused. The live/focus option was selected; the iris was closed until the cross on the paper came into focus and adjusted with the near/far or wide/narrow options. The piece of paper was removed and the Coomassie stained gel was placed on UV plate converter. The gel image was viewed through live/focus, freezed, then captured using the auto exposure option and saved.

2.8 Western blot analysis

Western blot analysis is a method used to identify and quantify specific proteins of interest. Proteins are separated according to their size using SDS-PAGE and thereafter transferred to a membrane, usually nitrocellulose or PVDF membranes, using an electrical current. Membranes are incubated with a primary antibody to detect the protein of

interest, followed by incubation with a secondary antibody coupled to horse radish peroxidase (HRP) to facilitate detection. Addition of a chemiluminescent substrate allows visualisation of proteins of interest. The detection signal is directly proportional to the concentration of the protein on the membrane.

2.8.1 Transfer

After SDS-PAGE electrophoresis, proteins were transferred to PVDF membranes using the Mini Trans-Blot Cell system (BioRad, USA). PVDF (Millipore, USA) membranes and Whatman paper (Whatman Ltd, UK) were cut according to the size of gel. The membrane was activated by gently shaking in 100% (v/v) methanol for 1 minute followed by 5 minutes in distilled water. Membranes, fibre pads, Whatman paper and gels were equilibrated by gently shaking in transfer buffer (25 mM Tris, 192 mM Glycine, 20% (v/v) methanol) for 20 minutes. The transfer sandwich was assembled by opening the transfer cassette, placing the black negative side face down in a container with transfer buffer, followed by the fibre pad, Whatman paper, gel, PVDF membrane, Whatman paper, fibre pad and then closed with the white positive side of the cassette. A roller bar was rolled over the transfer sandwich at each step to ensure that no air bubbles were trapped in the sandwich. Air bubbles hinder the transfer of proteins from the gel to the PVDF membrane.

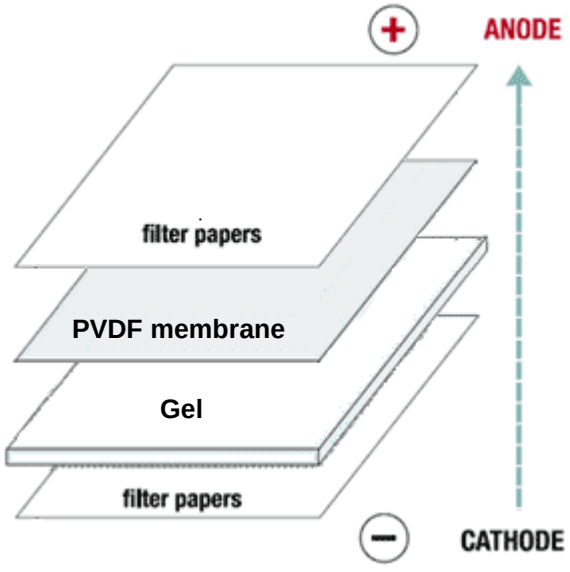

Figure 9. Diagrammatic illustration of Western blot transfer sandwich.

Transfer cassettes were placed between the electrodes of the Mini Trans-Blot Cell system according to manufacturer's instructions, black to black and red to red. An ice pack frozen at -20˚C was placed next to the black side of sandwich and a magnetic stirrer bar was added to the electrophoresis unit. The ice pack is used to ensure that the transfer system does not heat up due to the high voltage of electricity used, as well as to prevent degradation of proteins being transferred. The unit was filled with transfer buffer and placed on a magnetic stirrer (Sigma-Aldrich, USA). Proteins were allowed to transfer at 30-40 V overnight or at 160 V for 2 hours at room temperature.

After transfer, the cassette was disassembled and the protein side of the PVDF membrane was marked with a pencil. The membrane was stained with Ponceau stain (Sigma-Aldrich, USA) for five minutes then rinsed with distilled water to destain. Images were captured using the Bio-Rad ChemiDoc™ XRS+ image illuminator and Quantity One software. Imaging was performed as described in section 2.6, with the exception that the White Epi illumination options was selected on the scanner and in the acquisition window. The UV plate converter was also removed from the imager. The iris of imager camera was closed by using the open/close function in the acquisition window. The Ponceau stained blot was viewed through live/focus, freezed, then captured using the auto exposure option and saved. After imaging, membranes were washed with 1x Tris-buffered saline, pH 7.6 containing 0.2% (v/v) Tween-20 (TBST) until the Ponceau stain was removed. Ponceau stain is a rapid reversible protein staining method and does not have any deleterious effects on subsequent steps (Sigma-Aldrich, USA).

2.8.2 Blocking

PVDF membranes were blocked with 5% (w/v) non-fat milk powder (Elite Clover, SA) in TBST for 7 hours. Blocking of membranes is essential to prevent the non-specific binding of the detection antibody to other proteins or binding sites.

2.8.3 Primary antibody

After blocking the membrane, antibodies specific to the protein of interest were added to the membrane. The antibodies used in the study are indicated in Table 2. Antibodies were diluted in TBST according to the manufacturer's instructions. Membranes were placed in 50 ml skirted tubes and the antibody solution overlaid in the section of the membrane where the antibody of interest is expected to bind. Tubes were positioned on a shaker (Stuart, UK) in a cold room at 4ºC overnight for 16 to 17 hours.

Table 2. Primary antibodies used in study

Antibody	Source	Type	Dilution
pAMPK	Rabbit	mAb†	1:500
AMPK	Rabbit	pAb‡	1:1000
ACC	Rabbit	mAb†	1:1000
UCP2	Goat	mAb†	1:2500
PPARγ	Rabbit	mAb†	1:1000
PRARα	Rabbit	pAb‡	1:1000
β-tubulin	Rabbit	pAb‡	1:1000
β-actin	Mouse	mAb†	1:250

†Monoclonal antibody, produced in a single B-lymphocyte generating antibodies to one specific epitope on antigen

‡Polyclonal antibody, produced by multiple B-lymphocytes generating antibodies to target various epitopes on antigen

2.8.4 Secondary antibody

The following day, membranes were washed with TBST for 3x 15 seconds, then 1x 15 minutes and again for 3x 5 minutes. After washing, membranes were incubated with host specific secondary antibody (Table 3), in 2.5% (w/v) non-fat milk powder in TBST for 90 minutes at room temperature with shaking on a belly dancer (StoVoll, USA).

Table 3. Secondary antibodies used in study

Antibody	Source	Dilution
Mouse HRP IgG	Donkey	1:4000
Rabbit HRP IgG	Donkey	1:4000
Goat HRP IgG	Donkey	1:4000

Secondary antibodies, specific to the primary antibodies used, were labelled with horseradish peroxidase to facilitate detection.

2.8.5 Protein detection

Membranes were washed as described previously, and incubated with LumiGLO Chemiluminescent Substrate Kit (KPL, USA) for 1 minute. LumiGlo chemiluminescent solution was prepared an hour in advance as to the manufacturer's instructions, by mixing one part solution A (luminal solution) with two parts solution B (reaction buffer) and left at room temperature for 1 hour to acclimatise. Proteins of interest were then detected with the Bio-Rad ChemiDoc^{TM} XRS^{+} image illuminator and Quantity One software.

Imaging was performed as described in section 2.6, with the exception that the Epi-White switch on the imager and the Chemi Hi Sensitivity option in the acquisition window of the software was selected. The iris of the camera was completely opened until the black cross on the paper disappeared and the BioRad logo with lanes on the ruler became visible through live/focus. The camera lens was focused near/far or wide/narrow to obtain a clear image of BioRad logo and the lanes on the ruler. The piece of paper and ruler was then removed and the blot placed in the centre of A4 sheet on the glass plate. The blot was brought into focus and the Epi-White switched off on the imager. The live acquire option

was selected with a total exposure time of 1 to 2 minutes with 10 sec intervals. Images acquired were saved for quantification and analysis.

2.8.6 Quantification

Quantification of Western blot images was done using the Quantity One software (BioRad, USA). The Quantity One software programme was opened on the computer desktop. The saved western blot image e.g. pAMPK was opened. The image of the blot was then aligned and cropped to view distinctive linear, protein bands using the crop function in the image tools bar. Protein bands of interest were encircled using the rectangular action tool in the volume tools bar. An empty space on the blot where no protein binding was present was also encircled with the rectangular volumes tool. The empty space was used as a blank to subtract non-specific background binding from the blot image for quantification of protein bands. The volume report option was then selected in the volumes tools bar for the volume density analysis. Results from the volume density report were exported to Microsoft Excel 2003, for further analysis. The total expression of the protein of interest was determined by dividing its band volume density with that of a house keeping protein, β tubulin or β actin. A house keeping protein is expressed at constant levels and is not usually affected by the treatment or experiment.

2.8.7 Stripping

To allow for reprobing of membranes with another protein of interest, PVDF membranes were stripped with 10 ml of stripping buffer (Thermo Scientific, USA) to remove primary and secondary antibody. Stripping buffer was incubated for 15 minutes, the solution decanted and the membrane gently washed in TBST and stored at 4°C. To assess the efficiency of stripping, stripped membranes were incubated with LumiGLO Chemiluminescent Substrate Kit as described previously. This was only done with the first stripping procedure.

2.9 Enzyme-linked immunosorbent assay

The AMPKα [pT172] kit from Invitrogen (Life technologies, USA) is a solid phase sandwich enzyme-linked immunosorbent assay (ELISA). A monoclonal antibody specific

to AMPKα (regardless of its phosphorylation state) has been coated on a microtiter strip. The coated antibody binds to AMPKα protein in tissue lysates, trapping it to the microtiter strip. The addition of an antibody directed at AMPKα phosphorylated at Thr172 binds to the immobilized AMPKα protein if phosphorylated. Addition of an anti-rabbit IgG HRP antibody which binds to the detection antibody completes the four member sandwich as illustrated in Figure 10. Addition of the Tetramethylbenzidine (TMB) substrate will then result in an enzymatic color reaction whose intensity is directly proportional to the concentration of AMPKα phosphorylated at Thr 172 in the sample.

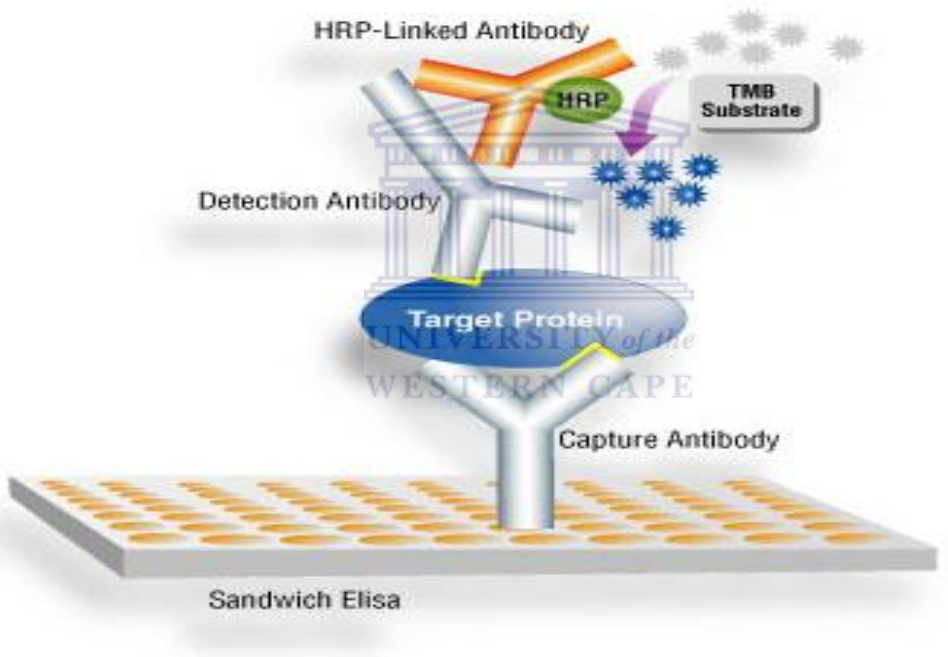

Figure 10. Illustration of the AMPK [pAMPK-T172] double sandwich ELISA.
The capture antibody which is attached to the microtiter plate binds the target protein during incubation with the tissue lysate. Addition of a target specific detection antibody binds to the stationary captured target protein. An HRP-linked antibody is then added to bind and detect the detection antibody. Addition of the TMB substrate results in an enzymatic color reaction which may be detected using a spectrophotometer at a wavelength of 450 nm.

2.9.1 Acclimatization of reagents and solutions

All reagents and buffers were allowed to reach room temperature before use, and thereafter gently mixed. All ELISA reagents are listed in appendix A and the recipes of solutions used listed in appendix B. The desired number of 8 well strips to be used was allowed to reach room temperature and the rest of the strips resealed and stored until required.

2.9.2 Incubation with standards and protein lysate

One hundred microliters of standard diluent buffer was added to the wells to be used, leaving the wells reserved for the chromogenic blank empty as illustrated in Figure 11. One hundred microliters of standards, controls and diluted samples were added to the appropriate microtiter plate wells as illustrated in Figure 11 and mixed by gently tapping the side of plate. Wells were covered with a plate cover and incubated for 2 hours at room temperature at 25ºC. The solution in the microtiter wells was decanted and discarded after incubation. Wells were washed 4 times by flooding with washing solution using a squirt bottle. Thereafter, solutions were decanted and the plate inverted on absorbent tissue to dry.

	1	2	3	4	5	6	7	8	9	10	11	12
A	100	U1	U1	U9	U9	U11	U11					
B	50	U2	U2	U10	U10	U12	U12					
C	25	U3	U3	U19	U19	U13	U13					
D	12.5	U4	U4	U20	U20	U14	U14					
E	6.25	U5	U5			U15	U15					
F	3.16	U6	U6			U16	U16					
G	1.6	U7	U7			U17	U17					
H	0	U8	U8	CB	CB	U18	U18					

Figure 11. Representative 96 well microtiter plate layout for ELISA.
Unknown (U), Chromogenic Blank (CB).

AMPKα standards were pipetted into the wells shaded in dark blue (100 U/ml, 50 U/ml, 25 U/ml, 12.5 U/ml, 6.25 U/ml, 3.16 U/ml, and 1.6 U/ml). The chromogenic blank (CB) was pipetted into wells H4 and H5. To avoid inaccuracies, no more than 20 unknowns (e.g. U1) (Lanes 2-7) was analyzed in duplicate per assay.

2.9.3 Incubation with detection antibody

One hundred microliters of AMPKα [pT172] detection antibody solution was added to each well except for the chromogenic blank well then gently mixed by tapping the side of the plate. The microtiter plate was covered with the plate cover and incubated for 1 hour at room temperature. The solution in the wells was discarded after incubation and the wells were washed 4 times as previously described.

2.9.4 Incubation with HRP anti-rabbit antibody

One hundred microliters of the anti-rabbit IgG HRP working solution was added to each well except for the chromogenic blank wells, and gently mixed by tapping the side of the plate. The microtiter plate was covered with a plate cover and incubated for 30 minutes at room temperature. The solution in the microtiter well strips was discarded after incubation and the wells were washed 4 times as described previously.

2.9.5 Incubation with stabilized chromogenic solution

One hundred microliters of stabilized chromogenic solution was added to each well including the chromogenic blank wells, and gently mixed by tapping the side of the plate. The microtiter plate was covered with a plate cover and incubated for 30 minutes at room temperature.

2.9.6 Incubation with stop solution and detection at 450 nm

One hundred microliters of stop solution was added to each well and gently mixed by tapping the side of the plate. The color of the solution in the wells changed from blue to yellow. The absorbance of each well was read 30 minutes after the addition of the stop solution at 450 nm using a spectrophotometer (BioTek, USA). Data was exported to Excel (Microsoft Office, Version 2003) for analysis.

2.9.7 Quantification

A standard curve was plotted using the known pAMPK standards (x axis) against their corresponding optical density readings (y axis) in Microsoft Excel using the scatter plot diagram option. Phosphorylated AMPK expression in samples were determined by solving for x using the linear regression equation (y=mx+c) provided with the standard curve in Excel.

2.10 Histological analysis of retroperitoneal fat pads

Histology is the study of the microscopic anatomy of cells and tissues of plants and animals. It entails the sectioning of tissue biopsies, their staining and observational analysis by microscopy. Haematoxylin and eosin is the most commonly used stains, providing contrast to tissues for visualisation as well as highlighting particular features of interest. Haematoxylin is a cationic or basophilic dye binding to negatively charged tissue ions such as chromatin in the nucleus. Eosin is an anionic or acidophilic dye binding to positively charge tissue ions such as the amino groups of proteins, cytoplasm. Adipocytes appear as translucent vacuoles surrounded by a thin cytoplasmic rims when H&E stained (Figure 12).

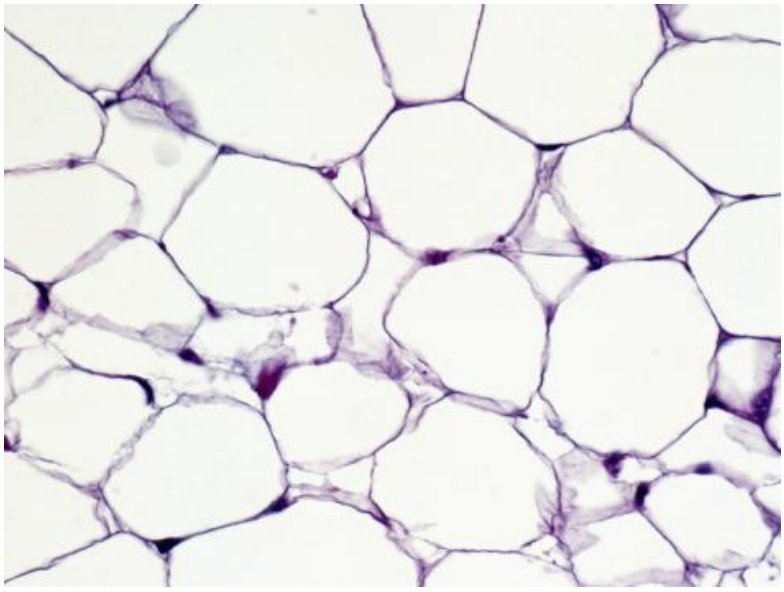

Figure 12. Representative picture of H&E straining of retroperitoneal fat.

Histology of retroperitoneal fat (RF) pads was done to determine the effect of *C. maculata* on adipocyte size and number. Retroperitoneal fat is an important visceral fat depot store. The retroperitoneal fat depot is sensitive to the storage and release of fatty acids, thereby influencing their morphology and cell number (Bjørndal *et al*., 2011).

2.10.1 Slide preparation and dewaxing

Retroperitoneal fat biopsies from Wistar rats (Patel, 2012) were fixed in 4% (v/v) buffered formalin and embedded and preserved in paraffin wax blocks. Tissue was dissected into 1 millimeter sections and wet mounted onto glass slides. Slides were placed on slide racks and incubated at 60˚C for approximately 30 minutes or until most of the wax surrounding the sections had melted away. The tissue sections on the slides were de-waxed by placing in xylene (Merck, USA) for 10 minutes, then placed in a second container with xylene for another 10 minutes. The tissue was hydrated by placing in 95% (v/v) ethanol twice for 2 minutes followed by rinsing by 20 dips in water.

2.10.2 Haematoxylin staining

The slides were stained in Haematoxylin solution for 12 minutes, followed by a 10 dip wash in water. The slides were then immersed in a container with running tap water to induce “Bluing” of the stained tissue sections. Bluing is the process of converting the initially red soluble hemalum to a final insoluble blue form. Slides were then rinsed by a 10 dip wash in water.

2.10.3 Eosin staining

The slides were stained in 1% (w/v) Eosin solution for 5 minutes, followed by a 10 dip wash in water. The slides were hydrated by dipping 20 times in 95% (v/v) ethanol, followed by another 20 dips in 100% (v/v) ethanol.

2.10.4 Mounting of cover slip

Slides were dipped 20 times in xylene and then left in xylene for mounting of the cover slip. Mounting was done by adding one drop of Entallen (Merck, Germany) onto the slide

followed by the cover slip. Mounting preserves the integrity of the stained tissue as well as making it transparent, making examination of the slides easier.

2.10.5 Image capturing and analysis

Images of slides were captured with x20 magnification and 10 fields per section were captured using an Olympus BX50 light microscope (Olympus, Japan) interfaced with NIS-Element BR 3.0 software (Nikon instruments Inc, USA).

2.10.6 Quantification of images

The adipocyte sizes were measured with the Leica Qwin pro version 3 (Leica Microsystems, Germany) image analysis software program. The adipocyte cell sizes were expressed as mean arbitrary units per 10 fields. The Grubb's test (Graphpad Prism, USA) was used to detect outliers (http://graphpad.com/quickcalcs/grubbs2.cfm).

2.11 Statistical analysis

Data analysis was performed in Microsoft Excel (Microsoft Office version 2010, USA). Results are expressed as the mean ± standard error of the mean (SEM). The SEM was calculated by dividing the standard deviation (calculated by Microsoft Excel) by the square root of the number of samples analyzed. Statistical analysis was performed using GraphPad Prism (Version 5.01, USA). The two-tailed unpaired t-tests, corrected for by the Welch's correction, was used to compare two groups, while the one way analysis of variance (ANOVA) with a Tukey post doc test was performed to determine any statistical significant variation between groups. A p-value of <0.05 was considered statistically significant.

Chapter 3

Results

3. Results

3.1 Protein extraction

3.1.1 Optimization

SDS-PAGE of proteins extracted using the in-house lysis buffer and the TissueLyser showed smearing, suggesting protein degradation, contamination with cellular debris and salts, incorrect pH of buffers or incorrect gel pouring (Figure 13). To improve the purity of protein lysates, acetone precipitation, a technique that is used to remove chemicals and salts from protein samples (Rinderknecht *et al.,* 1939), was conducted. At low temperatures, proteins are insoluble in acetone while other chemicals and salts are soluble and precipitate out of lysates after high speed centrifugation (Rinderknecht *et al.,* 1939). Our results showed that although acetone precipitation improved protein quality, a loss of high and low molecular weight proteins was observed (Figure 14). In an attempt to improve protein quality without affecting protein yield, protein extraction was compared using two different lysis buffers (in-house buffer vs. commercial buffer) and two different homogenization methods (TissueLyser vs. Polytron).

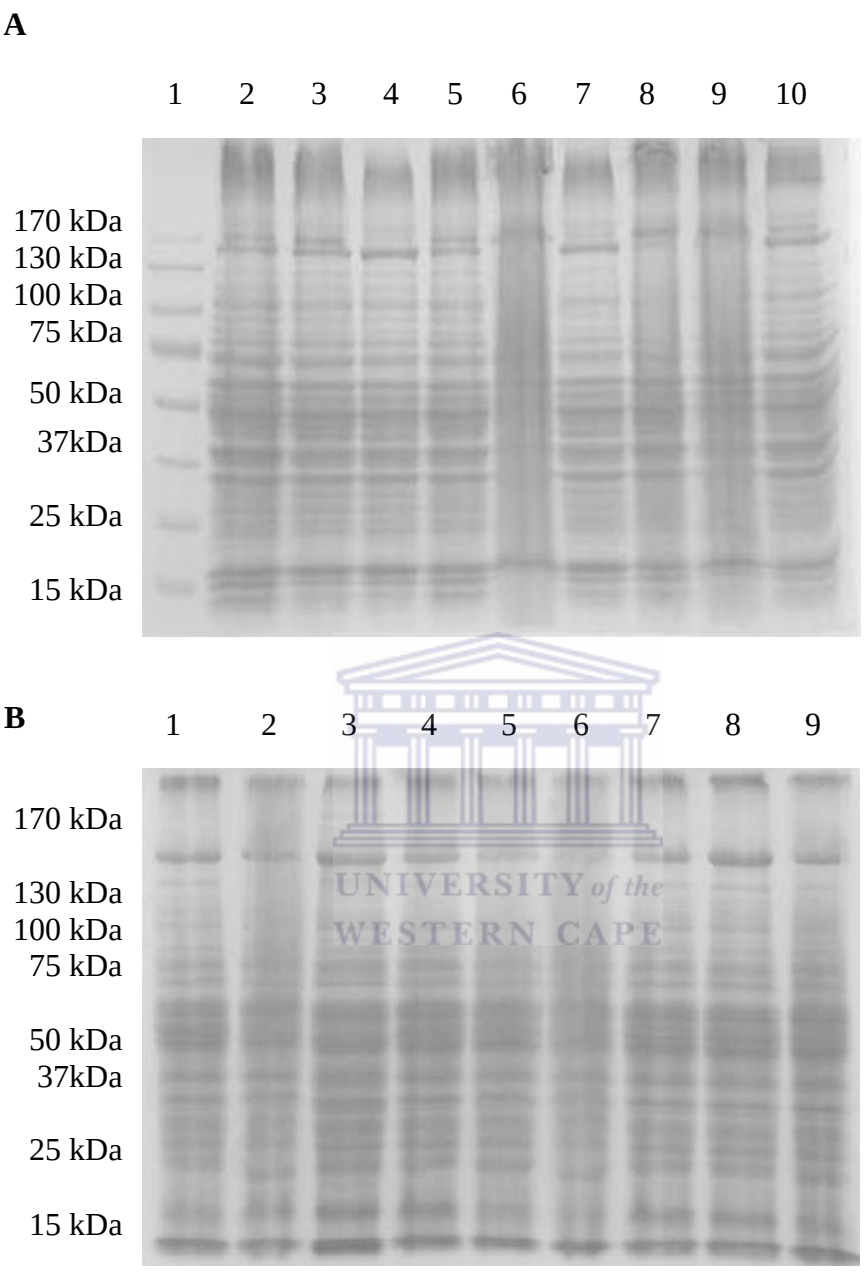

Figure 13. SDS PAGE of proteins before optimization.

Proteins were extracted from the liver of lean (**A, lanes 2-10**) and obese (**B, lanes 1-9**) rats using the in-house lysis buffer and the TissueLyser. Thereafter 10 µg of protein was separated by 10% SDS PAGE. The prestained protein ladder is indicated in lane 1 (A).

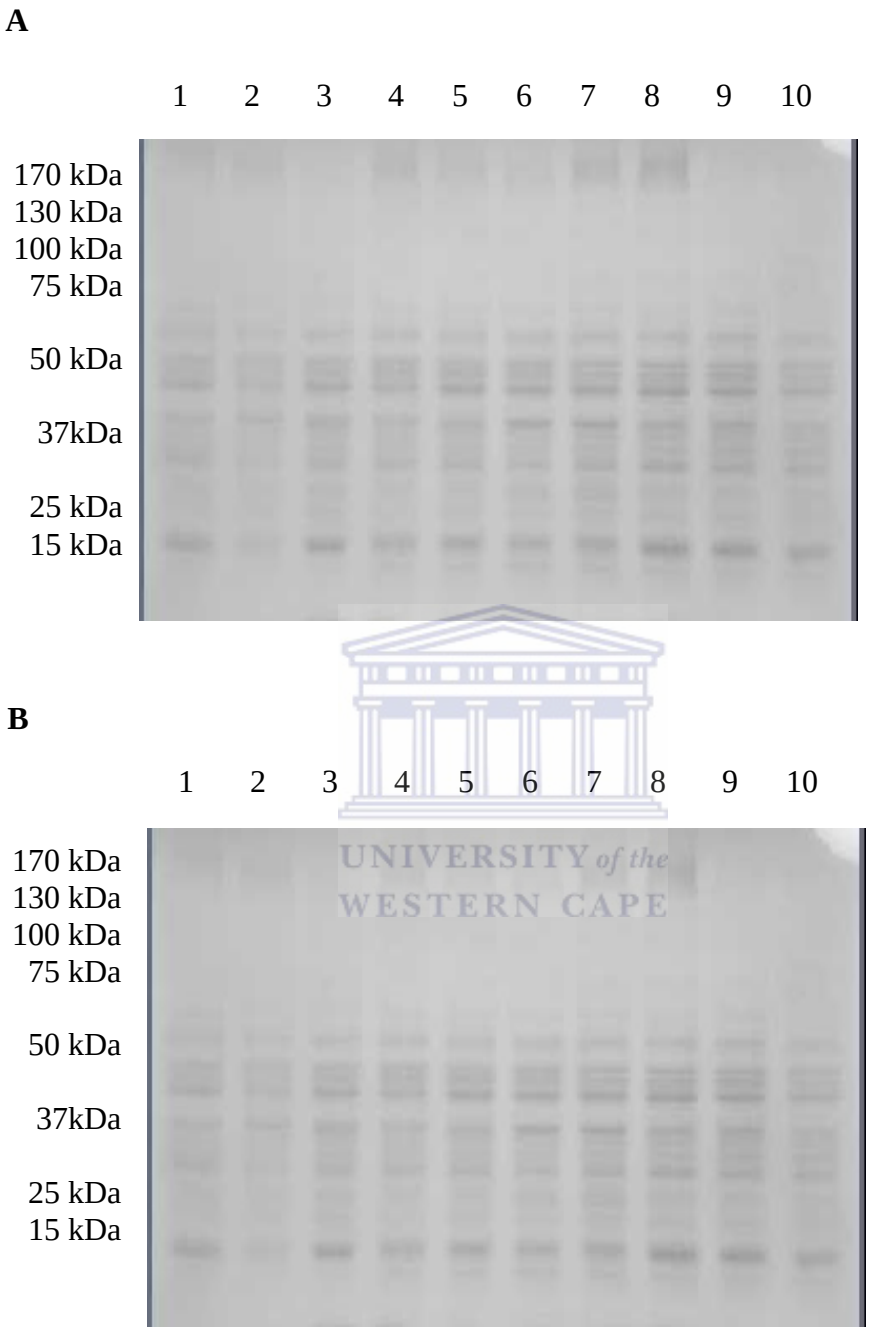

Figure 14 SDS PAGE of proteins after acetone precipitation.

Proteins were extracted from the liver of lean (**A, lanes 1-10**) and obese (**B, lanes 1-10**) rats using the in-house lysis buffer and the TissueLyser. Thereafter proteins were purified by acetone precipitation and 10 µg of protein was separated by 10% SDS PAGE.

3.1.1.1 Protein concentration

Protein concentrations were determined using the RC DC kit. As illustrated in Figure 15, high correlation coefficients (R^2) were obtained when using the in-house (0.996) and the commercial (0.994) lysis buffer as BSA diluents, thus supporting the use of these curves for protein concentration determination using the linear equation:

$$y=mx + c$$

y=absorbance, m=gradient, x=concentration and c=y-intercept.

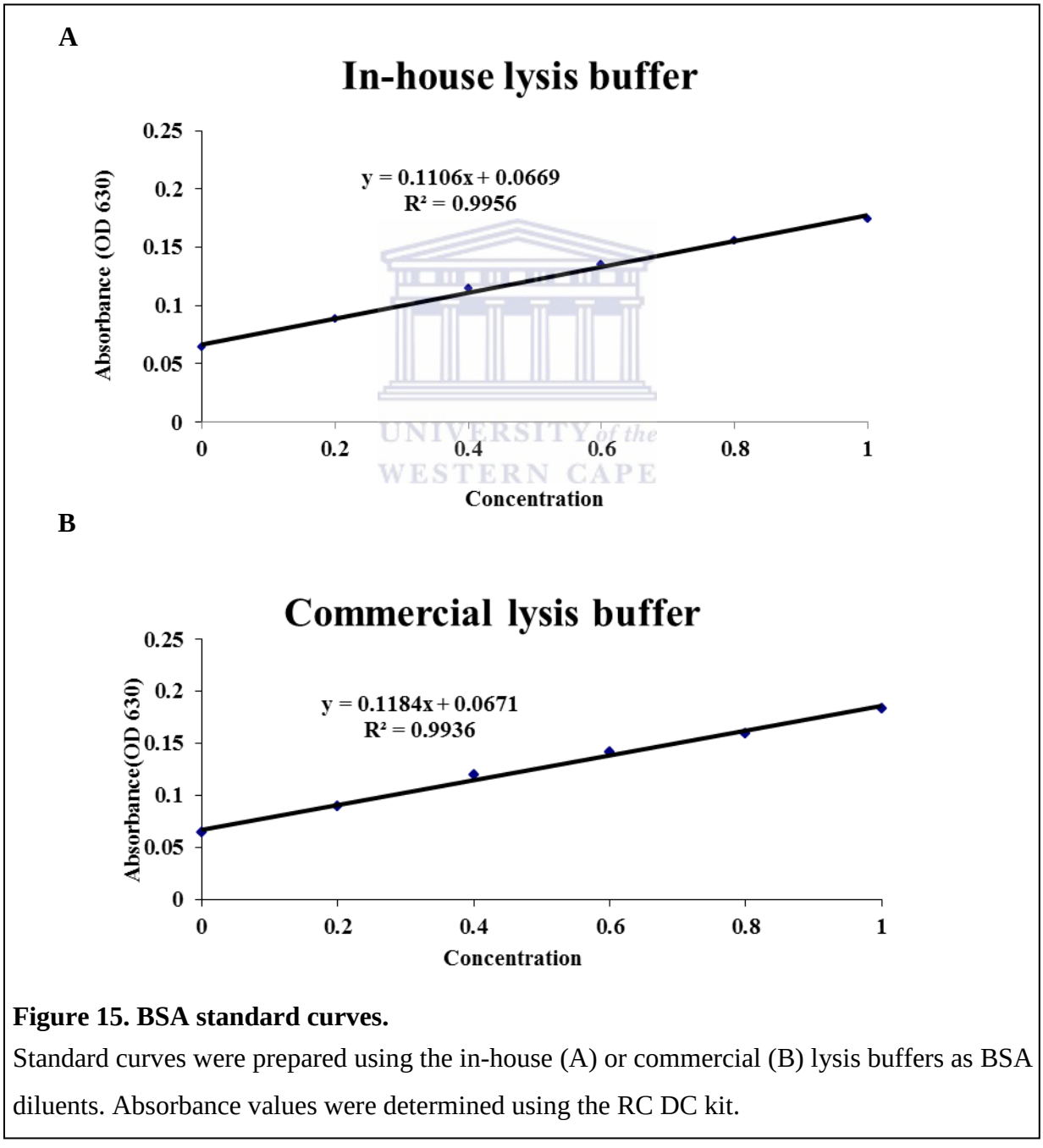

Figure 15. BSA standard curves.

Standard curves were prepared using the in-house (A) or commercial (B) lysis buffers as BSA diluents. Absorbance values were determined using the RC DC kit.

3.1.1.2 Protein yield

The total yield of proteins extracted using the two different extraction procedures was calculated. Protein yield varied according to tissue type, lysis buffer and homogenization method (Table 4, Figure 16).

The yield of proteins extracted from liver samples using the commercial lysis buffer was increased compared to the in-house lysis buffer, irrespective of homogenization method used (Polytron 44.60 ± 4.60 vs. 28.41 ± 6.02 (1.6-fold (p=0.0208)); TissueLyser 69.36 ± 10.83 vs. 36.48 ± 6.89 (1.9-fold (p=0.0114)).

For muscle samples, no significant differences in protein yield was observed when comparing the two different lysis buffers and the two homogenization methods (Table 4, Figure 16). Even though similar tissue weights used for protein extraction (100 mg), the protein yield of muscle samples were significantly lower than that of liver samples when comparing the same protein extraction procedures (commercial lysis buffer and Polytron 10.98 ± 0.98 vs. 44.60 ± 4.60 (4.1-fold (p=0.0002)); commercial lysis buffer and TissueLyser 11.27 ± 1.19 vs. 69.36±10.83 (6.2-fold (p=0.0008)); in-house lysis buffer and Polytron 11.64 ± 3.68 vs. 28.41±6.02 (3.2-fold (p=0.0146); in-house lysis buffer and TissueLyser 8.80 ± 1.16 vs. 36.48 ± 6.89 (4.2 fold (p=0.0024)).

Table 4. Protein concentration and yield after optimization.

Tissue	Lysis buffer	Homogenization	Sample	No	Concentration (mg/ml)	Total Yield (mg)
Liver	Commercial	Polytron	D71	1	61.64	49.31
			B51	2	50.15	40.12
			B53	3	55.47	44.38
			Average		**55.75**	**44.60 ± 4.60*$^{###}$**
		TissueLyser	D71	4	81.74	65.39
			B51	5	102.01	81.61
			B53	6	76.33	61.07
			Average		**86.69**	**69.36± 10.83$^{ǂ\$\$\$}$**
	In-house	Polytron	D71	7	42.36	33.89
			B51	8	36.73	29.38
			B53	9	27.45	21.96
			Average		**36.45**	**28.41 ± 6.02*^{ψ}**
		TissueLyser	D71	10	36.45	29.16
			B51	11	53.55	42.84
			B53	12	46.82	37.45
			Average		**45.61**	**36.48 ± 6.89^{ǂ††}**
Muscle	Commercial	Polytron	D71	13	15.02	12.01
			B51	14	12.57	10.05
			B53	15	13.58	10.86
			Average		**13.72**	**10.98 ± 0.98$^{###}$**
		TissueLyser	D71	16	15.78	12.62
			B51	17	13.50	10.80
			B53	18	12.99	10.39
			Average		**14.09**	**11.27 ± 1.19$^{\$\$\$}$**
	In-house	Polytron	D71	19	12.45	9.96
			B51	20	19.82	15.85

			B53	21	11.36	9.09
			Average		**14.55**	**11.64 ± 3.68$^{\Psi}$**
		TissueLyser	D71	22	11.00	8.80
			B51	23	9.55	7.64
			B53	24	12.45	9.96
			Average		**11.00**	**8.80 ± 1.16††**

Proteins were extracted from liver and muscle samples using the commercial or in-house lysis buffers and the Polytron or TissueLyser. Concentrations were determined using the RC DC kit and protein yield was calculated by multiplying the concentration obtained by the final volume. Results are expressed as the mean ± standard error of mean.
*Commercial lysis buffer and Polytron vs. In-house lysis buffer and Polytron
ǂCommercial lysis buffer and TissueLyser vs. In-house lysis buffer and TissueLyser
$^{\#}$Commercial lysis buffer and Polytron: liver vs. muscle
$^{\$}$Commercial lysis buffer and TissueLyser: liver vs. muscle
$^{\Psi}$In-house lysis buffer and Polytron: liver vs. muscle
†In-house lysis buffer and TissueLyser: liver vs. muscle
*$^{ǂ\Psi}$P value < 0.05, ††P value < 0.01, $^{\#\#\#,\$\$\$}$P value < 0.001.

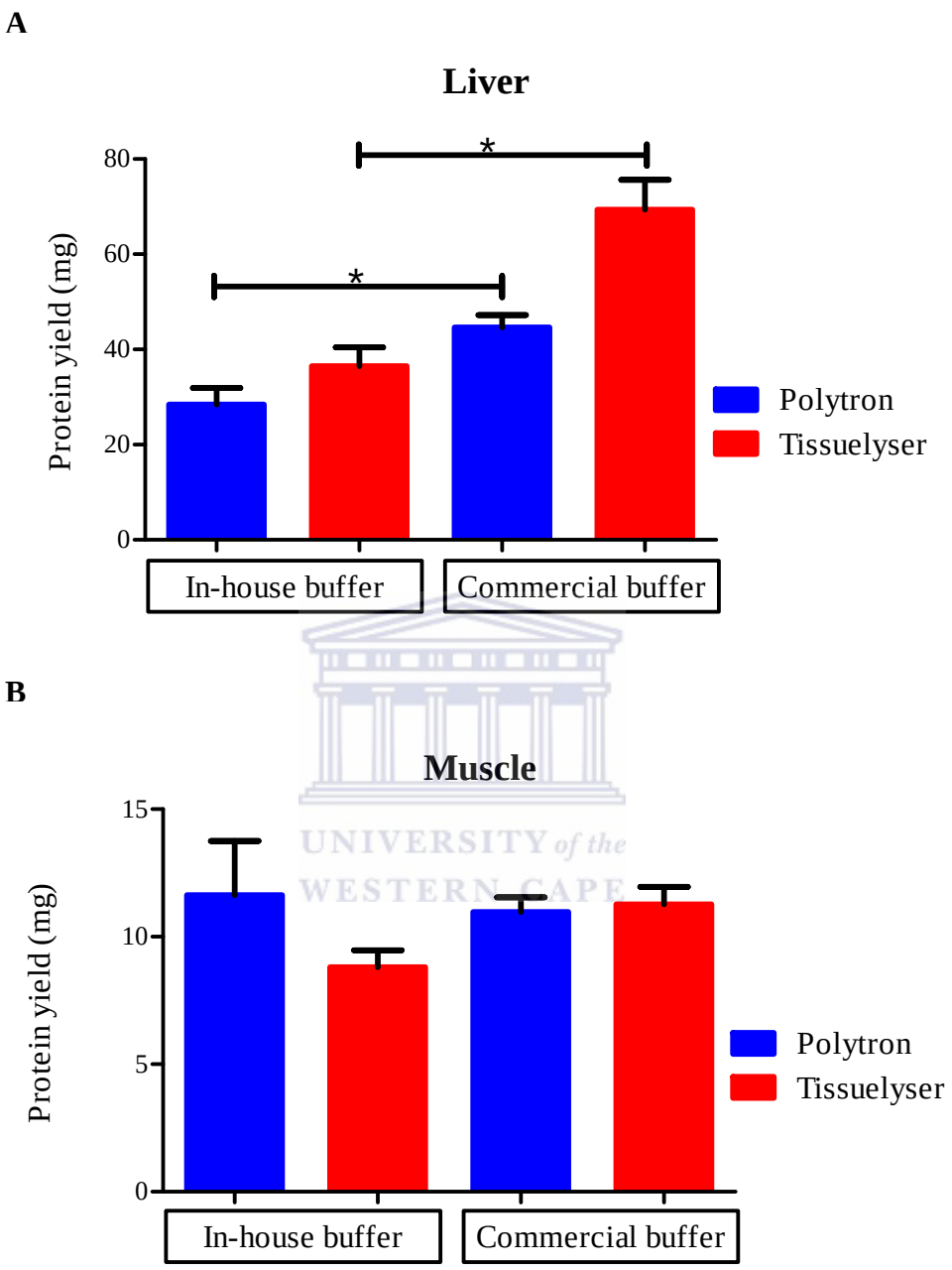

Figure 16. Graphical representation of protein yield after optimization.
Proteins were extracted from liver (**A**) and muscle (**B**) tissue using two different lysis buffers (in-house vs. commercial) and two different homogenization methods (Polytron vs. TissueLyser). Protein yield was determined by multiplying the concentrations obtained by the total volume. Results are expressed as the mean ± standard error of mean. * $p < 0.05$.

3.1.1.3 Protein profiling

To visually examine the quality of the proteins extracted using the different optimization conditions, 10 µg or 60 µg of protein was separated by 10% SDS-PAGE (Table 5 and 6 respectively), stained with Coomassie blue and visualized with the ChemiDoc illuminator. A low (10 µg) and a high (60 µg) concentration of protein was used to investigate whether protein amount affected banding patterns. No difference in protein profiles were observed in liver samples, irrespective of the lysis buffer or homogenization method used and the amount loaded (Figures 17 and 19). Muscle proteins that were extracted using the commercial lysis buffer, regardless of whether the Polytron or TissueLyser was used, displayed more low and high molecular weight protein bands compared to proteins extracted using the in-house lysis buffer (Figures 18 and 20).

Table 5. Volumes of proteins (10 µg) for SDS-PAGE profiling.

Sample No.	Protein concentration	Volume† used (µl)	Volume† water (µl)	2x Sample buffer (µl)	Volume for gel‡ (µl)	Tissue type
1	61.64	1	9	10	3.2	liver
2	50.15	1	9	10	4.0	liver
3	55.47	1	9	10	3.6	liver
4	81.74	1	9	10	2.4	liver
5	102.01	1	9	10	2.0	liver
6	76.33	1	9	10	2.6	liver
7	42.36	1	9	10	4.7	liver
8	36.73	1	9	10	5.4	liver
9	27.45	1	9	10	7.3	liver
10	36.45	1	9	10	5.5	liver
11	53.55	1	9	10	3.7	liver
12	46.82	1	9	10	4.3	liver
13	15.02	1	9	10	13.3	muscle
14	15.78	1	9	10	15.9	muscle
15	13.50	1	9	10	14.7	muscle
16	12.99	1	9	10	12.7	muscle
17	15.78	1	9	10	14.8	muscle
18	13.50	1	9	10	15.4	muscle
19	12.45	1	9	10	16.1	muscle
20	11.00	1	9	10	10.1	muscle
21	9.55	1	9	10	17.6	muscle
22	12.45	1	9	10	18.2	muscle
23	11.00	1	9	10	21.0	muscle
24	9.55	1	9	10	16.1	muscle

†Protein samples were diluted 1:10 to facilitate loading onto the gel.
‡A volume equal to 10 µg of protein and an equal volume of 2x sample buffer was loaded onto gels.

Table 6. Volumes of proteins (60 µg) for SDS-PAGE profiling.

Sample No.	Starting concentration (µg/µl)	For 120 µg† (µl)	2x Sample buffer (µl)	Volume (60 µg)for gel‡ (µl)	Tissue type
1	61.64	1.9	1.9	1.9	liver
2	50.15	2.4	2.4	2.3	liver
3	55.47	2.1	2.1	2.1	liver
4	81.74	1.4	1.4	1.4	liver
5	102.01	1.2	1.2	1.2	liver
6	76.33	1.5	1.5	1.5	liver
7	42.36	2.8	2.8	2.8	liver
8	36.73	3.2	3.2	3.2	liver
9	27.45	4.3	4.3	4.3	liver
10	36.45	3.3	3.3	3.3	liver
11	53.55	2.2	2.2	2.2	liver
12	46.82	2.5	2.5	2.5	liver
13	15.02	8	8	8	muscle
14	15.78	9.5	9.5	9.5	muscle
15	13.50	8.8	8.8	8.8	muscle
16	12.99	7.6	7.6	7.6	muscle
17	15.78	8.9	8.9	8.9	muscle
18	13.50	9.2	9.2	9.2	muscle
19	12.45	9.6	9.6	9.6	muscle
20	11.00	6.0	6.0	6.0	muscle
21	9.55	10.5	10.5	10.5	muscle
22	12.45	10.9	10.9	10.9	muscle
23	11.00	12.5	12.5	12.5	muscle
24	9.55	9.6	9.6	9.6	muscle

†120 µg of protein was used to prepare the mixture for loading in case of protein loss during pipetting

‡ The half (60 µg) was loaded onto the gel.

A

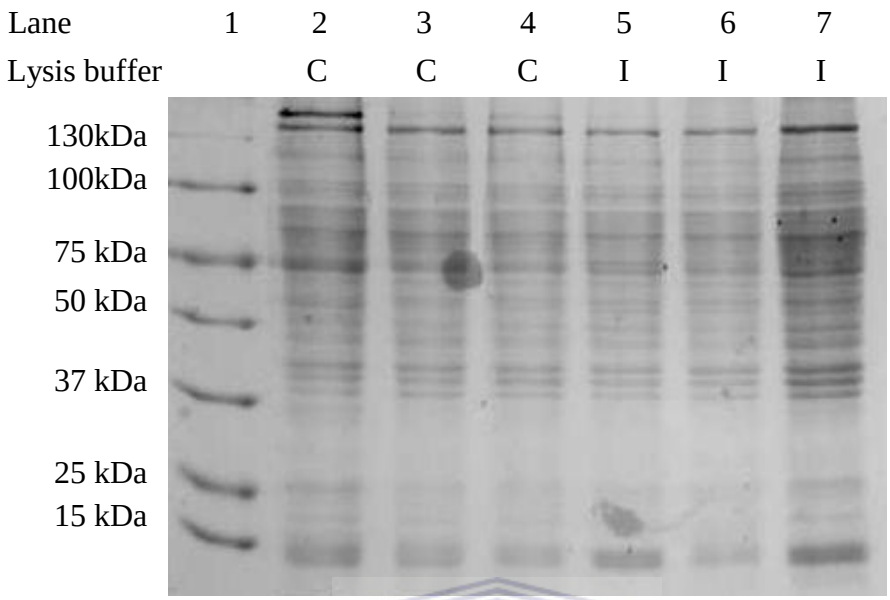

B

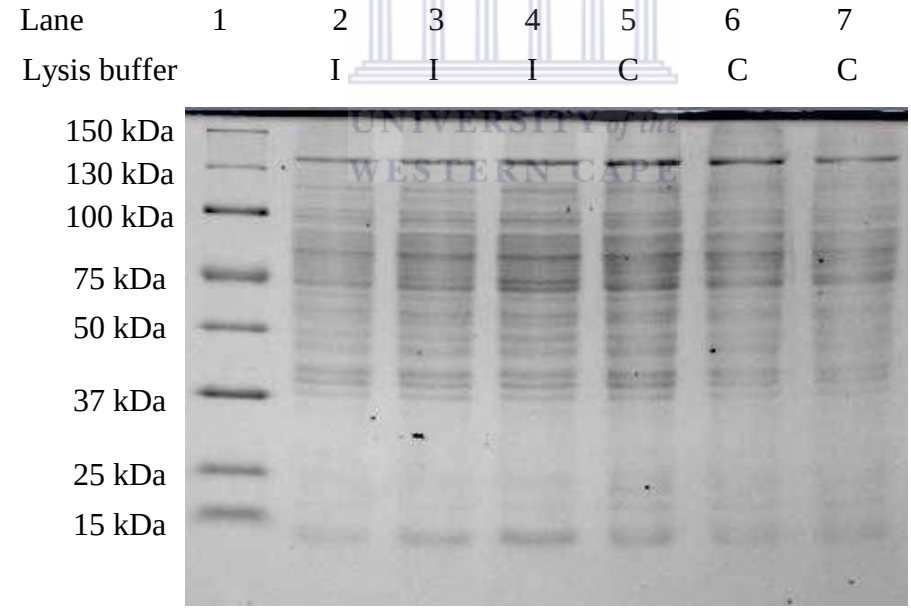

Figure 17. SDS-PAGE using 10 µg of liver protein.

Proteins were extracted from liver tissue using a commercial (C) or an in-house (I) lysis buffer and homogenized with the Polytron (**A**) or the TissueLyser (**B**). Lane 1, Protein ladder, Lanes 2-7 protein lysates.

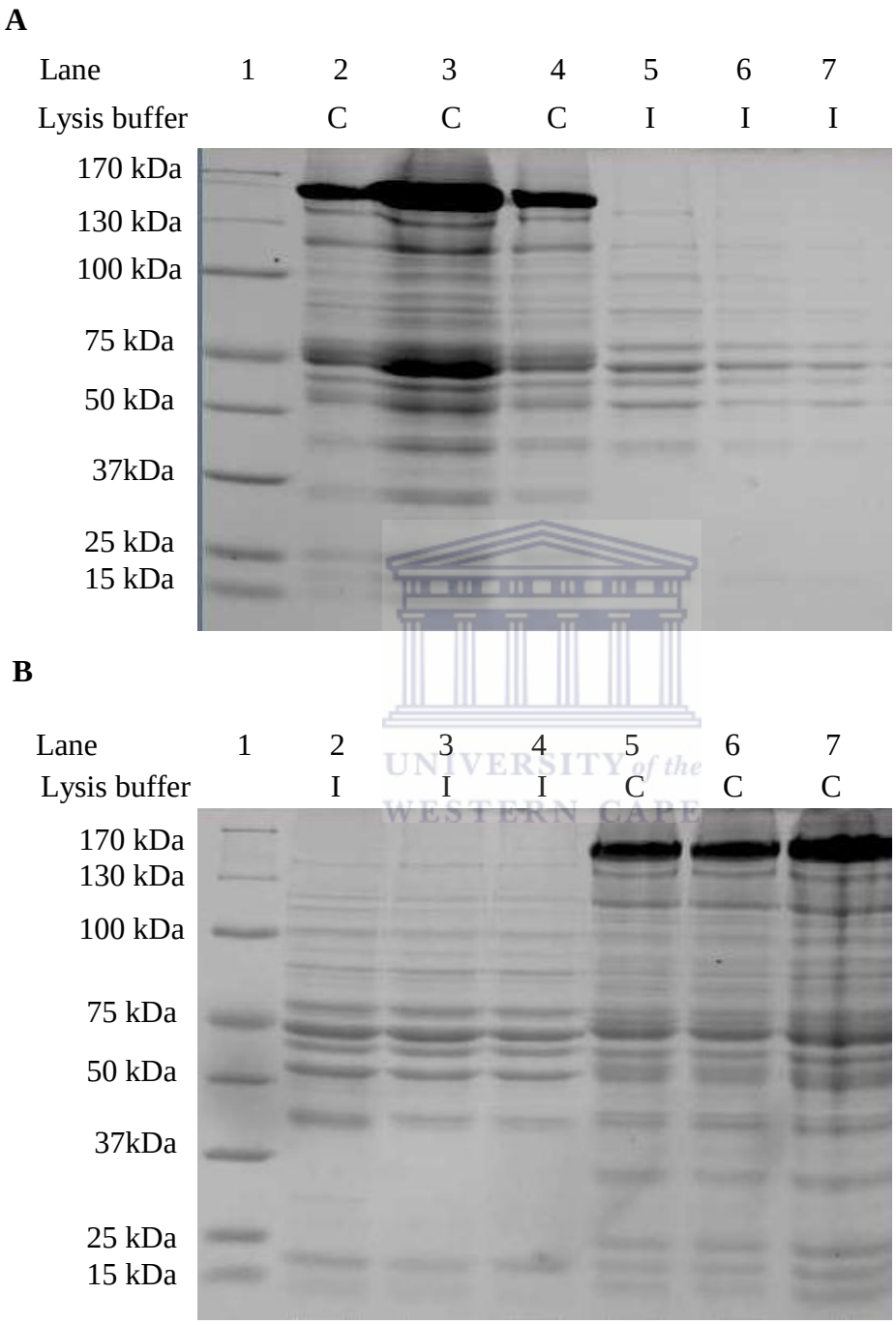

Figure 18. SDS-PAGE using 10 µg of muscle protein.

Proteins were extracted from muscle tissue using a commercial (C) or an in-house (I) lysis buffer and homogenized with the Polytron (**A**) or the TissueLyser (**B**). Lane 1, Protein ladder, Lanes 2-7 protein lysates.

A

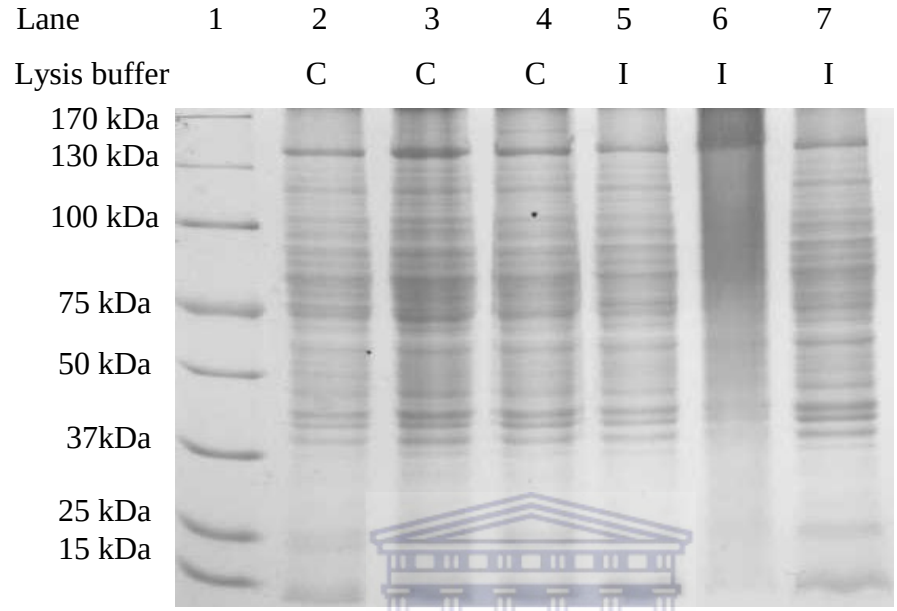

B

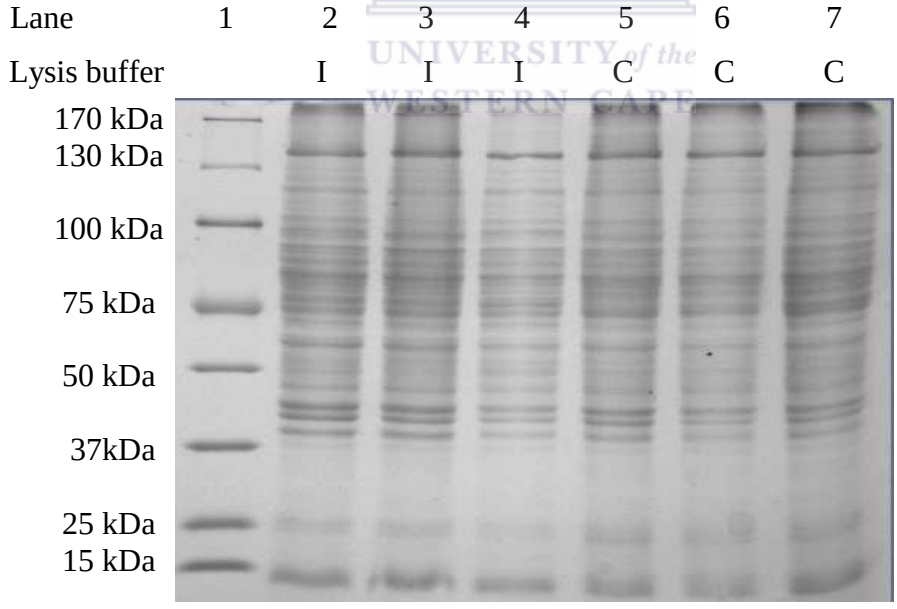

Figure 19. SDS-PAGE using 60 µg of liver protein.

Proteins were extracted from liver tissue using a commercial (C) or an in-house (I) lysis buffer and homogenized with the Polytron (**A**) or the Tissue Lyser (**B**). Lane 1, Protein ladder, Lanes 2-7 protein lysates.

A

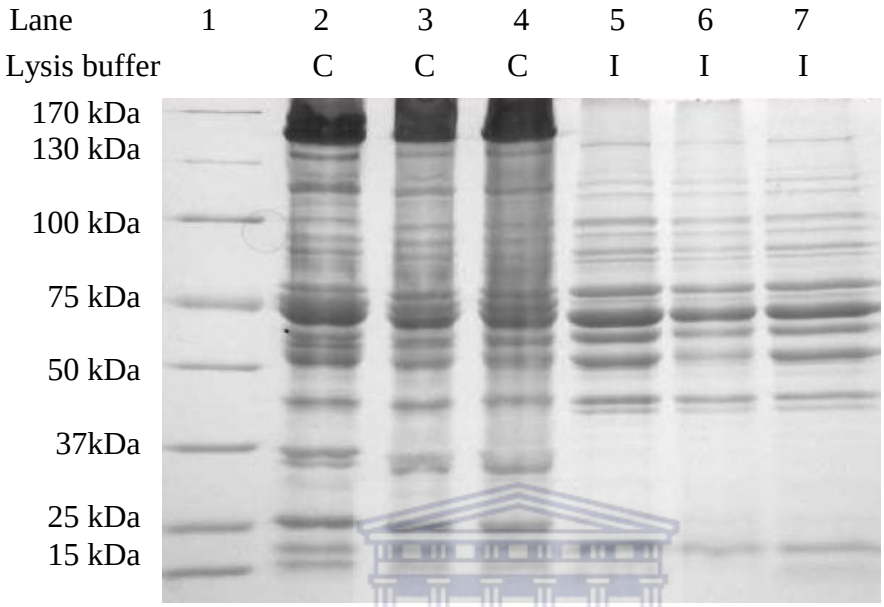

B

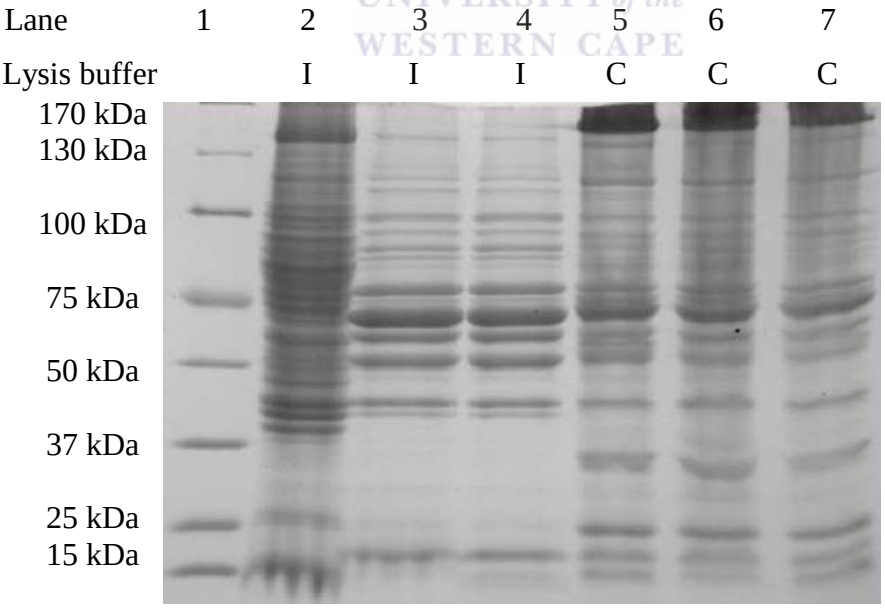

Figure 20. SDS-PAGE using 60 µg of muscle protein.

Proteins were extracted from muscle tissue using a commercial (C) or an in-house (I) lysis buffer and homogenized with the Polytron (**A**) or the Tissue Lyser (**B**). Lane 1, Protein ladder, Lanes 2-7 protein lysates.

3.1.1.4 Selection of protein extraction conditions

We decided to use the commercial lysis buffer and homogenization with the TissueLyser for the extraction of proteins from liver and muscle tissues of experimental samples. This extraction method yielded the highest amounts of proteins in the liver and demonstrated more high and low molecular weight proteins in muscle compared the other methods used.

3.2 Western blot analysis

Western blot analysis was performed to determine if *C. maculata* affects AMPK activation, as demonstrated for other phytochemicals with anti-obesity effects (Kim *et al*., 2008; Niu *et al*., 2012; Steinberg and Kemp, 2009). Proteins from lean and obese Wistar rats that were fed a cafeteria diet (CD) for three months, with or without *C. maculata* treatment, were analyzed.

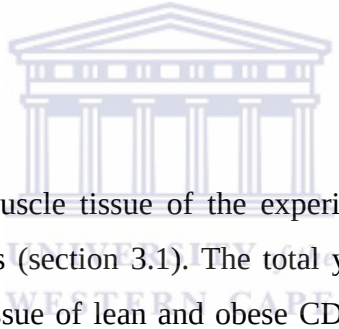

3.2.1 Protein extraction

Proteins from the liver and muscle tissue of the experimental samples were extracted using the optimized procedures (section 3.1). The total yield of proteins extracted from 100 mg of liver and muscle tissue of lean and obese CD-fed untreated and *C. maculata* treated rats is indicated in Table 7 and Figure 21.

Cyclopia maculata treatment had no effect on hepatic protein content of lean and obese rats (Table 7, Figure 21). Interestingly protein content was 2.4-fold higher ($p<0.001$) in obese rats compared to lean rats (untreated 26.0 ± 2.2 vs. 11.5 ± 0.6; treated 27.9 ± 2.3 vs. 11.0 ± 0.8).

Cyclopia maculata treatment similarly had no effect on muscle protein content of lean and obese rats (Table 7, Figure 21). Furthermore, although protein yield was increased in obese compared to lean rats (untreated 29.4 ± 2.3 vs. 26.8 ± 2.5; treated 30.3 ± 3.6 vs. 25.7 ± 3.7), the difference was not significant.

Table 7. Protein yield of liver and muscle tissue.

	Protein Yield (mg)			
	Non-obese		Obese	
	CD (n=10)	CD + *C. maculata* (n=10)	CD (n=10)	CD + *C. maculata* (n=10)
Liver	11.5 ± 0.6***	11.0 ± 0.8†††	26.0 ± 2.2***	27.9 ± 2.3†††
Muscle	26.8 ± 2.5	25.7 ± 3.7	29.4 ± 2.3	30.3 ± 3.6

Protein yield was obtained by multiplying the concentration by the total volume obtained. Results are expressed as the average ± standard error of mean.
***†††p<0.001. Lean vs. obese

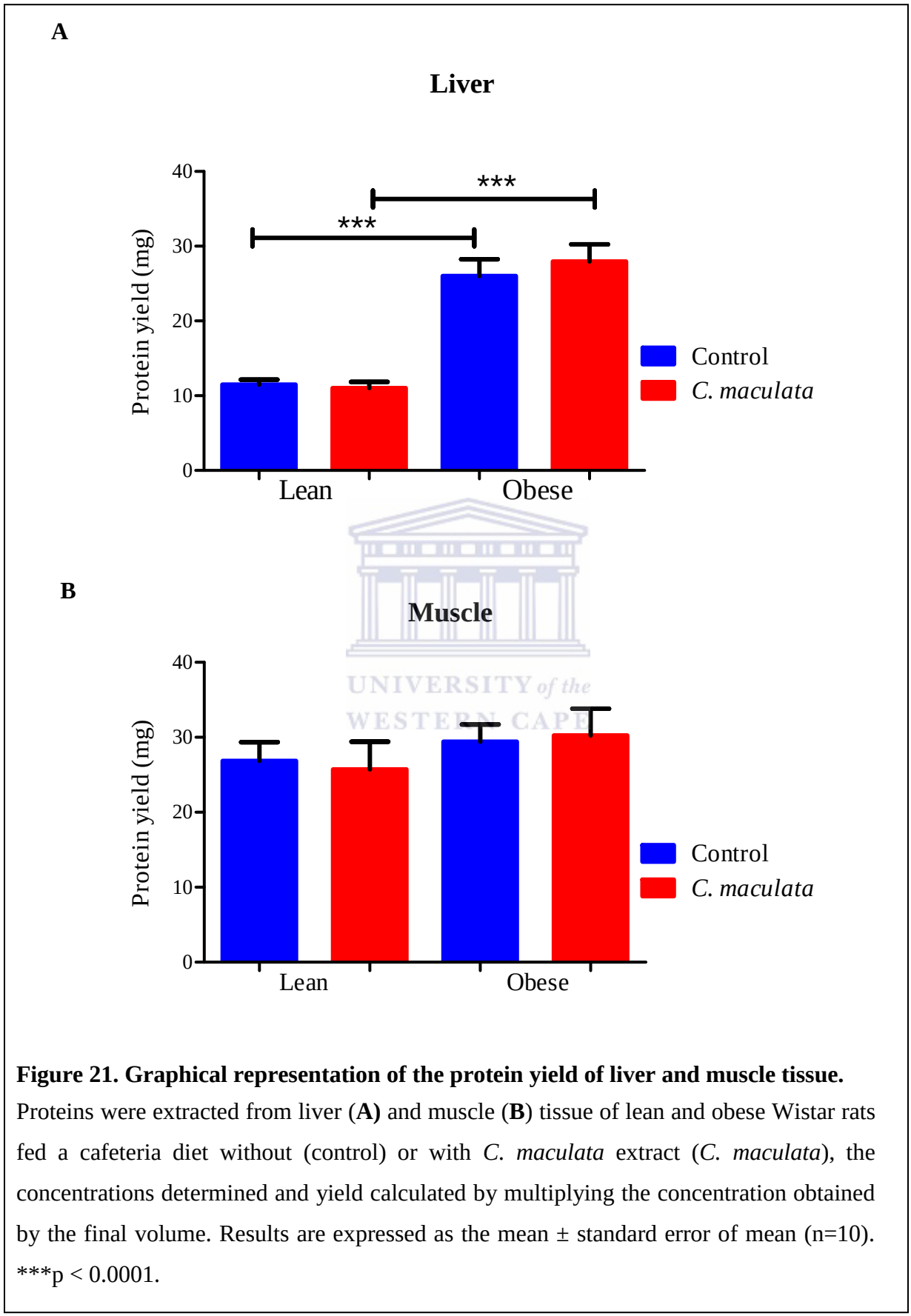

Figure 21. Graphical representation of the protein yield of liver and muscle tissue. Proteins were extracted from liver (**A)** and muscle (**B**) tissue of lean and obese Wistar rats fed a cafeteria diet without (control) or with *C. maculata* extract (*C. maculata*), the concentrations determined and yield calculated by multiplying the concentration obtained by the final volume. Results are expressed as the mean ± standard error of mean (n=10). ***p < 0.0001.

3.2.2 The effect of *C. maculata* treatment on AMPK expression

To investigate the effect of *C. maculata* on AMPK expression, proteins extracted from lean and obese Wistar rats were separated by 10% SDS PAGE, transferred to PVDF and probed with total AMPK and phosphorylated AMPK (an indication of AMPK activation) antibodies.

3.2.2.1 The effect of *C. maculata* on the expression of total AMPK

Although a slight increase was observed, *C. maculata* treatment had no significant effect on the expression of total AMPK in the liver of lean (115.4 ± 9.0 vs. 112.8 ± 7.2) and obese (126.1 ± 6.6 vs.154.8 ± 13.7) rats (Table 9, Figure 22). The expression of total AMPK was increased in liver of control obese rats compared to control lean rats (154.8 ± 13.7 vs. 112.8 ± 7.2; 1.4-fold, $p<0.05$).

In muscle, *C. maculata* treatment decreased AMPK expression in lean rats (606.5 ± 49.4 vs. 1451.4 ± 335.5; 2.3-fold, $p<0.05$) (Table 10, Figure 22). Treatment increased expression although not significant in obese rats (421.3 ± 54.5 vs. 377.2 ± 66.9). In contrast to the liver, the expression of total AMPK was decreased in control obese rats compared to control lean rats (377.2 ± 66.9 vs. 1451.4 ± 335.5; 3.8-fold, $p<0.0001$) (Table 10, Figure 22).

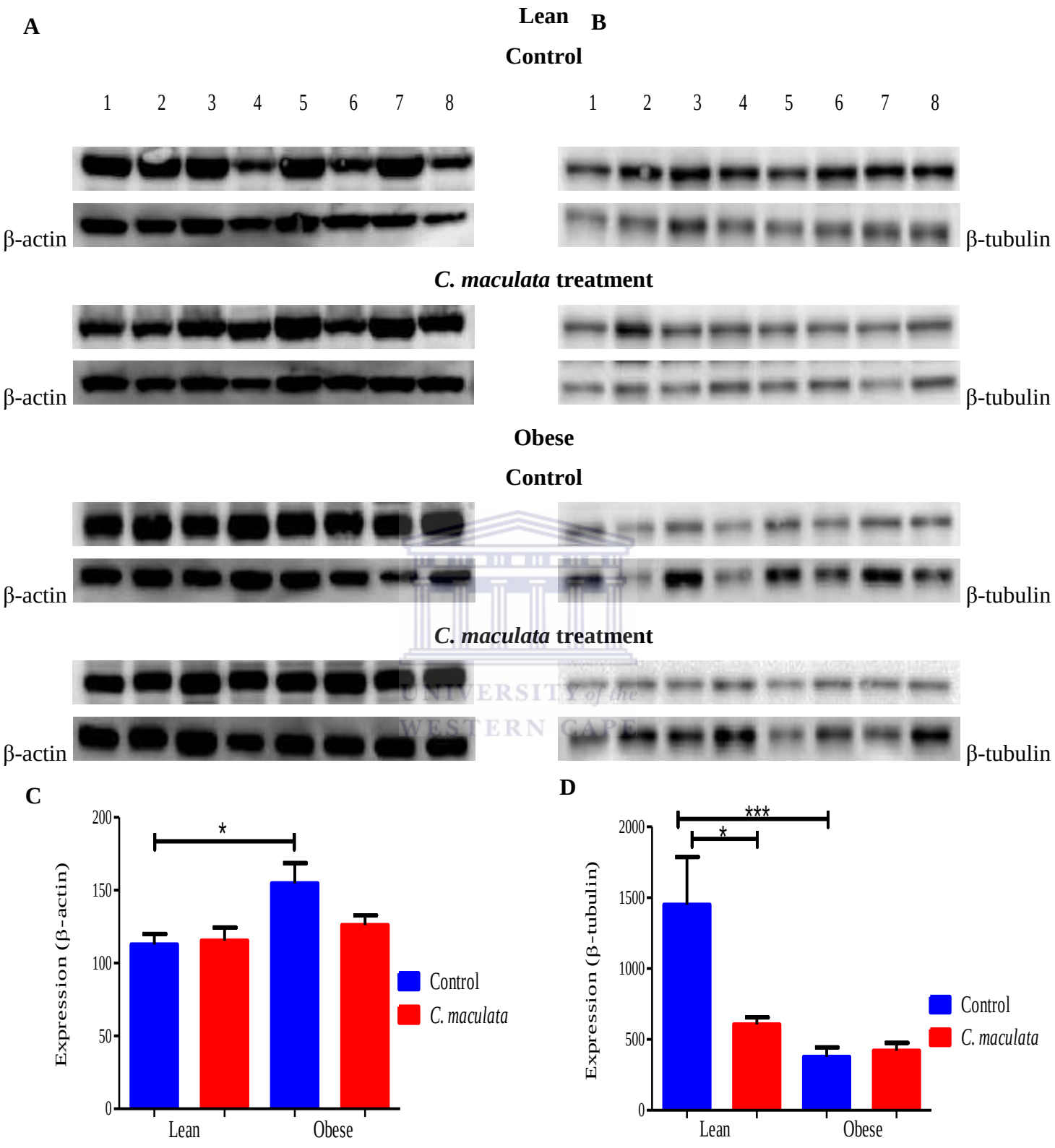

Figure 22. Total AMPK expression.

Densitometry blot images of total AMPK expression in liver (**A**) and muscle (**B**) tissue of lean and obese; control and *C. maculata* treated rats. Expression was normalized to β-actin or β-tubulin. Graphical representation of densitometry results for liver (**C**) and muscle (**D**) is expressed as the mean ± standard error of mean (n=8). *$p < 0.05$, *** $p < 0.0001$.

3.2.2.2 The effect of *C. maculata* on the expression of phosphorylated AMPK

AMPK activation is signified by its phosphorylation at threonine 172 in the activation loop of the α subunit catalytic domain by one or more upstream kinases (Hawley *et al*., 2003). Previous studies have demonstrated that plant extracts and phytochemicals may mediate their anti-obesity effects via AMPK activation (increase in phosphorylation) (Kim *et al*., 2008; Niu *et al*., 2012).

Cyclopia maculata treatment did not affect phosphorylated AMPK (pAMPK) expression in the liver of lean (120.0 ± 6.2 vs. 113.2 ± 5.6) and obese (117.0 ± 3.7 vs. 121.2 ± 5.8) rats (Table 9, Figure 23).

In muscle, *C. maculata* treatment induced a similar pattern of expression as observed for total AMPK; decreased expression of pAMPK was observed in lean rats after treatment (46.1 ± 7.9 vs. 246.2 ± 51.8; 5.3 fold, $p<0.0001$). Treatment did not effect pAMPK expression in obese rats (48.0 ± 8.3 vs. 44.5 ± 5.9). Phosphorylated AMPK expression was decreased in obese rats compared to lean rats, regardless of treatment (untreated 44.5 ± 5.9 vs. 246 ± 51.8; treated 48.0 ± 8.2 vs. 46.2 ± 7.9) the difference was significant in untreated rats only (46.2 ± 7.9 vs. 246 ± 51.8; 3.1 fold, $p<0.0001$) (Table 10, Figure 23).

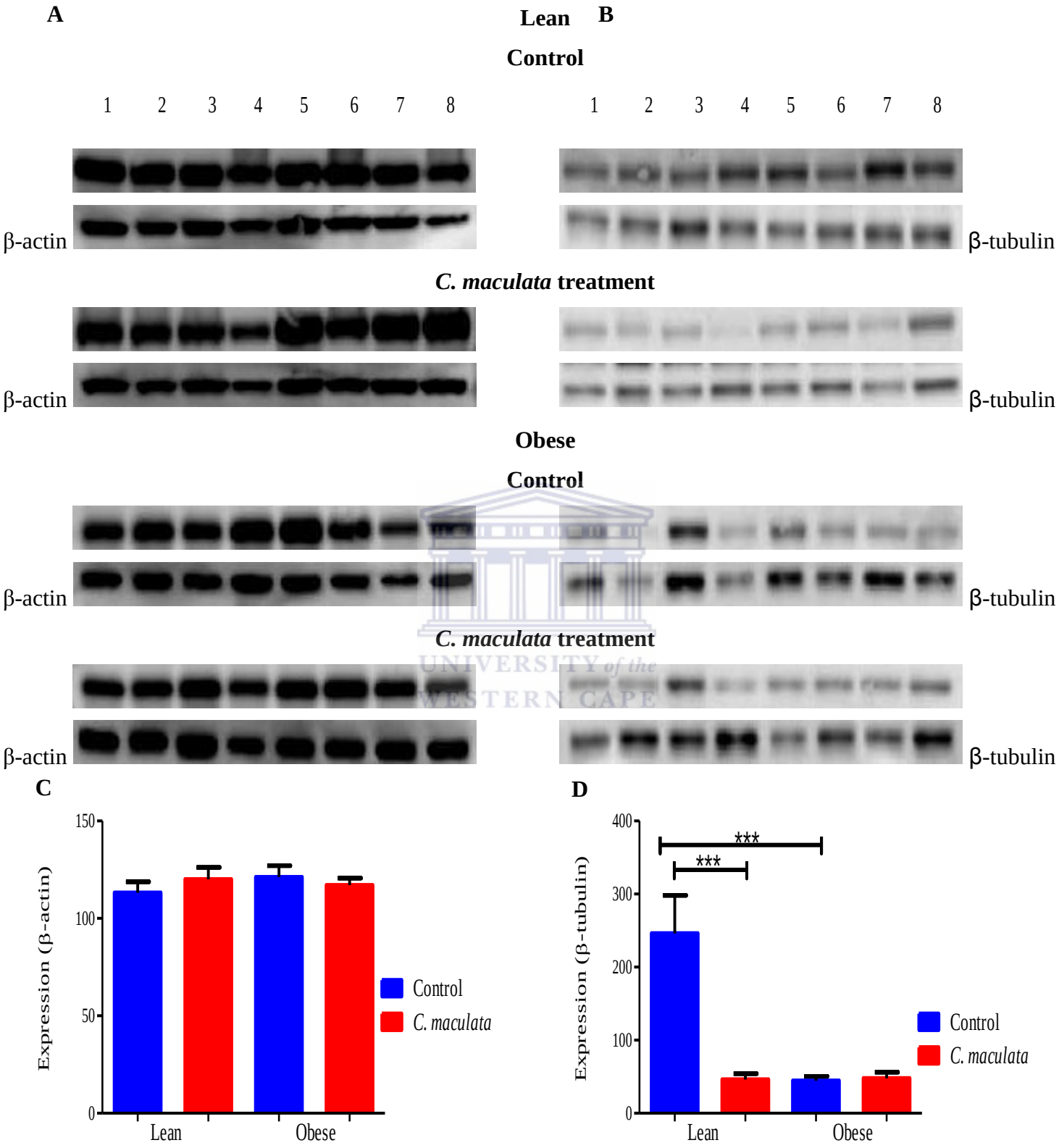

Figure 23. Phosphorylated AMPK expression.

Densitometry blot images of phosphorylated AMPK expression in liver (**A**) and muscle (**B**) tissue of lean and obese; control and *C. maculata* treated rats. Expression was normalized to β-actin or β-tubulin. Graphical representation of densitometry results for liver (**C**) and muscle (**D**) is expressed as the mean ± standard error of mean (n=8). ***p < 0.0001.

3.2.2.3 Phosphorylated AMPK as a ratio of total AMPK (Activated AMPK)

Activated AMPK expression was determined by dividing the relative phosphorylated AMPK expression by the relative total AMPK expression. *Cyclopia maculata* treatment increased AMPK activation in lean (107.6 ± 7.9 vs. 102.4 ± 6.7) and obese (94.2 ± 4.7 vs. 82 ± 7.2) rats, although the differences was not significant (Table 8, Figure 24). The activation of AMPK was found to be lower in the liver of untreated obese rats compared to untreated lean rats (82 ± 7.2 vs. 102.4 ± 6.7; 1.3-fold), but it was not significant (Table 8, Figure 24).

In muscle, *Cyclopia maculata* treatment decreased AMPK activation in both lean (8.3 ± 2.0 vs. 19.0 ± 3.8; 2.3-fold, $p<0.05$) and obese (11.7 ± 2.1 vs. 15.0 ± 3.9) rats, although the decrease observed in obese rats was not significant (Table 8, Figure 24). Similar to the results observed in the liver, AMPK activation was decreased in control (15.0 ± 3.9 vs. 19.0 ± 3.8; 1.3-fold) and *C. maculata* treated (11.7 ± 2.1 vs. 8.3 ± 2.0) obese rats compared to lean rats, although not significant (Table 8, Figure 24).

Table 8. Activated AMPK expression in liver and muscle of lean and obese rats.

	AMPK activation			
	Lean		Obese	
	CD (n=8)	CD + *C. maculata* (n=8)	CD (n=8)	CD + *C. maculata* (n=8)
Liver	102.4 ± 6.7	107.6 ± 7.9	82 ± 7.2	94.2 ± 4.7
Muscle	19.0 ± 3.8*	8.3 ± 2.0*	15.0 ± 3.9	11.7 ± 2.1

AMPK activation was determined by dividing the relative expression of phosphorylated AMPK by the total AMPK expression. Results are expressed as the mean ± standard error of mean.
*$p < 0.05$.

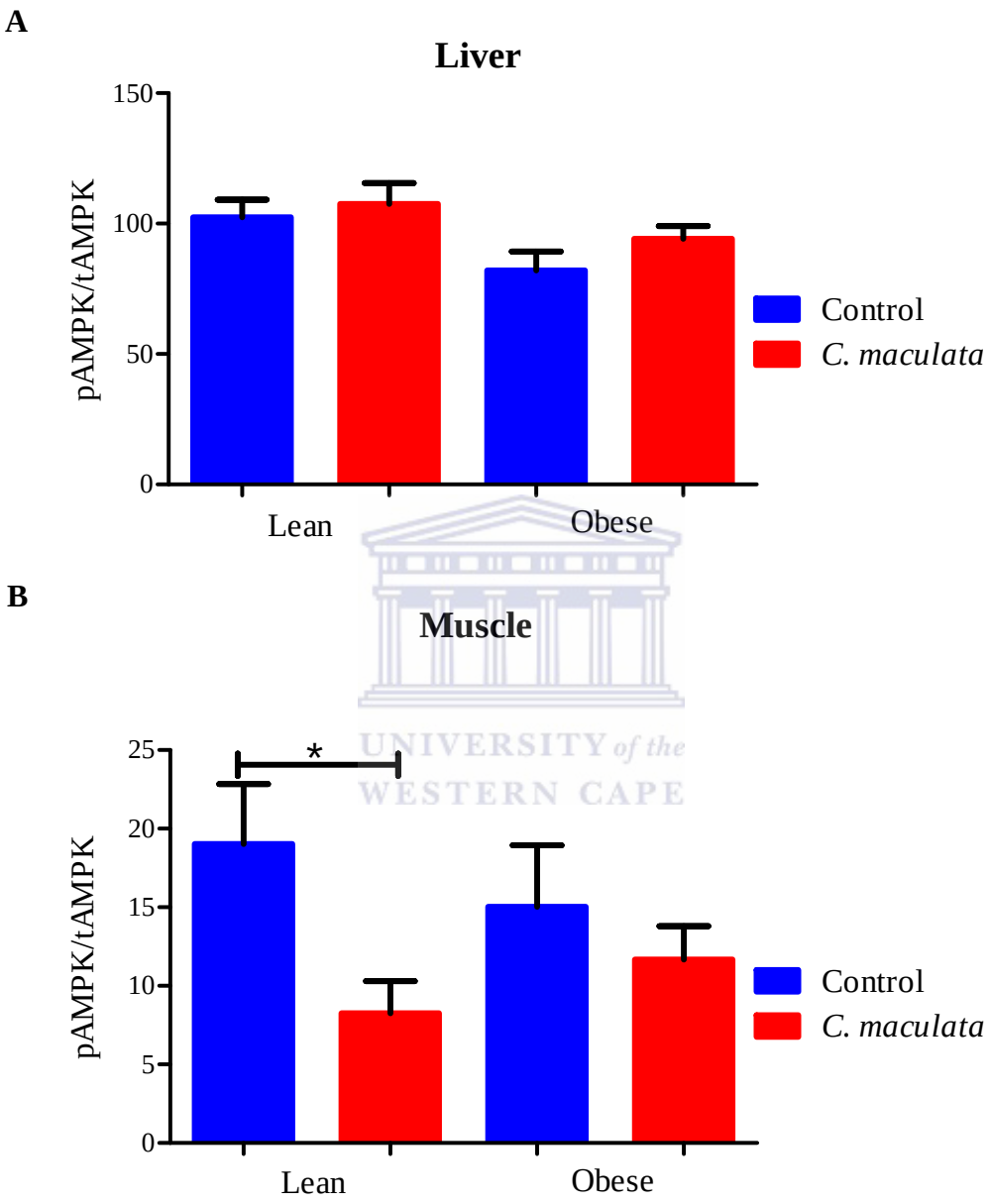

Figure 24. Activated AMPK.

AMPK activity in liver (**A**) and muscle (**B**) tissue was determined by dividing the expression of phosphorylated AMPK (pAMPK) by the expression of total AMPK (tAMPK). Results are expressed as the mean ± standard error of mean (n=8). * $p < 0.05$.

3.2.3 The effect of *C. maculata* treatment on PPARα expression

Peroxisomal proliferator activated receptor α (PPARα) is a downstream protein target of AMPK activation that is involved in the metabolic regulation of fatty acids by increasing fatty acid uptake and β-oxidation (Yoon, 2009 and Lee *et al*., 2006). PPARα is predominantly expressed in tissues with high rates of mitochondrial and peroxisomal fatty acid metabolism including the liver, heart, skeletal muscle and kidneys (Yoon, 2009). To investigate the effect of *C. maculata* on lipolysis and β-oxidation, the expression of PPARα was determined in liver and muscle of lean and obese control and treated rats.

Cyclopia maculata treatment decreased PPARα expression in lean rats (331.6 ± 55.3 vs. 444.0 ± 38) although the difference was not significant. In obese rats, treatment decreased PPARα expression (738.2 ± 75.3 vs. 1387.4 ± 334.1; 2.7-fold) although not significantly. The expression of PPARα expression was 2.7-fold higher in untreated obese rats compared to untreated lean rats (1387.4 ± 334.1 vs. 444.0 ± 38; $p<0.001$). Similarly PPARα expression was higher in *C. maculata* treated obese compared to *C. maculata* treated lean rats (738.2 ± 75.3 vs. 331.6 ± 55.3) although not significant (Table 9, Figure 25).

The expression of PPARα in muscle was too low for Western blot analysis and quantification.

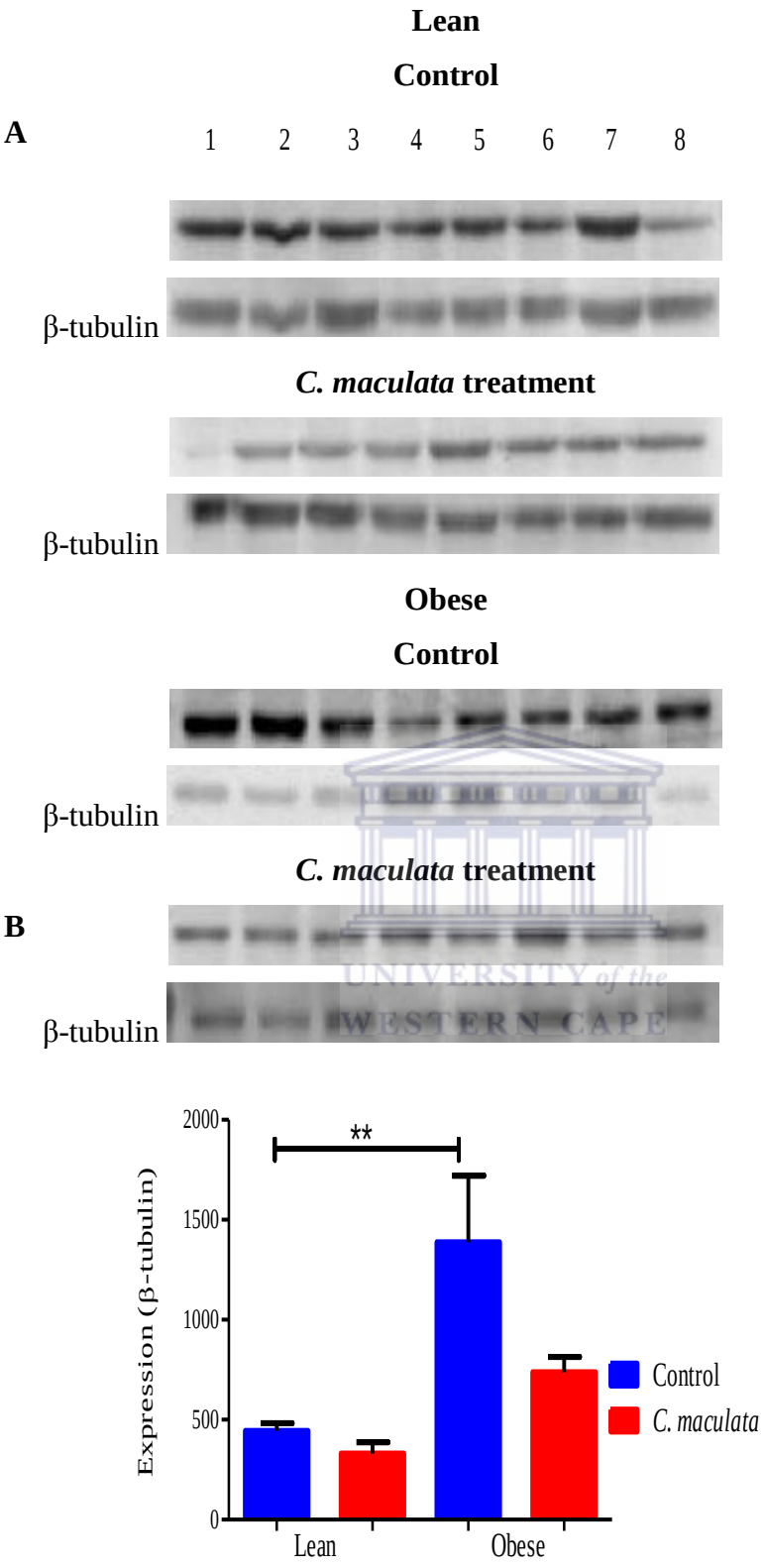

Figure 25. PPARα expression.

Densitometry blot images of PPARα expression in liver (**A**) and muscle (**B**) tissue of lean and obese; control and *C. maculata* treated rats. Expression was normalized to β-actin or β-tubulin. Graphical representation of densitometry results for liver (**C**) and muscle (**D**) is expressed as the mean ± standard error of mean (n=8). **p < 0.001.

3.2.4 The effect of *C. maculata* treatment on UCP2 expression

To investigate the effect of *C. maculata* on the β-oxidation of free fatty acids, the expression of uncoupling protein 2 (UCP2) was measure in the liver and muscle of lean and obese rats. UCP2 uncouples ATP and heat production from the metabolism of free fatty acids (Yonezawa *et al*., 2009; Schrauwen and Hesselink, 2002).

Cyclopia maculata treatment increased UCP2 expression in the liver of lean (1605 ± 379.4 vs. 1541.1 ± 287.2) and obese (4952.4 ± 1473 vs. 4604.1 ± 1057) rats, although not significant (Table 9, Figure 26). UCP2 expression was 2.9-fold higher, although not significant in the liver of control obese rats compared to control lean rats (4604.1 ± 1057 vs. 1541.1 ± 287.2 1) (Table 9, Figure 26).

In muscle, *C. maculata* treatment decreased UCP2 expression in lean rats (337.6 ± 31.6 vs. 937.7 ± 86.6; 2.8-fold, $p<0.0001$) (Table 10, Figure 26). Similarly treatment decreased UCP2 expression in obese rats, although it was not significant (372.7 ± 53.1 vs. 500.3 ± 66.1). Contrary to the liver, UCP2 expression was 1.4-fold higher in control lean rats compared to control obese rats (937.7 ± 86.6 vs. 500.3 ± 66.1; $p<0.0001$) (Table 10, Figure 26).

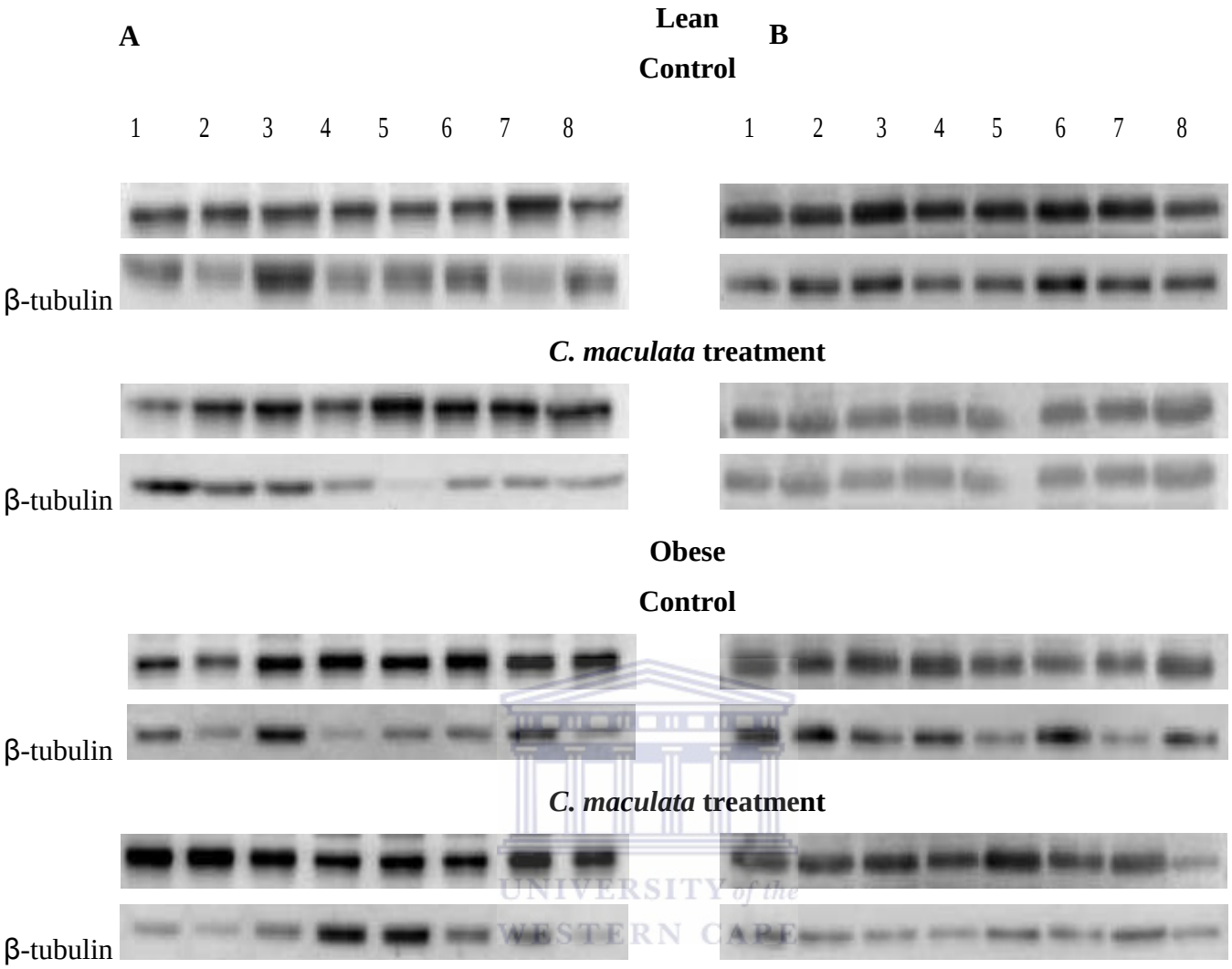

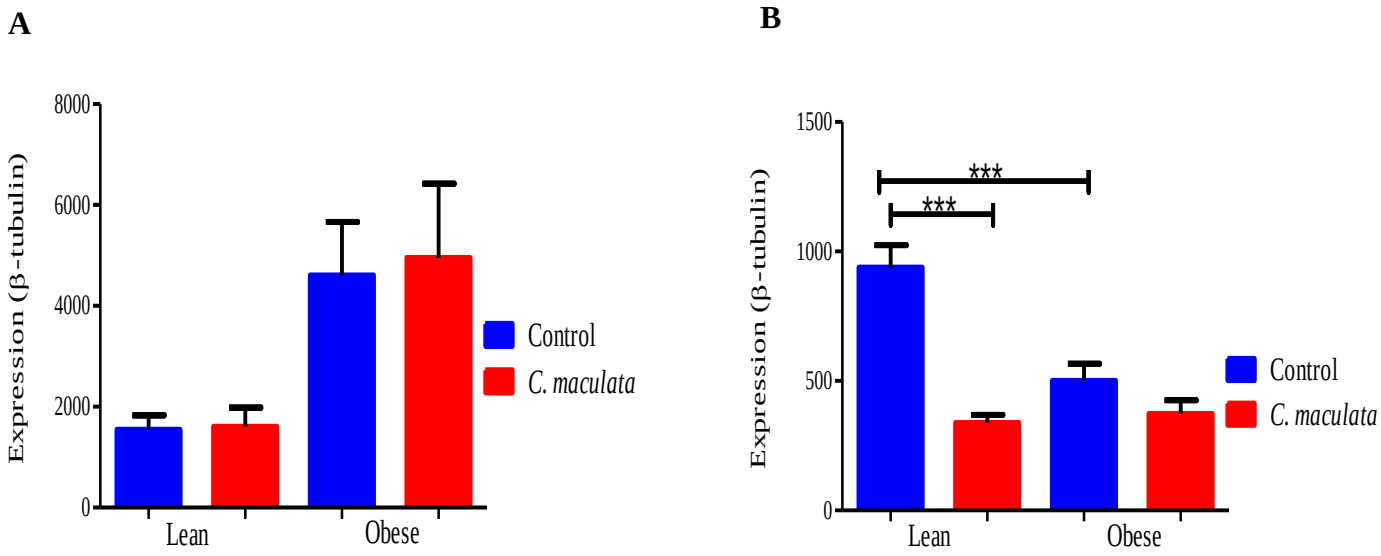

Figure 26. UCP2 expression.

Densitometry blot images of total AMPK expression in liver (**A**) and muscle (**B**) tissue of lean and obese; control and *C. maculata* treated rats. Expression was normalized to β-actin or β-tubulin. Graphical representation of densitometry results for liver (**C**) and muscle (**D**) is expressed as the mean ± standard error of mean (n=8). ***p < 0.0001.

Table 9. Summary of Western blot results for liver tissue.

Protein of interest	†Expression			
	Lean rats		Obese rats	
	Cafeteria diet (n=8)	Cafeteria diet + *C. maculata* (n=8)	Cafeteria diet (n=8)	Cafeteria diet + *C. maculata* (n=8)
tAMPK	112.8 ± 7.2*	115.4 ± 9.0	154.8 ± 13.7*	126.1 ± 6.7
pAMPK	113.2 ± 5.6	120.0 ± 6.2	121.2 ± 5.8	117.0 ± 3.7
PPAR-α	444.0 ± 38.0***	331.6 ± 55.3	1387.4 ± 334.1***	738.2 ± 75.36
UCP-2	1541.1 ± 287.2	1605 ± 379.4	4604.1 ± 1057	4952.4 ± 1473
PPAR-γ	ND	ND	ND	ND
ACC	ND	ND	ND	ND

†Expression was calculated by normalizing to β actin or β-tubulin
Results are expressed as the mean ± standard error of mean
ND indicates that the Western blot failed to identify the protein of interest
* $p < 0.05$, *** $p < 0.0001$.

Table 10. Summary of Western blot results for muscle tissue.

Protein of interest	†Expression			
	Lean rats		Obese rats	
	Cafeteria diet (n=8)	Cafeteria diet + *C. maculata* (n=8)	Cafeteria diet (n=8)	Cafeteria diet + *C. maculata* (n=8)
tAMPK	1451.4 ± 335.5*†††	606.5 ± 49.4*	377.2 ± 66.9†††	421.3 ± 54.5
pAMPK	246.2 ± 51.8***†††	46.2 ± 7.9***	44.5 ± 5.9†††	48.0 ± 8.3
UCP-2	937.7 ± 86.6***†††	337.6 ± 31.6***	500.3 ± 66.1***†††	372.7 ± 53.1
PPAR-α	ND	ND	ND	ND
PPAR-γ	ND	ND	ND	ND
ACC	ND	ND	ND	ND

†Expression was calculated by normalizing to β-tubulin
Results are expressed as the mean ± standard error of mean
ND indicates that the Western blot failed to identify the protein of interest.
*$p < 0.05$, ***$^{†††}p < 0.0001$.

3.2.5 Other proteins investigated

Investigation of the effect of *Cyclopia maculata* treatment on Peroxisome proliferator activated receptor gamma (PPARγ) and acetyl CoA carboxylase (ACC) was unsuccessful. PPARγ is the rate limiting transcriptional regulator involved in adipocyte differentiation and growth (Wu *et al*., 2010). Regulation of PPARγ activity by pharmaceutical and phytochemical treatments decreases adipogenesis, triglyceride accumulation and body weight gain (Hwang *et al*., 2007). Western blot analysis of PPARγ for liver and muscle tissue resulted nonspecific background binding with no quantifiable distinctive protein bands (Table 9 and 10).

ACC is the rate limiting enzyme for the conversion of acetyl CoA to malonyl-CoA, either for fatty acid synthesis or inhibition of β-oxidation by the blocking of carnitine palmitate tranferase 1 (CPT1) (Coleman *et al*., 2002). Inhibition of ACC through its direct phosphorylation by AMPK reduces fatty acid synthesis and promotes the β-oxidation of long fatty acids and decrease body weight gain (Do *et al*., 2012). Western blot analysis of ACC for liver and muscle tissue was unsuccessful due to nonspecific background binding with no quantifiable distinct protein bands (Table 9 and 10).

3.3 Phosphorylated AMPK ELISA

An ELISA was used to confirm our Western blot results for phosphorylated (activated) AMPK. The ELISA measures the expression of AMPK phosphorylated at threonine 172 and results are given relative to total AMPK. The ELISA therefore does not indicate absolute values of total and phosphorylated AMPK, but rather the ratio of pAMPK to tAMPK.

ELISA confirmed Western blot results where a slight increase in the activation of AMPK was observed in the liver of lean (23.7 ± 7.0 vs. 22.1 ± 6.4) and obese rats (21.1 ± 6.6 vs. 19.9 ± 4.3) after *C. maculata* treatment, although not significant (Table 11, Figure 27).

Due to financial constraints, only the muscle tissue of lean rats was investigated by ELISA. In contrast to Western blot analysis where *C. maculata* treatment decreased AMPK activation in lean rats (although not statistically significant), ELISA showed no effect (2.0 ± 1.1 vs. 1.7 ± 1.5) (Table 11, Figure 27).

Table 11. ELISA results

	Lean rats		**Obese rats**	
	CD (n=10)	CD + *C. maculata* (n=10)	CD (n=10)	CD + *C. maculata* (n=10)
Liver	22.1 ± 6.4	23.7 ± 7.0	19.9 ± 4.3	21.1 ± 6.6
Muscle	1.7 ± 1.5	2.0 ± 1.1	ND	ND

The AMPKα [pT172] kit from Invitrogen is a solid phase sandwich enzyme linked immunosorbent Assay (ELISA). A monoclonal antibody specific to AMPKα is coated on a microtiter strip which binds to AMPKα protein in tissue lysates, trapping it to the microtiter strip. The addition of an antibody directed at AMPKα phosphorylated at Thr172 binds to the immobilized AMPKα protein if phosphorylated

‡Results are expressed as the average ± standard error of mean

ND, not determined.

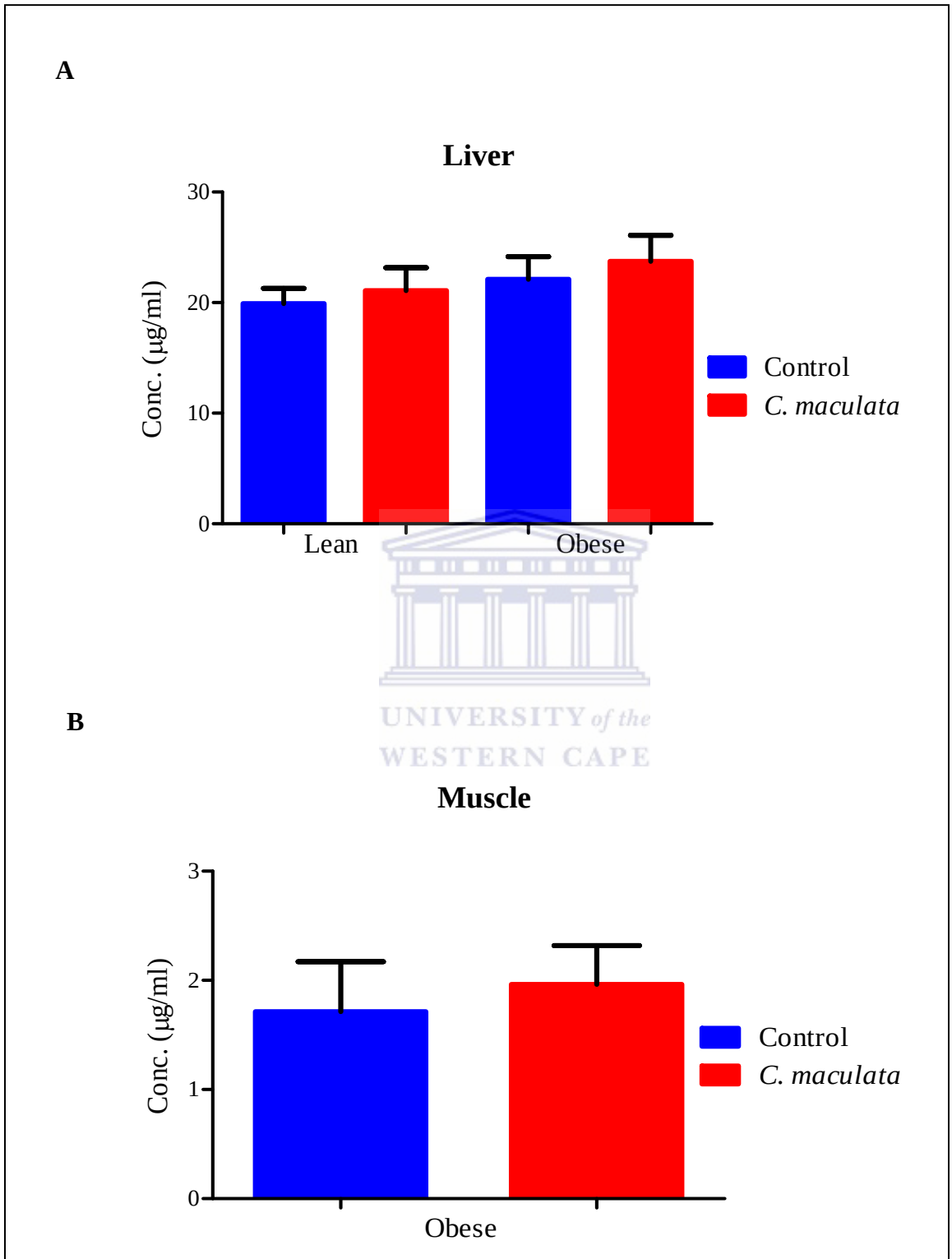

Figure 27. Phosphorylated AMPK [pT172] ELISA results.

(A) Phosphorylated AMPK expression in liver (A) and muscle (B) of lean and obese Wistar rats. Results are expressed as the average ± standard error of mean.

3.4 Histological analysis of retroperitoneal fat of Wistar rats

Haematoxylin and Eosin (H&E) staining of the retroperitoneal fat (RF) pads was performed to determine the effect of *C. maculata* treatment on fat accumulation and adipocyte morphology. Retroperitoneal fat is an important visceral fat depot store and is sensitive to the storage and release of fatty acids, thereby influencing their morphology and cell number (Bjørndal *et al*., 2011). Lipid metabolic regulatory effects of *C. maculata* could possibly be observed in the morphology and number of adipocytes in this active visceral fat depot.

Cyclopia maculata treatment did not affect adipocyte size in lean (106397 ± 1993 vs. 106779 ± 3758) and obese (102834 ± 1838 vs. 107612 ± 1393) rats (Table 12, Figure 28). Adipocyte size was increased in obese compared to lean rats, but was not significant (Table 12, Figure 28).

Cyclopia maculata treatment did not affect the number of adipocyte in lean (8.2 ± 0.9 vs. 8.2 ± 1.2) rats; a slight increase in obese (8.0 ± 0.7 vs. 7.6 ± 0.4) rats, but it was not significant. The number of adipocyte observed in the retroperitoneal fat of obese was lower than that in lean rats, although not significant (Table 12, Figure 28).

Table 12. Histological results of retroperitoneal fat.

	Lean rats		**Obese rats**	
	CD (n=10)	CD + *C. maculata* (n=10)	CD (n=10)	CD + *C. maculata* (n=10)
Adipocyte size	106779 ± 3758	106397 ± 1993	107612 ± 1393	102834 ± 1838
Adipocyte number	8.2 ± 1.2	8.2 ± 0.9	7.6 ± 0.4	8.0 ± 0.7

Results for adipocyte size are expressed as arbitrary units, while the number of adipocytes per microscopic field (average of 10 fields) is given.
Results are expressed as the average ± standard error of mean

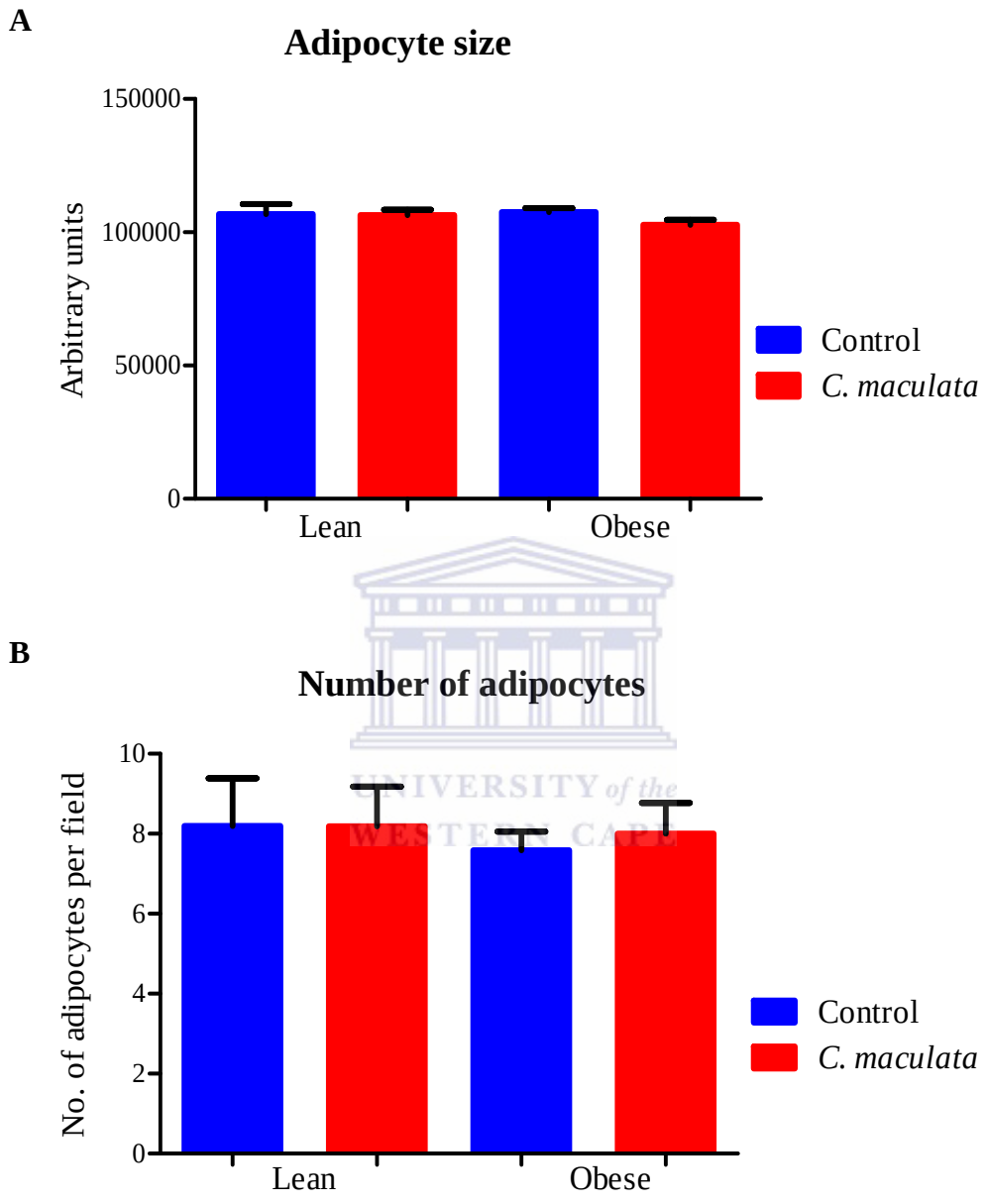

Figure 28. Histological results of retroperitoneal fat.

Adipocyte size (**A**) and number (**B**) in the retroperitoneal fat pads of lean and obese Wistar rats fed the cafeteria with or without the *C. maculata* extract. Results are expressed as the as the average ± standard error of mean.

Chapter 4

Discussion

4. Discussion

Natural plants and their phytochemicals possess a number of health effects including anti-oxidant, anti-mutagenic, anti-inflammatory and anti-cancer properties, mediated by activating the AMPK signaling pathway (Hwang *et al*., 2009). The increase in AMPK expression and phosphorylation by phytochemicals including mangiferin, a constituent of *C. maculata* has been shown to regulate body weight gain by promoting lipid catabolism (Niu *et al*., 2012). Recent investigations in our laboratory have shown that a hot water extract of fermented *C. maculata* regulates lipid metabolism *in vitro* (Dhudia *et al*., 2013). Patel investigated the effect of *C. maculata* on diet-induced obesity in Wistar rats (Patel, 2012). The aim of this study was to investigate whether *C. maculata* treatment in Wistar rats activates the AMPK signaling pathway.

4.1 Protein optimization

Protein lysate purity is important during Western blot analysis. Salts, debris and other impurities may impede the migration of proteins during SDS-PAGE (Westermeier, 2000). Furthermore, impurities may contain enzymes and compounds which degrade proteins. Impurities may also result in smearing of gels, hindering protein band visibility and density, thus causing bands to be indistinguishable, resulting in non-specific binding of antibodies to proteins of interest during western blot analysis

Protein extraction was optimized by comparing two different lysis buffers and two different homogenization methods, and using two different tissues, liver and muscle. The protein yield of liver was significantly higher when the commercial lysis buffer was used compared to the in-house lysis buffer, with both methods of homogenization. The TissueLyser homogenization method was superior to the Polytron, in terms of protein yield. The different optimization methods yielded no significant differences in muscle tissue, thus the commercial lysis buffer and the TissueLyser was selected for protein extraction from liver and muscle tissue samples. Protein yield for the liver was also significantly higher compared to muscle protein yield, irrespective of lysis buffer and homogenization method used. Protein content differences between the liver and muscle

may be due to the different structure and function of these tissues. The liver is a soft tissue consisting of simple hepatocytes whereas muscle is composed of striated rigid fibers that do not lyse easily.

The commercial lysis buffer contains a proprietary detergent and was supplemented with protease and phosphatase inhibitor tablets according to the manufacturer's instructions, whereas the in-house lysis buffer was prepared according to our standard operation procedure for protein extraction and was supplemented with less protease and phosphatase inhibitor tablets. The difference in protein yield obtained between the two extraction buffers may be due to the greater ability of the commercial lysis buffer to protect against enzymatic degradation by phosphatase and protease enzymes in the lysates, as well as the proprietary detergent removing excess salts and debris thereby increasing lysate purity and quality.

For liver samples, the TissueLyser was superior to the Polytron. Differences in the protein yield between the TissueLyser and the Polytron may be due to their different homogenization procedures. The TissueLyser works by high speed crushing of the tissue with steel beads and the Polytron homogenizes tissue with a serrated blade. Furthermore, during homogenization with the Polytron the lysate is transferred to multiple tubes which may lead to a loss in volume. The TissueLyser homogenization is a single step process in which homogenization occurs in a 2 ml tube without volume loss. The Polytron yielded residual debris after homogenization which may also account for its reduced protein yield compared to the TissueLyser.

4.2 Lean and obese rats

A lean and an obese group (Patel, 2012) were used for this study. The lean rats were 21 day old weanlings who were fed the cafeteria diet over the experimental period of 12 weeks. The obese rats were 21 day old weanlings who were fed a cafeteria diet for 16 weeks *ad libitum* to induce nutritional obesity prior to the experimental period (3 months). Both groups of rats were treated with the hot water extract of fermented *C. maculata* at a dose of 300 mg/kg throughout the 3 month experimental period. The lean rats that were

treated with the *C. maculata* extract had a 2.4% reduction in body weight gain at the end of the study, whereas the obese rats showed a 2.4% increase in body weight gain over the experimental period. These two groups were investigated to determine how *C. maculata* treatment affected AMPK activity in lean and obese individuals.

4.3 Western blot analysis

4.3.1 Protein yield results

Proteins were extracted with an optimized method using the commercial lysis buffer and the TissueLyser as described previously. *Cyclopia maculata* treatment did not affect the protein yield of liver and muscle tissue of lean and obese rats. Interestingly, 100 mg of liver tissue from obese rats yielded significantly more proteins than 100 mg of liver tissue from lean rats. The increased protein yield observed in the livers of obese rats compared to lean rats, is possibly part of an adaptive response to the increased lipid overload from the cafeteria diet (Estornell *et al*., 1995; Fillios and Saito, 1965). Increased hepatic protein turnover in obese fa/fa Zucker rats and in obese woman has been linked to increased microsomal and peroxisomal protein turnover in response to lipid over feeding (Estornell *et al*., 1995; Fillios and Saito, 1965). The increased protein turnover is thought to facilitate the synthesis of enzymes to regulate the increased lipid accumulation within cells (Waterlow *et al*., 1995; Fillios and Saito, 1965).

Similar to the liver, the protein yield in muscle tissue of obese rats was higher to the protein yield obtained in lean rats, although the difference was not statistically significant. Difference in protein yield between tissues is suggested to be dependent on tissue structure and functional activity (Anderson *et al*., 2008; Hwang *et al*., 2010). Our results suggest that the liver, and to a lesser extent the muscle, is an important site for protein synthesis in the obese state. Contrary to the optimization experiment, no difference in protein yield was observed between liver and muscle of lean and obese rat. Difference in protein yield between experiments could be due to differences in the tissue samples for the optimization experiments.

4.3.2 *Cyclopia maculata* and AMPK activity (pAMPK/tAMPK)

Recent investigations have shown that many plants mediate their biological actions by inducing the AMPK pathway (Kim *et al*., 2008; Do *et al*., 2012; Kang *et al*., 2012). The effect of *C. maculata* treatment on AMPK activity was determined as the ratio of pAMPK/tAMPK.

Although total AMPK was significantly higher in the liver of obese rats, activated AMPK (pAMPK/tAMPK) was lower in these rats. Total AMPK and activated AMPK were lower in the muscle of obese rats. Other studies have reported that AMPK activity is dysregulated in the liver and muscle during lipid overload, obesity and raised blood glucose levels (Martin *et al*., 2006; Kraegen *et al*., 2006). The obese rats used in this study were fed a cafeteria diet to induce obesity and insulin resistance (Patel, 2012), possibly explaining the decreased AMPK activity in these rats. Furthermore, the blood glucose concentrations of these rats were raised, and they were 4 months older than lean rats (Patel, 2012), further contributing to the decreased AMPK activity observed.

Although a slight increase in AMPK activity was observed after *C. maculata* treatment in the liver of lean and obese rats, the difference was not statistically significant. In muscle, *C. maculata* treatment decreased AMPK activity in lean and obese rats. Glycogen accumulation is known to inhibit AMPK activity (Viollet *et al*., 2003; Mcbride *et al*., 2009). Chellan *et al*. (2012) showed than another South African plant *Athrixia phylicoides,* stimulates glycogen accumulation, thus making it tempting to speculate that *C. maculata* also stimulates glycogen accumulation and that the decreased AMPK activity observed after *C. maculata* treatment is due to increased glycogen accumulation in the muscle of these animals. In support of this idea, other *Cyclopia* species have been shown to stimulate glucose uptake and utilization (Muller *et al*. 2012).

AMPK activity is tissue specific and differences in AMPK activity in the muscle and the liver have been reported (Viollet *et al*., 2010). AMPK may be expressed as 12 different isoforms, conferring different properties depending on their subcellular location (Amodeo *et al*., 2007). AMPK activity in the liver results in the overall inhibition of energy

consuming pathways, whereas AMPK activation in skeletal muscle results in the activation of ATP producing catabolic pathways, depending on their isoform combination and stimulus (Suzuki *et al*., 2007).

Although the beneficial effects of AMPK activation have been well reported (Kang *et al*., 2012), some evidence for the beneficial effects of AMPK inhibition during stroke and cancer has been reported (Li *et al*., 2007). The over activation of AMPK in response to ischemic injury is detrimental during ischemic reperfusion which my lead to further energy failure and cell death (McCullough *et al*., 2005; Viollet *et al*., 2010). AMPK inhibition by compound C was shown to provide sustained neuroprotection after stroke, benefiting cell survival (Li *et al*., 2007).

4.3.3 *Cyclopia maculata* and PPARα expression

The peroxisomal proliferator activated receptor α (PPARα) is a ligand activated transcription factor that belongs to the steroid hormone PPAR superfamily. Other members include PPARγ and PPARδ, each with their own ligand and tissue specific functions (Evans *et al*., 2004; Yoon *et al*., 2009). PPARα is predominantly expressed in tissues with high rates of mitochondrial and peroxisomal fatty acid metabolism such as the liver, heart, brown adipose tissue, skeletal muscle and kidneys (Yoon *et al*., 2009). PPARα functions by regulating the gene expression of key enzymes involved in the transport, uptake and oxidation of lipids such as fatty acid transport protein, carnitine palmityol transferase-1 (CPT1) and the uncoupling proteins (UCP1, UCP2 and UCP3) (Evans *et al*., 2004; Yoon *et al*., 2009). PPARα is activated by high circulating free fatty acids, fibrates, ligand steroids and various hormones including leptin and adiponectin (Kersten *et al*., 1999; Armstrong and Towle, 2001). PPARα has been shown to be a downstream protein target of the AMPK pathway, activated under conditions of energy deprivation and lipid overload (Armstrong and Towle 2001).

PPARα expression was significantly higher in the liver of obese rats compared to their lean counterparts. PPARα gene expression is associated with Fatty acid synthase (FAS) expression and is regulated by lipid content (Chakravarthy *et al*., 2009). Increased PPARα

expression is associated with increased circulating free fatty acids and their derivatives during a high fat diet (Armstrong and Towle, 2001), thus possibly explaining the increased PPARα expression in obese rats.

Cyclopia maculata treatment decreased PPARα expression in the liver of both lean and obese rats. Dudhia (2012) also demonstrated decreased PPARα protein expression in 3T3-L1 adipocytes after *C. maculata* treatment. In this study, decreased PPARα protein expression correlated with decreased expression of PPARγ and adipogenesis.

Cyclopia maculata was shown to possess phytoestrogen activity (Verhoog, 2006). Phytoestrogens are plant polyphenols with estrogen activity (Cederroth *et al*., 2008). Estrogens have been shown to reduce PPARα activity (Jeong *et al*., 2004; Yoon *et al*., 2009), thus possibly explaining the decreased PPARα expression in the rats after *C. maculata* treatment

4.3.4 The effect of *C. maculata* on uncoupling protein 2 expression

Uncoupling proteins (UCPs) are mitochondrial transporters present in the inner mitochondrial membrane (Villarroya *et al*., 2007). UCP1 was the first one to be identified and plays an important role in the adaptive thermogenesis of brown adipose tissue (Del *et al*., 2000). The UCP1 protein was found to enhance the uncoupling of protons down the respiratory chain in the mitochondria for the production of heat in response to cold temperatures or high circulating fatty acids (Nicholls and Locke, 1985). UCP2 and UCP3 were recently identified sharing 72% and 57% amino acid homology to UCP1 (Fleury *et al*., 1997; Gimeno *et al*., 1997). UCP2 is ubiquitously expressed in a variety of tissues in the body, including the skeletal muscle, white adipose tissue, liver, spleen, lungs and macrophages (Armstrong and Towle, 2001). UCP3 is predominantly expressed in skeletal muscle (Weigle *et al*., 1998). Unlike UCP1 which is solely involved in the adaptive thermogenesis to cold temperatures, UCP2 and UCP3 have been shown to respond to high circulating FFAs and reactive oxygen species (ROS), conferring to them lipid metabolic regulatory functions (Samec *et al*., 1998). UCPs are activated by unsaturated fatty acids

and are under the transcriptional control of PPARα and PGC1 which are downstream components of the AMPK pathway (Jager *et al*., 2007).

Cyclopia maculata treatment did not effect UCP2 expression in the liver of lean and obese rats. However, UCP2 expression in the liver of obese rats was 2.9-fold higher compared to lean rats. Over feeding and a diet high in unsaturated fats has been associated with increased expression of UCP1, a homologue of UCP2, in brown adipose tissue and skeletal muscle of rodents decreasing the metabolic efficiency and preventing the development of obesity (Himms-Hagen, 1984). Fasting has been associated with an increase in metabolic efficiency and a decrease in UCP1 expression and activity (Rothwell *et al*., 1984). Thus the increased UCP2 expression in the liver of obese rats may be due to increased adiposity and circulating free fatty acids caused by the cafeteria diet. UCP2 has been shown to regulate free radical production from fatty acid oxidation, by reducing the proton gradient across the mitochondrial membrane preventing damage to lipids, proteins and DNA by ROS (Schrauwen and Hesselink, 2002). Increased UCP2 expression in obese rats may be due to the fact that these rats were older and have increased ROS production (Samec *et al*., 1998; Katsanos *et al*., 2009).

In muscle, UCP2 protein was decreased in obese rats and after *C. maculata* treatment of lean rats. These results differ to those observed in the liver and is possibly is due to tissue specificity of UCP2. UCP3 is the predominant UCP in muscle (Rousset *et al*., 2004). The decreased UCP2 expression after *C. maculata* treatment in lean rats could be due to an adaptive response, where *C. maculata* decreases ROS due to its anti-oxidant properties (Marnewick *et al*., 2000; Joubert *et al*., 2008) and thus leads to less UCP2 expression. However, this is a speculation and requires further investigation.

4. 4 Phosphorylated AMPK [pT172] ELISA

ELISA results, similar to Western blot results, showed that *C. maculata* treatment increased AMPK activation, although not significantly.

ELISA is a quantitative assay that investigates intact native proteins whereas Western blot is a semi quantitative assay that investigates denatured proteins (Yang and Ma, 2009). ELISAs are easier to perform and are less time-consuming than Western blots. However, Western blots may give information about protein purity and size, whereas ELISAs do not.

4.5 Adipocyte size and number

Obesity is known to be due to the enlargement of adipose tissue to store excess energy intake (Jo *et al*., 2009). Adipose tissue grows by two mechanisms: hyperplasia, which is the increase in cell number and hypertrophy, which is the increase in adipocyte size (Jo *et al*., 2009). Adiposity is influenced by diet and genetic susceptibility of a person to its environment and their interaction (Marti *et al*., 2009; Prentice, 2006). Adipose tissue itself is stored in special depots such as the visceral and subcutaneous fat depots, whose rates of adiposity are determinants of weight gain and obesity (Matsuzawa *et al*., 1995; Huang *et al*., 2001). The investigation of these depots by visual staining techniques such Haematoxylin and Eosin staining has provided crucial phenotypical evidence of adipocyte size and number, influenced by nutritional intake and genetic susceptibility (Pang *et al*., 2008; Azin *et al*., 2000).

Cyclopia maculata treatment did not significantly affect adipocyte number and size in the retroperitoneal fat of lean ad obese Wistar rats. The retroperitoneal fat is a depot of visceral fat accumulation which is detrimental in the development of obesity and metabolic syndrome (Huang *et al*., 2001). Anti-obesity treatments have been shown to decrease adipocyte hyperplasia and hypertrophy in visceral fat depots such as retroperitoneal fat (Pang *et al*., 2008).

The failure to observe significant differences in adipocyte size and number between lean and obese rats is unexpected and could be due to technical difficulties with the quantification method used. Due to time constraints, it was not possible to repeat the analysis.

4.6 Limitations of study and future work

The main limitation of the study is the small weight reduction observed in these rats after *C. maculata* treatment. This could possibly explain our failure to observe AMPK activation. Furthermore, it has been suggested that AMPK activation plays a more prominent role in genetic models of obesity compared to diet-induced models of obesity. Testing of different doses of *C. maculata* could improve bioactivity (weight reduction) and AMPK activation.

C. maculata decreased UCP2 expression in the muscle of lean rats, but not in obese rats. However, no difference in UCP2 expression in the liver was observed after treatment. Future studies should focus on investigation of these tissue specific differences as it may provide important clues about metabolic regulation in lean and obese individuals.

4.7 Conclusion

Safe effective treatments to combat weight gain and obesity have become a serious concern due to the increased prevalence of obesity and the metabolic syndrome epidemic. Phytochemical treatments have been shown to regulate weight gain and reduce the detrimental effects of obesity in the development of NCDs, exhibiting their effects through the regulation of key metabolic process, such as AMPK signaling. *Cyclopia maculata* is a polyphenolic rich plant with a range of biological activities including anti-mutagenic, anti-oxidative, anti-cancer and phytoestrogen activity. This study has shown that treatment of diet-induced obese Wistar rats with 300 mg/kg of *C. maculata* does not affect the AMPK signaling pathway.

Although treatment did not affect AMPK activation in lean and obese rats, protein content in the liver of obese animals was increased compared to their lean counterparts. Similarly, an increase in PPARα and UCP2 expression was observed in obese rats compared to lean rats and suggests an adaptive response to the increased circulating free fatty acids and an increase in β-oxidation in these animals.

Chapter 5

References

5. References

- Abu-Elheiga L., Matzuk MM., Abo-Hashema KA. and Wakil SJ. Continuous fatty acid oxidation and reduced fat storage in mice lacking acetyl-CoA carboxylase 2. Science, 2001; 291: 2613-2616.
- Ajmo JM., Liang X., Rogers CQ., Pennock B. and You M. Resveratrol alleviates alcoholic fatty liver in mice. American Journal of Physiology, Gastrointestinal and Liver Physiology, 2008; 259: 833-842.
- American heart association. Statistical fact sheet; Overweight and Obesity. 2012
- Amodeo GA., Rudolph MJ. and Tong L. Crystal structure of the heterotrimeric core of *Saccharomyces cerevisiae* AMPK homologue SNFI. Nature, 2007; 449: 492-495.
- Andersson U., Filipsson K., Abbott CR., Woods A., Smith K., Bloom SR., Carling D. and Small CJ. AMP-activated protein kinase plays a role in the control of food intake. Journal of Biological Chemistry, 2004; 279(13): 12005-12008.
- Anderson SR., Gilge DA., Stieber AL. and Previs SF. Diet induced obesity alters protein synthesis: tissue-specific effects in fasted versus fed mice. Metabolism Clinical and Experimental, 2008; 57: 347-354.
- Andreadis EA., Tsourous GI., Tzavara CK., Georgiopoulos DX., Katsanou PM., Marakomichelakis GE. and Diamantopoulos EJ. Metabolic syndrome and incident cardiovascular morbidity and mortality in a Mediterranean hypertensive population. American Journal of Hypertension, 2007; 20: 558-564.
- Armstrong MB. and Towle HC. Polyunsaturated fatty acids stimulate hepatic UCP-2 expression via a PPARα-mediated pathway. American Journal of Physiology and Endocrinology Metabolism, 2001; 281(6): 1197-1204.
- Azin MJ., Hausman DB., Sisk MB., Flat WP. and Jewell DE. Dietary conjugated Linoleic acid reduces rat adipose tissue cell size rather than cell number. Journal of Nutrition, 2000; 130: 1548–1554.
- Barazzoni R., Bosutti A. and Stebel M. Ghrelin regulate mitochondrial lipid metabolism gene expression and tissue fat distribution in liver and skeletal muscle. American Journal of Physiology and Endocrinology Metabolism, 2005; 288: 228-235.

- Bateman A. The structure of a domain common to archaebacteria and homocystinuria disease protein. Trends in Biochemical Science, 1997; 22: 12-13.
- Berg AH., Combs TP., and Scherer PE. ACRP30/Adiponectin: an adipokine regulating glucose and lipid metabolism. Trends Endocrinology Metabolism, 2002; 13: 84-89.
- Bergeron R., Previs SF., Cline GW., Perret P., Russell RR ^{3rd}., Young LH. and Shulman GI. Effect of 5-aminoimidazole-4-carboxamide-1-beta-D-ribofuranoside infusion on *in vivo* glucose and lipid metabolism in lean and obese Zucker rats. Diabetes, 2001: 50(5): 1076-1082.
- Bjørndal B., Burri L., Staalesen V., Skorve J. and Berge RK. Different adipose depots: their role in the development of metabolic syndrome and mitochondrial response to hypolipidemic agents. Journal of Obesity, 2011; 2011:490650
- Bowie J. Sketches of the Botany of South Africa. South African Quarterly Journal, 1830; 1: 27-36.
- Brabant G., Muller G., Horn R., Anderwald C., Roden M. and Nave H. Hepatic leptin signaling in obesity. FASEB Journal, 2005; 19: 1048-1050.
- Carling D. AMPK-activated protein kinase: balancing the scales. Biochemistry. 2005; 87(1): 87-91.
- Cederroth CR., Vinciguerra M., Gjinovci A., Kuhne F., Klein M., Cederroth M., Caille D., Suter M., Neumann D. and James RW. Dietary phytoestrogens active AMP-activated protein kinase with improvement in lipid and glucose metabolism. Diabetes, 2008; 57(5): 1176-1185.
- Chakravarthy MV., Lodhi IJ., Malapaka RRV., Xu HR., Turk J. and Semenkovich CF. Identification of a physiologically relevant endogenous ligand from PPARα in liver. Cell, 2009; 138: 476-488.
- Chellan N., Muller CJF., De Beer D., Joubert E., Page BJ. and Low J. An *in vitro* assessment of the effect of *Athrixia phylicoides* DC. aqueous extract on glucose metabolism. Phytomedicine, 2012; 9: 730-736.
- Coleman RA., Lewin TM., Van Hoorn SG. and Gonzalez-Baro. Do long-chain acyl-CoA synthetases regulate fatty acid entry into synthetic or degradative pathways?. Journal of Nutrition, 2002; 132: 2123–2126.

- Collins SP., Reoma JL., Gamm DM. and Uhler MD. LKB-1, a novel serine/threonine protein kinase and potential tumour suppressor, is phosphorylated by cAMP-dependent protein kinase (PKA) and prenylated *in vivo*. Biochemical Journal, 2000; 345(3): 673-680.
- Collins QF., Liu HY., Pi J., Liu Z., Quon MJ. and Cao W. Epigallocatechin-3-gallate (EGCG), a green tea polyphenol, suppresses hepatic gluconeogenesis through 5-AMP-activated protein kinase. Journal of Biological Chemistry, 2007; 282: 30143-30149.
- Cool B., Zinker B., Chiou W., Kifle L., Cao N., Perham M., Dickinson R., Adler A., Gagne G. and Iyengar R. Identification and characterization of a small molecule AMPK activator that treat key components of type 2 diabetes and the metabolic syndrome. Cellular Metabolism, 2006; 437: 1109-1111.
- De Beer D. and Joubert E. Development of HPLC method for *Cyclopia subternata* phenolic compound analysis and application to other *Cyclopia* spp. Journal of Food Composition and Analysis, 2010; 23: 289–297.
- De Nyssechen AM., Van Wyk BE., Van Heerden FR. and Schutte AL. The major phenolic compounds in the leaves of *Cyclopia species* (Honeybush Tea). Biochemical Systematics and Ecology, 1996; 24(3): 243-246.
- Del-Mar Gonzalez-Barroso M., Ricquier D. and Cassard-Doulcier AM. The human uncoupling protein-1 gene (UCP1): present status and perspectives in obesity research. Obesity Reviews, 2000; 1(2): 61-42.
- Do GM., Jung UJ., Park HJ., Kwon EY., Jeon SM., McGregor RA. and Choi MS. Resveratrol ameliorates diabetes-related metabolic changes via activation of AMP-activated protein kinase and its downstream targets in db/db mice. Molecular Nutritional Food Research, 2012; 56(8): 1282-1291.
- Dudhia Z. The effect of *Cyclopia maculata* on lipogenesis and lipolysis in 3T3-L1 pre-adipocytes and adipocytes. Masters of Science, University of Stellenbosch, 2012

- Dudhia Z. The effect of *Cyclopia maculata* on lipogenesis and lipolysis in 3T3-L1 pre-adipocytes and adipocytes. In Phytomedicine (press), 2013.

- Du Toit J., Joubert E. and Britz TJ. Honeybush Tea – A rediscovered indigenous South African Herbal Tea. Journal of Sustainable Agriculture, 1998; 12(2/3): 67-84.
- Encinosa WE. and Hellinger FJ. The impact of medical errors on ninety-day costs and outcomes: an examination of surgical patients. Health Service Research, 2008; 43(6): 2067–2085.
- Evans RM., Barish GD. and Wang YX. PPARs and the complex journey to obesity. Nature Medicine, 2004; 10(4): 355 - 361
- Estornell E., Cabo J. and Barber T. Protein synthesis is stimulated in nutritionally obese rats. Journal of Nutrition, 1995: 125(5): 1309-1315.
- Ferreira D., Kamara BI., Brandt EV. and Joubert E. Phenolic compounds from *Cyclopia intermedia* (honeybush tea). Journal of Agricultural and Food Chemistry, 1998; 46: 3406-4310.
- Fillios LC. and Saito S. Hepatic protein synthesis and lipid metabolism in genetically obese rats. Metabolism, 1965; 14(6): 734-745.
- Finkelstein EA., Trogdon JG., Cohen JW. and Dietz W. Annual medical spending attributable to obesity: payer and service specific estimates. Health Affairs. (Millwood), 2009; 28: 822-31.
- Finucane MM., Stevens GA. and Cowan MJ. For the global burden of metabolic risk factors of chronic disease collaborating group (Body mass index). National, regional and global trends in body mass index since 1980: systematic analysis of health examination surveys and epidemiological studies with 960 country-years and 9.1 million participants. Lancet, 2011; 377(9): 16-24.
- Flegal KM., Caroll MD., Ogden CL. and Curtin LR. Prevalence and trends in obesity among US adults, 1999-2008. American Medical Association, 2010.
- Fleury C., Neverova M., Collins S., Raimbault S., Champigny O., Levi-Meyrueis C., Bouillaud F., Seldin MF., Surwit RS., Ricquier D. and Warden CH. Uncoupling protein 2: a novel gene linked to obesity and hyperinsulinemia. Natural Genetics, 1997; 15(3): 269-272.

- Fogarty S. and Hardie DG. Development of protein kinase activators: AMPK as a target in metabolic disorders and cancer. Biochemical Biophysical Activation, 2010; 1804: 581–591
- Ford ES. Risks for all-cause mortality, cardiovascular disease and diabetes associated with the metabolic syndrome: a summary of the evidence. Diabetes Care, 2005; 28: 1769-1778.
- Friedman JM. and Halaas JL. Leptin and the regulation of body weight in mammals. Nature, 1998; 395: 763–770.
- Fujii N., Jessen N. and Goodyear LJ. MAPK-activated protein kinase and regulation of glucose transport. American Journal of Physiology and Endocrinology Metabolism, 2006; 291: 867-877.
- Galassi A., Reynolds K. and He J. Metabolic syndrome and risk of cardiovascular disease: a meta-analysis. American Journal of Medicine, 2006; 119: 812-819.
- Galati EM., Monforte MT., Kirjavainen S., Forestieri AM., Trovato A. and Tripodo MM. Biological effects of hesperidin, a citrus flavonoid: anti-inflammatory and analgesic activity. Pharmacology, 1994; 40: 709-126.
- Gill GW. H&E staining; oversight and insights. Connection, 2010: 104-114.
- Gimeno RE., Dembski M., Weng X., Denig NH., Shyian AW., Gimeno CJ., Iris F., Ellis SJ., Woolf F. and Tartagalia LA. Cloning and characterization of an uncoupling protein homolog: a potential molecular mediator of human thermogenesis. Diabetes, 1997; 46: 900-906.
- Goldstein BJ. and Scalia R. Adiponectin: A novel adipokine linking adipocytes and vascular function. Journal of Clinical Endocrinology Metabolism, 2004; 89: 2563-2568.
- Hall JE. The kidney, hypertension and obesity. Hypertension, 2003; 41: 625-633.
- Hardie DG. and Sakamoto K. AMPK: A Key Sensor of Fuel and Energy Status in Skeletal Muscle. Physiology, 2006; 21: 48-60.
- Haslam DW. And James WP. Obesity. Lancet, 2005; 366:1197-209.
- Hawley SA., Boudeau J., Reid JL., Mustard KJ., Udd L., Mäkelä TP., Alessi DR. and Hardie DG. Complexes between the LKB1 tumor suppressor, STRAD alpha/beta and

MO25 alpha/beta are upstream kinases in the AMP-activated protein kinase cascade. Journal of Biology, 2003; 2:28.

- Hawley SA., Pan DA., Mustard KJ., Ross L. and Bain J. Calmodulin-dependent protein kinase-β is an alternative upstream kinase for AMP-activated protein kinase. Cell Metabolism, 2005; 2: 9-19
- Hemmingsen B., Lund SS., Wetterslev J. and Vaag A. Oral hypoglycaemic agents, insulin resistance and cardiovascular disease in patients with type 2 diabetes. European Journal of Endocrinology, 2009; 161: 1–9.
- Hemminki A., Markie D., Tomlinson I., Avizent E., Roth S., Loukola A., Bignell G., Warren W., Aminoff M., Hoglund P., Jarvinen H., Kristo P., Pelin K., Ridanpaa M., Salovaara R., Torro T., Bodmer W., Olschwang S., Olsen AS., Stratton MR., de la Chapelle A. and Aaltonen LA. A serine/threonine kinase gene defective in Peutz Jeghers syndrome. Nature, 1998; 391: 184-187.
- Himms-Hagen J. and Harper ME. Physiological role of UCP3 may export of fatty acids from mitochondria when fatty acid oxidation predominates: an hypothesis. Experimental Biology Medicine, 2001; 226:78-84.
- Huang TT., Johnson MS., Figueroa-Colon R., Dwyer JH. and Goran MI. Growth of visceral fat, subcutaneous abdominal fat, and total body fat in children. Obesity Research, 2001: 9(5): 283-289.
- Hudson ER., Pan DA. and James J. A novel domain in AMP-activated protein kinase causes glycogen storage bodies similar to those seen in hereditary cardiac arrhythmias. Current Biology, 2003; 13: 861-866.
- Hurley RL., Anderson KA., Franzone JM., Kemp BE., Means AR. and Witters LA. The Ca^{2+}/Calmodulin-dependent protein kinase kinases. Journal of Biological Chemistry, 2005; 280: 29060-29066.
- Hwang H., Bowen BP., Lefort N., Flynn CR., De Filippis EA., Roberts C., Smoke CC., Meyer C., Hojlund K., Yi Z. and Mandarino LJ. Proteomics analysis of human skeletal muscle levels novel abnormalities in obesity and type 2 diabetes. Diabetes, 2010; 59 (1): 33-42.

- Hwang JT., Kwon DY. and Yoon SH. AMPK–activated kinase: a potential target for the disease prevention by natural occurring polyphenols. New Biotechnology, 2009; 26(1-2): 17–22.
- Hwang JT., Ha J., Park IJ., Lee SK., Baik HW., Kim YM. and Park OJ. Apoptotic effect of EGCG in HT-29 colon cancer cells via AMPK signal pathway. Cancer Letters, 2007; 247: 115–121.
- Hwang JT., Park IJ., Shin JI., Lee YK., Lee SK., Baik HW., Ha J. and Park O J. Genistein, EGCG, and capsaicin inhibit adipocyte differentiation process via activating AMP-activated protein kinase. Biochemical and Biophysical Research Communications, 2005; 338: 694-699.
- Jager S., Handschin C., St Pierre J. and Spiegelman BM. AMP-activated protein kinase (AMPK) action in skeletal muscle via direct phosphorylation of PGC-1α. National Academy of Science, 2007; 104: 12017-12022.
- James WPT., Caterson ID., Coutinho W., Finer N., Van Gaal LF., Maggioni AP., Torp-Pedersen C., Sharma AM., Sheperd GM., Rode RA. and Renz CL. Effect of sibutramine on cardiovascular outcomes in overweight and obese subjects. Diabetes Care, 2010; 363: 909-917.
- Jenne DE., Reimann H., Nezu J., Friedel W., Loff S., Jeschke R., Muller O., Back W. and Zimmer M. Peutz- Jeghers syndrome is caused by mutations in a novel serine threonine kinase. Natural Genetics, 1998; 18: 38-43.
- Jeong S., Han M., Lee H., Kim M., Kim J., Nicol CJ., Kim BH., Choi JH., Nam KH., Oh GT. and Yoon M. Effects of fenofibrate on high-fat diet-induced body weight gain and adiposity in female C57BL/6J mice. Metabolism, 2004; 53(10): 1284-1289.
- Jiang WJ. Sirtuins: Novel targets for metabolic disease in drug development. Biochemical and Biophysical Research Communications, 2008; 373(3): 341-344.
- Jo J., Gavrilova O., Pack S., Jou W., Mullen S., Summer AE., Cushmen SW. and Periwal V. Hypertrophy and/or Hyperplasia: Dynamics of adipose Tissue Growth. PLoS Computational Biology, 2009; 5(3):1-11.
- Jorgensen SB., Violett B., Andreelli F., Frosig C., Birk JB., Schjerling P., Vaulont S., Richter EA. and Wojtaszewski JF. Knockout of alpha2 but not alpha 5-AMP-activated

protein kinase isoform abolishes 5-aminoimidazole-4-carboxamide-1-beta-4-ribofuranoside but not contraction induced glucose uptake in skeletal muscle. Journal of Biological Chemistry, 2004; 279: 1070-1079.

- Joubert E., Gelderbloem WCA., Louw A. and De Beer D. South African Herbal Teas: *Aspalathus linearis*, *Cyclopia spp.* and *Anthrixia phylicoides* – A review. Journal of Ethnopharmacology, 2008; 119: 376-412.
- Joubert E., Joubert ME., Bester C., De Beer D. and De Lange JH. Honeybush (*Cyclopia spp.*): From local cottage industry to global markets – The catalytic and supporting role of research. South African Journal of Botany, 2011; 77: 887-907.
- Joubert J., Norman R., Bradshaw D., Goedecke JH., Steyn NP. and Puoane. Estimating the burden of disease attributable to excess body weight in South Africa in 2000. South African Comparative Risk Assessment Collaborating Group. South African Medical Journal, 2007; 97(8): 683-690.
- Kahn BB., Alquier T., Carling D. and Hardie DG. AMP-activated protein kinase: ancient energy gauge provides clues to modern understanding of metabolism. Cell Metabolism, 2005; 1(1): 15-25.
- Kahn SE., Hull RL. and Utzschneider KM. Mechanisms linking obesity to insulin resistance and type 2 diabetes. Nature, 2006; 444: 840-846.
- Kamara BI., Brandt EV., Ferreira D. and Joubert E. Polyphenols from honeybush tea (*Cyclopia intermedia*). Journal of Agricultural and Food Chemistry, 2003; 51: 3874-3879.
- Kamara BI., Brandt EV. and Joubert E. Phenolic metabolites from honeybush tea (*Cyclopia subternata*). Journal of Agricultural and Food Chemistry, 2004; 52: 5391-5395.
- Kang SI., Shin HS., Kim HM., Hong YS., Yoon S A., Kang SW., Kim JH ., Kim MH., Ko HC. and Kim SJ. Immature *Citrus sunki* peel extract exhibits anti-obesity effects by β-oxidation and lipolysis in high fat diet induced obese mice. Biological Pharmacology Bulletin, 2012; 35(2): 223-230.
- Katsanos CS. and Mandarino LJ. Protein metabolism in human obesity: a shift in focus from whole-body to skeletal Muscle. Obesity, 2011; 19(3): 469-475.

- Kersten S., Seydoux J., Peters JM., Gonzales FJ., Desvergne B. and Wahli W. The peroxisome proliferator activated alpha receptor α mediates t adaptive response to fasting. Journal of Clinical Investment, 1999; 103: 1489-1498.
- Khaodhiar L. and Apovian CM. Current perspective of obesity and its treatment. Management Care Interface, 2007; 20: 24-31.
- Kim MJ., Yoo KH., Kim JH., Seo YT., Ha BW., Kho JH., Shin YG. and Chung CH. Effect of pinitol on glucose metabolism and adipocytokines in uncontrolled type 2 diabetes. Diabetes Research and Clinical Practice, 2007; 77: 247-251.
- Kim SJ., Jung JY., Kim HW. and Park T. Anti-obesity effects of *Juniperus chinensis* extract are associated with increased AMP-activated protein kinase expression and phosphorylation in the visceral adipose tissue of rats. Biological Pharmacology Bulletin, 2008; 31(7):1415-1421.
- Ko HC., Jang MG., Kang CH., Lee NH., Kang SI., Lee SR., Park DB. and Kim SJ. Preparation of a polymethoxyflavone-rich fraction (PRF) of *Citrus sunki* Hort. ex Tanaka and its anti-proliferative effects. Food Chemistry, 2010; 123: 484-488.
- Kokotkiewicz A., Luczkiewicz M., Sowinski P., Glod D., Gorynski K. and Bucinski A. Isolation and structure elucidation of phenolic compounds from *Cyclopia subternata* Vogel (honeybush) intact plant and *in vi*tro cultures. Food Chemistry, 2012; 133: 1373-1382.
- Kola B. Role of AMPK-activated protein kinase in the control of appetite. Journal of Neuroendocrinology, 2008; 20: 942-951.
- Kraegen EW., Saha AK., Preston E., Wilks D., Hoy AJ., Cooney GJ. and Ruderman NB. Increased malonyl-CoA and diacylglycerol content and reduced AMPK activity accompany insulin resistance induced by glucose infusion in muscle and liver of rats. American Journal of Physiology and Endocrine Metabolism, 2006; 290(3): 471-479.
- Lage R., Dieguez C., Vidal-Puig A. and López M. AMPK: a metabolic gauge regulating whole body energy homeostasis. Trends in Molecular Medicine, 2008; 14(2): 539-549.
- Lalloo UG. and Pillay S. Managing tuberculosis and HIV in sub-Saharan Africa. Current HIV/AIDS Report, 2008; 5(3): 132-139.

- Lavie CJ., Richard MD., Milani MD., Hector O. and Ventura MD. Obesity and cardiovascular disease risk factor, paradox and impact of weight loss. Journal of the American College of Cardiology, 2009; 35: 1925-1932.
- Lee H., Kang R. and Yoon. SH21B, an anti-obesity herbal composition, inhibits fat accumulation in 3T3-L1 adipocytes and high fat diet induced obese mice through the modulation of the adipogenesis pathway. Journal of Ethnopharmacology, 2010; 127: 709-717.
- Lee WJ., Kim M., Park HS., Kim HS., Jeon MJ., Oh KS., Koh EH., Won JC., Kim MS., Oh GT., Yoon M., Lee KU. and Park JY. AMPK activation increases fatty acid oxidation in skeletal muscle by activating PPARα and PGC-1. Biochemical and Biophysical Research Communication, 2006; 340: 291-295.
- Leeder S., Raymond S., Greenberg H., Liu H. and Esson K. A race against time: the challenge of cardiovascular disease in developing countries. New York: Trustees Columbia University, 2004.
- Li J., Zeng Z., Viollet B., Ronnett GV. and McCullough LD. Neuroprotective effects of adenosine monophosphate-activated protein kinase inhibition and gene deletion in stroke. Stroke, 2007; 38(11): 2992-2999.
- Lim CT., Kola B. and Korbonits M. AMPK as a mediator of hormonal signaling. Journal of Molecular Endocrinology, 2010; 44: 87-97.
- Lizcano JM., Goransson O., Toth R., Deak M., Morrice NA., Boudeau J., Hawley SA., Udd L., Makela TP., Hardie DG. and Alessi DR. LKB-1 is a master kinase that activates 13 kinases of the AMPK subfamily, including MARK/PAR-1. The EMBO Journal, 2004; 23: 833-843.
- Loos RJ. Genetic determinants of common obesity and their value in prediction. Best Practice and Research: Clinical Endocrinology and Metabolism, 2012; 26(2): 211-226.
- López M., Saha AK., Diéguez C. and Vidal-Puig A. The AMPK- malonyl-CoA-CPT1 axis in the control of hypothalamic neuronal function. Cell Metabolism, 2008; 8(3): 176.
- Marinou K., Tousoulis D., Antonopoulos AS., Stefanadi E. and Stefanadis C. Obesity and cardiovascular disease: from pathophysiology to risk stratification. International Journal of Cardiology, 2010; 138: 3-8.

- Marnewick JL., Gelderblom WCA. and Joubert E. An investigation on the antimutagenic properties of South African herbal teas. Mutation Research, 2000; 471(1-2): 157-166.
- Marnewick JL., Joubert E., Joseph S., Swanevelder S., Swart P. and Gelderbloem WCA. Inhibition of tumour promotion in mouse skin by extracts of rooibos (*Aspalanthis linearis)* and honeybush (*Cyclopia intermedia)*, unique South African herbal teas. Cancer Letters, 2005; 224: 193-202.
- Marti A., Martinez-Gonzales MA. and Martinez JA. Interaction between genes and lifestyle factors on obesity. Proceedings of the Nutrition Society, 2008; 67:1-8.
- Martin TL., Alquier T., Asakura K, Furukawa N., Preitner F. and Kahn BB. Diet-induced obesity alters AMPK kinase activity in hypothalamus and skeletal muscle. Journal of Biological Chemistry, 2006; 281: 18933-18941.
- Matsuzawa Y., Nakamura T., Shimomura I. and Kotani K.Visceral fat Accumulation and cardiovascular disease. Obesity Research, 1995; 3(5): 645-647.
- McBride A., Ghilagaber S., Nikolaev A. and Hardie DG. The glycogen-binding domain on the AMPK beta subunit allows the kinase to act as glycogen sensor. Cellular Metabolism, 2009; 9(1): 23-34.
- McCullough LD., Zeng Z., Li H., Landree LE., McFadden J., Ronnett GV. Pharmacological inhibition of AMP-activated protein kinase provides neuroprotection in stroke. Journal of Biological Chemistry, 2005; 280(21): 20493-20502.
- Mckay DL. and Blumberg JB. A Review of the bioactivity of South African herbal teas: Rooibos (*Aspalanthus linearis*) and Honeybush (*Cyclopia intermedia*). Phytotherapy Research, 2007; 21: 1-16.
- Menon VP. and Sudheer AR. Antioxidant and anti-inflammatory properties of curcumin. Advances in Experimental and Medical Biology, 2007; 595: 105-125.
- Minokoshi Y., Alquiler T., Furukawa N., Kim YB., Lee A., Xue B., Mu J., Foufelle F., Ferre P. and Birnbaum MJ. AMP-kinase regulates food intake by responding to hormonal and nutrient signals in the hypothalamus. Nature, 2004; 428: 569-574.
- Misra A. and Khurana L. Obesity and the metabolic syndrome in developing countries. Journal of Clinical Biology, 2009; 93(11): 9-30.

- Momcilovic M., Hong SP. and Carlson. Mammalian TAK1 activates Snf1 protein kinase in yeast and phosphorylates AMP-activated protein kinase *in vitro*. Journal of Biological Chemistry, 2006; 281: 25336-25343.
- Muller CJF., Joubert E., Gabuza K., De Beer D., Fey SJ. and Louw J. Assessment of the antidiabetic potential of an aqueous extract of honeybush (*Cyclopia intermedia*) in streptomycin and obese insulin resistant Wistar rats. Phytochemicals-Bioactivities and Impact on Health. 2011: 313-332.
- Must A., Spando J., Coakley EH., Field AE., Colditz G. and Dietz WZ. The disease burden associated with overweight and obesity. Journal of the American Health Association, 1999; 282: 1523-1529.
- Nicholls DG. and Locke RM. Thermogenic mechanisms in brown fat. Physiological Review, 1984; 64(1): 1-64.
- Niu Y., Li S., Na L., Feng R., Liu L., Li Y. and Sun C. Mangiferin decreases plasma free fatty acids through promoting its catabolism in liver by activation of AMPK. PLoS ONE, 2012; 7(1): e30782.
- Paeratakul S., Popkin BM., Keyou G., Adair LS. and Stevens J. Changes in diet and physical activity affect the body mass index of Chinese adults. International Journal of Obesity Relationship Metabolic Disorders, 1998; 22: 424-431.
- Patel O. The effect of *Cyclopia maculata* on adipogenesis in Wistar rats. Masters of Science, University of the Western Cape, 2012.
- Pang J., Choi Y. and Park T. *Ilex paraguariensis* extract ameliorates obesity induced by high-fat diet: potential role of AMPK in the visceral adipose tissue. Biochemistry and Biophysical, 2008. 476, 178–185.
- Persell S. Prevalence of resistant hypertension in the United-States, 2003-2008. Hypertension, 2011; 57: 1076-1080.
- Pierce Biotechnology Incorporated. Acetone precipitation of protein; technical resource, 2004.
- Pi-Sunyer FX. The obesity epidemic: pathophysiology and consequences of obesity. Obesity Research, 2002; 10:97–104.

- Polekhina G., Gupta A., Mitchell BJ., Van Denderen B., Murthy S. and Feil SC. AMPK beta subunit targets metabolic stress sensing to glycogen. Current Biology, 2003; 13: 867-871.
- Popkin BM., Adair LS. and Weng S. Global nutrition transition and pandemic of obesity in countries. Nutrition Reviews, 2011; 70(1); 3-21.
- Porrier P., Cornier MA., Mazzone T., Stiles S., Cummings S., Klein S., McCullough PA., Ren -Fielding C. and Franklin B. Bariatric surgery and cardiovascular risk factors: a surgery and cardiovascular risk factors: a scientific and cardiovascular risk factors: scientific statement from the American heart association. Circulation, 2011; 123: 1683-1701.
- Prentice AM. The emerging epidemic of obesity in developing countries. International Journal of Epidemiology, 2006; 35; 93-99.
- Puoane T., Steyn K., Bradshaw D., Laubscher R., Fourie J., Lambert VE. and Mbananga N. Obesity in South Africa: The South African demographic and health survey. Obesity Research, 2002; 10(10): 1038-1048.
- Redon J., Cifkova R., Laurent S., Nilsson P., Narkiewicz K., Erdine S. and Mancia G. Scientific Council of the European Society of Hypertension. The metabolic syndrome in hypertension. Journal Hypertension, 2008; 26: 1891-9000.
- Reis JP., Macera CA., Araneta MR., Lindsay SP., Marshal SJ. and Wingard DL. Comparison of overall obesity and fat distribution in predicting risk and mortality. Obesity, 2009; 17(6): 1232-1239.
- Rinderknecht H., Noble RL. and Williams PC. Preliminary extraction of gonadotrophic principle from pregnant mare serum. Biochemical Journal, 1939; 33(3):381-384.
- Robinson MK. Perioperative safety in the longitudinal assessment of bariatric surgery. New England Journal of Medicine, 2009; 361(5): 520-521.
- Rothwell NJ., Saville ME. and Stock MJ. Brown fat activity in fasted and refed rats. Bioscience Review, 1984; 4:351-357.
- Rousset S., Alves-Guerra MC., Mozo J., Miroux B., Cassard-Doulcier AM., Bouillaud F. and Ricquier D. The biology of mitochondrial uncoupling proteins. Diabetes, 2004; 53(1): 130-135.

- Samec S., Seydoux J. and Dulloo AG. Role of UCP homologues in skeletal muscles and brown adipose tissue: mediators of thermogenesis or regulators of lipids as fuel substrate. The FASEB Journal, 1998; 12(9): 715-724.
- Samuel VT., Petersen KF. and Shulman GI. Lipid induced insulin resistance: unravelling the mechanism. Lancet, 2010; 375: 2267-77.
- Sanders MJ., Grondin PO., Hegarty BD., Snowden MA. and Carling D. Investigating the mechanisms for AMP activation of the AMP-activated protein kinase cascades. Biochemical Journal, 2007; 403: 139-148.
- Sassi F. Obesity and the economics of prevention. In Obesity, online publication; page 29: fit not fat. Paris: OECD publishing, 2010.
- Schinner S., Scherbaum WA., Bornstein SR. and Barthel A. Molecular mechanisms of insulin resistance. Diabetes, 2005; 22: 674-682.
- Scholze J., Alegria E., Ferri C., Langham S., Stevens W., Jeffries D. and Uhl-Hochgraber K. Epidemiological and economic burden of metabolic syndrome and its consequences in patients with hypertension in Germany, Spain and Italy; a prevalence-based model. Biological Medicine Central Public Health, 2010; 10; 529.
- Schrauwen P. and Hesselink M. UCP2 and UCP3 in muscle controlling body metabolism. The Journal of Experimental Biology, 2002; 205: 2275-2285.
- Scott JW., Hawley SA., Green KA., Anis M., Stewart G. and Scullion GA. CBS domains from energy-sensing modules whose binding of adenosine ligands is disrupted by disease mutations. Journal of Clinical Investigations, 2004; 113: 274-284.
- Segura J., Banegas JR., Garcia-Donaire JA., Rodriguez-Artalejo F., de la Cruz JJ. and Praga M. Should hypertension guidelines be changed for hypertensive patients with metabolic syndrome?. Journal of Clinical Hypertension (Greenwich), 2007; 9: 595-600.
- Sigma-Aldrich. Ponceau stain data sheet, 2012
- Sironi AM., Gastaldelli A., Mari A., Ciociaro D., Positano V., Buzzigoli E., Ghione S., Turchi S., Lombardi M. and Ferrannini E. Visceral fat in hypertension: Influence on insulin resistance and beta-cell function. Hypertension, 2004; 44: 127–133.
- Smith BM, Smith JM. and Tsai JH. Discovery and structure-activity relationship of (1R)-8-chloro-2, 3, 4, 5–tetrahydro-1-methyl-1H-3-benzazepine (lorcaserin), a selective

serotonin 5-HT_{2c} receptor agonist for the treatment of obesity. Journal of Medical Chemistry, 2008;51:305–313.(a)

- Smith RS., Prosser WA., Donahue DJ., Morgan ME., Anderson CM. and Shanahan WR. Lorcaserin (APD356), a selective 5-HT2C agonist, reduces body weight in obese men and women. Obesity Journal, 2008;17: 494-503.(b)
- Srivastava AK., Qin X., Wedhas N., Arnush M., Linkhart TA., Chadwick RB. and Kumar A. Tumor necrosis factor-α augments matrix metalloproteinase-9 production in skeletal muscle cells through the activation of transforming growth factor-β-activated kinase 1 (TAK1)-dependent signaling pathway. Journal of Biological Chemistry 2007; 282(48): 35113-35124.
- Steinberg GR. and Kemp BE. AMPK in health and disease. Physiology Review, 2009; 89(3): 1025-1078.
- Suter M., Riek U., Tuerk R., Schlattner U., Wallimann T. and Neumann D. Dissecting the role of 5'-AMP for allosteric stimulations, activation and deactivation of AMP-activated protein kinase. Journal of Biological Chemistry, 2006; 281: 32207-32216.
- Suzuki A., Okamoto S., Lee S., Saito K., Shiuchi T. and Minokoshi Y. Leptin stimulates fatty acid oxidation and peroxisome proliferator-activated receptor alpha gene expression in mouse C2C12 myoblasts by changing the subcellular localization of the alpha2 form of AMP-activated protein kinase. Molecular and Cellular Biology, 2007; 27(12): 4317-4327.
- Tanaka T. Central melanocortin signaling restores skeletal muscle AMPK-activated protein kinase in mice fed a high fat diet. Cellular Metabolism, 2007: 5: 395-402.
- Torgerson JS., Hauptman J., Bolden MN. and Sjostrom L. Xenical in prevention of diabetes in obese subjects (XENDOS) study: a randomized study of orlistat as an adjunct to lifestyle changes for the prevention of type 2 diabetes in obese patients. Diabetes Care, 2004; 27: 155-161.
- Verhoog NJD. Evaluation of phytoestrogen activity of honeybush (Cyclopia). Masters of Science (Biochemistry), Stellenbosch University, 2006.
- Villarroya F., Iglesias R. and Giralt M. PPARs in control of uncoupling proteins gene expression. PPAR Research, doi:10.1155/2007/74364.

- Viollet B., Andreelli F., Jørgensen SB., Perrin C., Geloen A., Flamez D., Mu J., Lenzner C., Baud O., Bennoun M., Gomas E., Nicolas G., Wojtaszewski JF., Kahn A., Carling D., Schuit FC., Birnbaum MJ., Richter EA., Burcelin R. and Vaulont S. The AMP-activated protein kinase alpha2 catalytic subunit controls whole-body insulin sensitivity. Journal of Clinical Investment, 2003; 111(1): 91-98.
- Viollet B., Horman S,. Leclerc J., Lantier L., Foretz M., Billaud M., Giri S. and Andreelli F. AMPK inhibition in health and disease. Biochemistry and Molecular Biology, 2010; 45(4): 276-295.
- Wasir JS. and Misra A. The metabolic syndrome in Asian Indians: the impact of nutritional and socio-economic transition in India. Metabolic syndrome relationship disorder, 2004; 2: 14-23.
- Waterlow JC. Whole body protein turnover in humans- past, present and future. Annual Review Nutrition, 1995; 15:57-92.
- Weigle DS., Selfridge MW. and Schwartz MW. Elevated free fatty acids induce protein UCP3 expression in muscle: a potential explanation for the effect of fasting. Diabetes, 1998; 47(2): 298-302.
- Welborn TA., Dhaliwal SS. and Bennett SA. Waist-hip ratio is the dominant risk factor predicting cardiovascular death in Australia. Medical Journal of Australia, 2003; 179: 580-585.
- Welle S., Barnard RR., Statt M. and Amatruda JM. Increased protein turnover in obese women. Metabolism, 1992; 41(9): 1028-1034.
- Westermeier R. Electrophoresis. Electrophoresis in practice, a guide to methods and applications of DNA and protein separations, Third Edition. Wiley-VCH: Freiburg, Germany, 2000: 35-40.
- Wild S., Roglic G, Green A., Sicree R. and King H. Global prevalence of diabetes: estimates for the year 200 and projections for 2030. Diabetes Care, 2004; 27: 1047-1053.
- World health organization (WHO). Global Health Observatory (GHO), Overweigh and obesity, 2012.
- World health organization (WHO). Overweight and obesity fact sheet, 2012.

- Wu CH., Yang MY., Chan KC., Chung PJ., Ou TT. and Wang CJ. Improvement in high fat diet induced obesity and body fat accumulation by *Nelumbo nucifera* leaf flavonoid-rich extract in mice. Journal of Agriculture and Food Chemistry, 2010; 58: 7075-7081.
- Yang Y., Atasoy D., Su HH. and Sternson SM. Hunger states switch a flip flop memory circuit via a synaptic AMPK dependent positive feedback loop. Cell, 2011; 146: 992-1003.
- Yang Y. and Ma H. Western blotting and ELISA techniques. Researcher, 2009; 1(2): 67-86.
- Yamauchi T., Kamon J. and Minokoshi Y. Adiponectin stimulate glucose utilization and fatty acid oxidation by activating AMP-activated protein kinase. Natural Medicine, 2002; 8: 1288-1295.
- Yonezawa T., Kurata R., Hosomichi K. and Kono A. Nutritional and Hormonal regulation of Uncoupling Protein 2. Life, 2009; 61(12): 1123-1131.
- Yoon M. The role of PPARα in lipid metabolism and obesity: Focusing on the effects of estrogen on PPARα actions. Pharmacological Research, 2009; 60: 151-159.
- Yoshikawa M., Shimoda H., Nishida N., Takada M. and Matsuda H. *Salacia reticulata* and its polyphenolic constituents with lipase inhibitory and lipolytic activities have mild antiobesity effects in rats. Journal of Nutrition, 2002; 132(7): 1819-24.

Appendix A

Materials	Suppliers
Protein extraction	
• Glass plate	• BioRad, (USA)
• Scalpel and blades	• Sigma-Aldrich (USA)
• Forceps	• Lasec (RSA)
• 100% ethanol	• B&M Scientific (RSA)
• Gloves	• Lasec (RSA)
• Paper towels	• Nampak (RSA)
• Weighing paper	• Lasec (RSA)
• Ice	• Ice making machine
• Liquid nitrogen	• Afrox (RSA)
• Eppendorf tubes 2 ml, 1.5 ml, 0.5 ml	• Sigma-Aldrich (USA)
• Phosphate buffered saline (PBS)	• Roche (Germany)
• Standard lysis buffer	• According to SOP
• Tissue extraction reagent lysis buffer	• Invitrogen (USA)
• Trizma base	• Sigma-Aldrich (USA)
• Glycine	• Sigma-Aldrich (USA)
• NaCl	• B & M Sci (RSA)
• DTT	• Sigma-Aldrich (USA)

• NaF	• Sigma-Aldrich (USA)
• Na_3VO_4	• Sigma-Aldrich (USA)
• NP40	• Sigma-Aldrich (USA)
• Triton X 1140	• Sigma-Aldrich (USA)
• RNase	• Sigma-Aldrich (USA)
• 1 x Protease inhibitor cocktail tablets	• Roche (Germany)
• 1 x Phosphatase inhibitor tablets	• Roche (Germany)
• PMSF	• Thermo Scientific (USA)
• Stainless steel beads	• Qiagen (Germany)
• Pipette tips 10 µl, 20 µl, 100 µl, 200 µl and 1000 µl	• Sigma-Aldrich (USA)

Protein determination

• BioRad DC assay reagent kit	• BioRad, (USA)
• BSA	• BioRad, (USA)
• 96 well microtiter plate	• Sigma-Aldrich (USA)

SDS-PAGE

• Leammli sample buffer	• BioRad (USA)
• β-mercapatoethanol	• Sigma-Aldrich (USA)
• TEMED	• Sigma-Aldrich (USA)
• 40% Acrylamide	• BioRad, USA (USA)
• SDS	• Sigma-Aldrich (USA)
• APS	• Sigma-Aldrich (USA)
• Protein loading tips	• Sigma-Aldrich (USA)
• Precision Plus Dual Color Marker	• Thermo Scientific (USA)
• Fermentes Pre-stain Protein ladder	• Thermo Scientific (USA)
• Fermentes Un-stain Protein ladder	• Thermo Scientific (USA)
• Cruz marker	• SantaCruz (USA)
• Coomassie brilliant blue	• BioRad (USA)

Western blot

• Ponceau Stain	• Sigma-Aldrich (USA)
• Hybond-P (PVDF) membrane	• Millipore (USA)
• Whatmann paper	• Whatman Ltd (UK)
• Non-fat milk powder	• Clover (RSA)
• LumiGlo Chemiluminescent Substrate kit	• KPL (USA)

Primary antibodies

Antibody	Source	Type	Cat number	Supplier
• pAMPK	Rabbit	mAb	#2535	Cell Signalling (USA)
• tAMPK	Rabbit	pAb	#2757	Cell Signalling (USA)
• ACC	Rabbit	mAb	C20G5	Cell Signalling (USA)
• UCP2	Goat	mAb	AB77363	Abcam (USA)
• PPARγ	Rabbit	mAb	#2430	Cell Signalling (USA)
• PPARα	Rabbit	pAb	AB3484	Abcam (USA)
• β-tubulin	Rabbit	pAb	#2146	Cell Signalling (USA)
• β-actin	Mouse	mAb	SC47778	SantaCruz (USA)

Secondary antibodies

Antibody	Source	Cat number	Supplier
Mouse HRP† IgG	Donkey	#2535	Cell Signalling (USA)
Rabbit HRP IgG	Donkey	#2757	Cell Signalling (USA)
Goat HRP IgG	Donkey	C20G5	Cell Signalling (USA)

ELISA

AMPKα [pT172] ELISA kit Invitrogen (USA)

Reagent	96 Test kit
• AMPKα [pT172] standard	• 2 vials
• Standard diluent buffer	• 1 bottle
• Antibody coated wells, 12 x 8 well strips	• 1 plate
• AMPKα [pT172] Detection antibody	• 1 bottle
• Anti-rabbit IgG HRP (100 X)	• 1 vial
• HRP Diluent	• 1 bottle
• Wash buffer concentrate (25 X)	• 1 bottle
• Stabilized Chromogen, Tetramethylbenzidine (TMB)	• 1 bottle
• Stop solution	• 1 bottle
• Plate covers, adhesive strips	• 3

Histology

• Glass slides	• Lasec (RSA)
• Haematoxylin	• Lasec (RSA)
• Eosin	• Lasec (RSA)
• 100% Ethanol	• B&M Scientific (RSA)
• Xylene	• Merck (Germany)
• Entallen	• Merck (Germany)

Equipment

• Analytical balance	• Ohaus (UK)
• TissueLyser	• Qiagen (Germany)
• Polytron homogenizer	• Brinkmann/Kinematica (Switzerland)
• Centrifuge	• Labnet Inc. (USA)
• ELISA plate reader	• BioTek (USA)
• Plate shaker	• IKA® (Germany)
• BioRad Mini Protean Tetra Cell	• BioRad (USA)
• BioRad, USA power pac HC	• BioRad, (USA)
• Heating block	• Labnet (USA)
• BioRad, USA ChemiDoc™ XRS+ image illuminator	• BioRad (USA)
• Quantity One software	• BioRad (USA)
• Ice making machine	• Scotsman (USA)
• Pasteur pipettes	• Labnet Inc. (USA) • Greiner (Germany)
• Belly dancer/shaker	• StoVoll (USA)
• Olympus BX50 light microscope	• Olympus (Japan)
• NIS-Element BR 3.0 software	• Nikon instruments Inc,(USA)
• Leica Qwin pro version 3	• Leica Microsystems, Germany

Appendix B

Solutions

Protein extraction

1 M Tris, pH 7.5

Stock	Volume	Final Concentration
Tris, MW=121.1	12 g	1M
ddH_2O	100 ml	
pH to 7.5 with HCl		
	Make up to 100 ml with ddH2O	

50 mM Tris, pH 7.5

Stock	Volume	Final Concentration
1M Tris, pH 7.5	2.5 ml	50 mM
ddH_2O	to 50 ml	

1 mM DTT

Stock	Volume	Final Concentration
DTT, MW= 41.9 9	8 mg	50 mM
Lysis buffer	to 50 ml	

100 mM PMSF

Stock	Volume	Final Concentration
PMSF, MW=174.194	870 mg	100 mM
Isopropanol	to 50 ml	
1 ml aliquots were stored at -20˚C		

50 mM NaF

Stock	Volume	Final Concentration
NaF, MW= 41.9 g/mol	0.104 g	50 mM
ddH_2O	to 50 ml	

200 mM Na_3VO_4, pH 10

Stock	Volume	Final Concentration
Na_3VO_4, MW=183.91 g/mol	367.82 mg	200 mM
ddH_2O	to 100 ml	

10 mM Na_3VO_4

Stock	Volume	Final Concentration
200 mM Na_3VO_4	10 ml	10 mM
ddH_2O	to 200 ml	

1 ml aliquots were stored at -20˚C

70% Ethanol

Stock	Volume	Final Concentration
100%	700 ml	70%
ddH_2O	to 1 liter	

In-house lysis buffer

Stock	Volume	Final Concentration
1M Tris	2.5 ml	50 mM
100 mM DTT	0.8 mg	1mM
NaF	104 mg	50 mM
Na_3VO_4	500 µl	100 µM
NP40	500 µl	1%,
Triton	500 µl	1%
RNase	12.5 µl	25 µg/ml
Protease inhibitors	2 tablets	1x
Phosphatase inhibitors	5 tablets	1x
ddH_2O	to 50 ml	

Make 1 ml aliquots and store at -20°C.

100 mM PMSF	10 µl	1 mM

Add PMSF before use.

Commercial lysis buffer

Stock	Volume	Final Concentration
1 M Tris		50 mM
NaCl		250 mM
EDTA		5 mM,
Na_3VO_4		2 mM
NaF		1 mM
$Na_4P_2O_7$		20 mM,
NaN_3		0.02%
Proprietary detergent		
Protease inhibitors	10 tablets	1x
Phosphatase inhibitors	10 tablets	1x
ddH_2O	to 100 ml	
Make 1 ml aliquots and store at -20°C		
100 mM PMSF	10 µl	1 mM
Add PMSF before use		

Protein determination

Solution A

Stock	Volume	Final Concentration
BioRad, USA DC Reagent S	20 µl	
BioRad, USA DC Reagent A	1 m	

SDS PAGE

2x Sample buffer

Stock	Volume	Final Concentration
β-mercaptoethanol	50 µl	
Leammli sample buffer	950 µl	

10% SDS

Stock	Volume	Final Concentration
SDS	10 g	10%
ddH_2O	to 100 ml	

10% APS

Stock	Volume	Final Concentration
APS	100 mg	10%
ddH_2O	in 1 ml	

10% Resolving gel

Stock	Volume	Final Concentration
3M Tris	1.25 ml	
40% Acrylamide	2.5 ml	10%
10 % SDS	100 µl	
99% TEMED	10 µl	
10% APS	75 µl	
ddH_2O	6.1 ml	

4% Resolving gel

Stock	Volume	Final Concentration
0.5M Tris	1.25 ml	
40% Acrylamide	1 ml	4%
10 % SDS	100 µl	
99% TEMED	10 µl	
10% APS	50 µl	
ddH_2O	7.59 ml	

10 x running buffer

Stock	Volume	Final Concentration
Tris, MW=121.1	30.28 g	25 mM
Glycine, MW=75.07	142.63 g	1.9 M
10% SDS	100 µl	1 %
ddH_2O	to 1 L	

1 x running buffer

Stock	Volume	Final Concentration
10 x running buffer stock	100 ml	1 x
ddH_2O	900 ml	

Destain

Stock	Volume	Final Concentration
Acetic acid	200 ml	10%
Methanol	600 ml	30%
ddH_2O	to 2 L	

Western blot analysis

Transfer buffer

Stock	Volume	Final Concentration
Tris,	6.06 g	25 mM
Glycine	28.83 g	192 mM
Methanol	400 ml	20%
ddH_2O	to 2 L	

10 x TBS

Stock	Volume	Final Concentration
Tris	24.22 g	25 mM
NaCl	80.06 g	1.37 M
ddH_2O	to 1 L.	

1 x TBST

Stock	Volume	Final Concentration
10 x TBS	100 ml	1 x
ddH_2O	900 ml	
Tween ®20	1 ml	

5% Blocking buffer

Stock	Volume	Final Concentration
Fat free powder milk	5 g	5%
1x TBST	100 ml	

.

AMPK [pT172] ELISA

100 Units/ml AMPK [pT172] standard

Stock	Volume	Final Concentration
AMPK [pT172] standard		100 Units/ml
Standard diluent buffer	800 µl	

Dilution of AMPKα [pT172] standards

Standard	Add:	Into
100 Units/ml		
50 Units/ml	0.25 mL of 100 Units/mL	0.25 mL of Diluent buffer
25 Units/ml	0.25 mL of 50 Units/mL	0.25 mL of Diluent buffer
12.5 Units/ml	0.25 mL of 25 Units/mL	0.25 mL of Diluent buffer
6.25 Units/ml	0.25 mL of 12.5 Units/mL	0.25 mL of Diluent buffer
3.12 Units/ml	0.25 mL of 6.25 Units/mL	0.25 mL of Diluent buffer
1.6 Units/ml	0.25 mL of 3.12 Units/mL	0.25 mL of Diluent buffer
0 Units/ml	0.25 mL of diluent buffer	An empty tube

Anti-rabbit IgG HRP working solution

Stock	Volume	Final Concentration
Anti-Rabbit IgG HRP (100x)	1 µl	1 x working solution
HRP Diluent	1 ml	
Sufficient for analysis of 10 samples		

Wash buffer solution

Stock	Volume	Final Concentration
Washing buffer concentrate (25x)	25 ml	1 x working wash buffer
ddH_2O	to 600 ml	